

Online ISSN : 2395-602X

Print ISSN : 2395-6011

www.ijrst.com



**Conference
Proceedings**

**One Day National Conference On Recent
Advances In Chemical and Biochemical Sciences**

RACBCS-2025

27th February 2025

Organized By

Ajitha Education Society's,
Department of Chemistry, Sant Dnyaneshwar Mahavidyalaya,
Soegaon, Maharashtra, India

&

Dr. Babasaheb Ambedkar Marathwada University,
Chhatrapati, Sambhajinagar, Maharashtra, India

VOLUME 12, ISSUE 10, JANUARY-FEBRUARY-2025

**INTERNATIONAL JOURNAL OF SCIENTIFIC
RESEARCH IN SCIENCE AND TECHNOLOGY**

PEER REVIEWED AND REFEREED INTERNATIONAL SCIENTIFIC RESEARCH JOURNAL

Scientific Journal Impact Factor : 8.627

Email : editor@ijrst.com Website : <http://ijrst.com>



**One Day National Conference On Recent Advances in
Chemical and Biochemical Sciences
(RACBCS-2025)**

17th February 2025

Organized by

Ajintha Education Society's,
Department of Chemistry, Sant Dnyaneshwar Mahavidyalaya, Soegaon,
Maharashtra, India

&

Dr. Babasaheb Ambedkar Marathwada University, Chhatrapati,
Sambhajinagar, Maharashtra, India

In Collaboration with

Society of Science, Technology and Humanity, Kalyan

Published By

International Journal of Scientific Research in Science and Technology

Print ISSN: 2395-6011 Online ISSN: 2395-602X

Volume 12, Issue 10, January-February-2025

International Peer Reviewed, Open Access Journal

Published By

Technoscience Academy

website: www.technoscienceacademy.com

Patrons

Hon.Shri Rangnath Kale

President
Ajintha Education Society

Hon.Shri Prakash Kale

Secretary
Ajintha Education Society

Chief Organizer

Dr. Shirish Pawar

I/C Principal

Organizing Secretary

Dr. Raosaheb Barote

Vice - Principal

Convener

Dr. Rameshwar Magar

Head, Dept. of Chemistry

Co-Convener

Dr. Sunil Choudhare

(Contact No. 8275321259)

Dr. Santosh Padghan

(Contact No. 8275334170)

Dr. Manojkumar Chopade

(Contact No. 9011093483)

Coordinator

Mr. Shyam Takle

(Contact No. 9921684561)

Dr. Pankaj Gavit

(Contact No. 9689488471)

Organizing Committee Members

Dr. Vinod Barote
Dr. Dilip Birute
Dr.Santosh Tandale
Dr. Nilesh Gadekar
Dr. Deepak Pardhe
Dr.Pandit Nalawade
Dr. Pramod Pawar
Dr.Jyoti Adhane
Dr.Ulhas Patil

Dr.Pradip Golhare
Dr.Chhatragun Bhore
Dr.Vikram Bhutekar
Mr. Kishor Nale
Dr.Sushil Jawle
Dr.Bhaskar Tekale
Dr.Pandurang Dapke
Mr.Pankaj Sable
Mr.Ravindra Jadhav

And all teaching and Non-teaching Staff

Contact

Dr. Rameshwar Magar

Mob.9423185053 / 9763873135

Email : racbcs2025@gmail.com

National Advisory Committee

Dr. Avinash Palodkar, Senior Scientist, Indian Institute of Petroleum, Dehradun
Dr. Farsa Ram, Indian Institute of Science (IISC), Bengaluru
Dr. Sachin Undre, Indian Institute of Teacher Education (IITE), Gandhinagar, Gujarat
Dr. N.N.Karade, Dept. of Chemistry, RTM Nagpur university, Nagpur
Dr. Vijay Bhosale, Yashwant Mahavidyalaya, Nanded
Dr. Anil Chopade, KBP Mahavidyalaya, Pandharpur
Dr. Sachin Gadekar, KBCNMU, Jalgaon
Dr. Rajendra Tayade, institute of Science, Nagpur

Local Advisory Committee

Prof. S. G. Shankarwar, Head, Dept. of Chemistry, Dr. BAMU, Chhatrapati Sambhajnagar
Prof. M. K. Lande, Dept. of Chemistry, Dr. BAMU, Chhatrapati Sambhajnagar
Prof. S. T. Gaikwad, Dept. of Chemistry, Dr. BAMU, Chhatrapati Sambhajnagar
Prof. A. S. Rajbhoj, Dept. of Chemistry, Dr. BAMU, Chhatrapati Sambhajnagar
Prof. B. B. Shingate, Dept. of Chemistry, Dr. BAMU, Chhatrapati Sambhajnagar
Prof. Arif Pathan, BOS Chairman, Maulana Azad College, Chhatrapati Sambhajnagar
Dr. G. M. Bondale, Dept. of Chemistry, Dr. BAMU, Chhatrapati Sambhajnagar
Dr. A. S. Chavan, Dept. of Chemistry, Dr. BAMU, Chhatrapati Sambhajnagar
Prof. S. R. Mirgane, Principal, Rajashri Shahu College, Pathri
Prof. B. K. Magar, Shivaji College Kannad
Dr. Ganesh Pawar, MGM University, Chhatrapati Sambhajnagar
Dr. Sandip Deshmukh, BOS Member, RP College, Dharashiv

Eminent Resource Persons



Dr. Rohan Erande
Indian Institute of
Technology (IIT), Jodhpur



Dr. B. M. Krishna Mariserla
Indian Institute of
Technology (IIT), Jodhpur



Dr. B. R. Sathe
Dr. B.A.M. University,
Chhatrapati Sambhajnagar

About the Society

Late Baburaoji Kale, a great freedom-fighter established Ajintha Education Society in 1970. Considering the problems faced by students in higher education in both urban and rural area, he established Pandit Jawaharlal Nehru Mahavidyalaya at Chhatrapati Sambhajinagar and Sant Dnyaneshwar Mahavidyalaya at Soegaon in June 1971. After Late Baburaoji Kale, Shri Rangnath Baburaoji Kale, the President of Ajintha Education Society and Shri. Prakash Baburaoji Kale, the Secretary of Ajintha Education Society were shouldered the responsibility of society. Since then, the Society has contributed a lot for the development of both of the institutions. In memory of their father, they established Late Baburaoji Kale Arts, Commerce and Science College at Ajintha, Dist. Chhatrapati Sambhajinagar in the year 2000. They incessantly strive hard to fulfil the noble dreams of Late Baburaoji Kale.

About the College

Sant Dnyaneshwar Mahavidyalaya, Soegaon was established in the year 1971. The College is affiliated to Dr. Babasaheb Ambedkar Marathwada University, Chhatrapati Sambhajinagar. It is included in 2(f) and 12 (B) of the UGC Act 1956. Our college has been accredited by NAAC with B Grade (CGPA 2.42 II Cycle). The College offers BA, B.Com, B. Sc. And B.Sc. in Computer at the UG level. M Sc. in Chemistry, Physics, Botany, Zoology, M. A. in Marathi, History, Political Science, Geography and M. Com. at PG level. The college is located near the vicinity of the world famous Ajintha Caves. The college provides higher education to mostly rural and hilly area students and focuses on the holistic development of students.

About the Department

The UG course of department of Chemistry was started in 2006 and PG course in Organic Chemistry was started in 2022. Department has highly qualified, young and dynamic faculty members. The department provides quality education in chemical sciences under UG and PG courses.

About the Conference

The Department of Chemistry is organizing one day National Conference on Recent Advances in Chemical and Biochemical Sciences-2025. The conference will provide an opportunity to share research idea with the eminent scientist, academician and industrialists.

Thrust area of the Conference

Organic Synthesis	Green Chemistry
Bio-Chemistry and Biotechnology	Drug Chemistry
Material Science	Polymer Chemistry
Catalysis	Inorganic Chemistry
Nanotechnology	Physical Chemistry

Any other topic related to the theme of the conference

Call for Full length paper/Abstract

Original research papers/abstract on the above mentioned area are invited from participant for oral and poster presentation on or before 20th February 2025 on the email address racbcs2025@gmail.com.

Guidelines for Abstract Submission

- Abstract of the research paper should be maximum 250 words type only MS word format Times New Roman , Font size 12 and 1.5 line spacing with 1" margin on all size on A4 size paper.
- The title should be bold with font size 14 followed by authors name(s) and Affiliation (font size 12) which is followed by email address(font size10)
- Presenting author should be underlined

Guidelines for Oral Presentation

- Authors are requested to make 10-15 slides for oral presentation.
- Each presentation has time 5-7 min.

Guidelines for Poster Presentation

- Poster size should be 1 X 1 meter size
- Each presentation has time 5 min.

Full length paper

It is proposed to publish the selected research paper presented in the conference in the International Journal of Scientific Research in Science and Technology after peer review

Important Dates

Abstract Submission	20 th February 2025
Intimation of Acceptance	21 st February 2025
Submission of Full length Paper	22 nd February 2025
Last Date of Registration	25 th February 2025

Venue

**Late Baburaoji Kale Auditorium
Sant Dnyaneshwar Mahavidyalaya, Soegaon
Dist.Chhatrapati Sambhaji Nagar**

CONTENT

SR. NO	ARTICLE/PAPER	PAGE NO
1	A Review on an Efficient Pyrazole Derivatives and Its Biological Activity Mr. Arun E. Bharade, Dr. Satish B. Jadhav, Dr. Bharat K. Dhotre, Dr. Balaji D. Rupnar	01-05
2	Medicinal Properties and Health Benefits of Giloy Plant (Tinospora Cordifolia) Dr. Deepak Devilal Pardhe	06-14
3	Facile Synthesis and Characterization of Nio Nanoparticles by Ultrasound Assisted Sol-Gel Method Dr. Sharada D. Shirole, Dr. Yogesh S. Suryawanshi	15-19
4	Mesoporous Al-SBA-15 Zeolite: An Efficient and Reusable Heterogeneous Catalyst for Green Synthesis of Pyrimido [4, 5-d] Pyrimidine Derivatives Ganesh T. Pawar, Rameshwar R. Magar, Bhagwat B. Nagolkar, Machhindra K. Lande	20-30
5	A Review on Biological Routes to Palladium Nanoparticle Synthesis: A Path toward Sustainable Nanomaterials M. B. Suwarnkar, G. V. Shitre, S. N. Sinkar	31-36
6	Advanced Chemical Synthesis and Characterization of γ-Fe₂O₃ Nanoparticles Mugale Y. G, Suryawanshi V. S	37-48
7	Ecofriendly Natural and Synthetic Approach for Synthesis of Coumarin Derivatives – A Review A. V. Sonone, R. U. Bhagyawant, M. D. Jadhav, R. D. More	49-53
8	Review on Synthesis, Characterization, and Properties of Soft Substituted Ferrite Nanoparticles A. P. Chavan, N. D. Chaudhari, G. B. Andhale, A. M. Kute, A. O. Dhokte, P. R. Kute	54-57
9	Synthesis and Characterization of Copper Doped TiO₂ Nanoparticles Sandip B. Deshmukh, Kalyani H. Deshmukh, Appasaheb W. Suryawanshi, Maheshkumar L. Mane	58-69
10	Study of Structural and Electrical Properties of Zinc Sulphide Films Prepared By Spray Pyrolysis Techniques Asif Karim, Sayed Mujeeb	70-73
11	Comprehensive Insights into Phenol Sulfonamides : Synthesis, Mechanistic Pathways, and Applications Sumit R. Nikume, Atul B. Patil, Ratnamala S. Bendre	74-84

A Review on an Efficient Pyrazole Derivatives and Its Biological Activity

Mr. Arun E. Bharade¹, Dr. Satish B. Jadhav¹, Dr. Bharat K. Dhotre¹, Dr. Balaji D. Rupnar²

¹Department of Chemistry, R.B. Attal Arts, Science & Commerce College, Georai, Maharashtra, India

²Department of Chemistry, Swami Vivekanand Senior College, Mantha, Jalna, Maharashtra, India

ARTICLE INFO

Article History:

Published : 27 January 2025

Publication Issue :

Volume 12, Issue 10

January-February 2025

Page Number :

01-05

ABSTRACT

Pyrazole is a heterocyclic organic compound having a 5-membered ring structure with three carbon atoms and two neighbour nitrogen atoms. There are several applications of pyrazole core based organic molecules in various areas including pharmacy and agro-chemical industries. There is an increase in the interest of synthesizing, analyzing different properties, and seeking possible applications of pyrazole derivatives. Our research efforts have been focusing on different aspects of pyrazoles including facile synthesis,

Researcher have synthesized and evaluated pyrazoles against several biological agents. This review Study novel structures of pyrazoles have been synthesised with their corresponding biological activities.

Keywords: Pyrazole derivatives; biological activities; synthesis; green chemistry;

I. INTRODUCTION

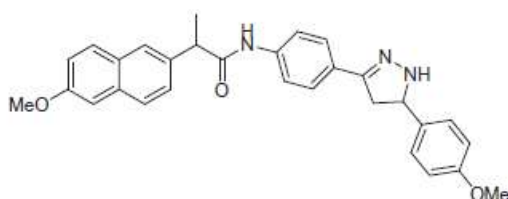
Over the years increasing attention has been paid to pyrazole derivatives which are synthesized based on the pyrazole as the central core[1]. The central core contains a five-membered heterocyclic organic compound with two adjacent nitrogen atoms. In the chemical, pharmaceutical, and agrochemical industries, pyrazole derivatives are of great interest [2, 3]. We aim to discuss recent research on pyrazole derivatives in this brief review, which was primarily published in the last years.

Biological active compounds of significance include pyrazoles and their substituted derivatives. Antiviral, antiparasitic, anti-tubercular, antifungal, antibacterial, antitumor, and insecticidal agents are among their uses. Certain compounds have also demonstrated analgesic, anesthetic, anti-inflammatory, and anti-diabetic effects. This research paper focuses on the most recent studies on pyrazole derivatives that have documented their antimicrobial qualities[4].

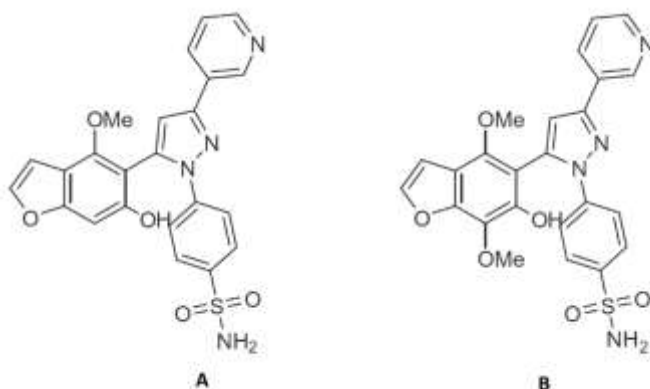
Biological Activity of various pyrazole derivatives

1. Analgesic and anti-inflammatory activity-

Rheumatoid arthritis and other inflammatory illnesses are frequently treated with NSAIDs, which have antipyretic and analgesic properties. NSAIDs have been associated with a number of adverse consequences, including stroke and bleeding from the gastrointestinal tract. Furthermore, people with a past of a cardiac event have been found to have an elevated risk for heart disease while using Non-steroidal anti-inflammatory drugs [5]. El-Sehemi and coworkers substituted other heterocycles for naproxene's carboxylic acid group, an NSAID. A variety of substances were acquired and evaluated for their potential ulcerogenic, analgesic, and anti-inflammatory properties. The pyrazoles derivative showed significant analgesic activity and exhibited no ulcerogenic effect [6].



Hassan et al. used benzofuran to create celecoxib analogs assessed their COX-2 inhibitory potential. With respective IC₅₀ values of 0.40 μM and 0.36 μM, molecules A and B exhibited the most anti-inflammatory action, while celecoxib's was 0.28 μM.23[8]



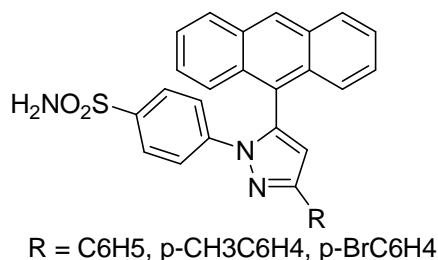
2. Antibacterial activity

Resistant to multiple drugs microbial infections are becoming more common, which is a global health concern. The development of novel antimicrobials with increased activity and decreased toxicity is always needed [7]. Aggarwal et al. synthesized fifteen compounds and tested them against a variety of bacterial strains to determine their in vitro antibacterial activity. Trifluoromethyl (CF₃) groups found in a number of pyrazoles have demonstrated exceptional antibacterial qualities[9].



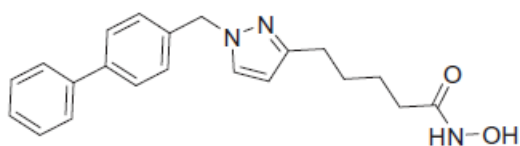
3. Pyrazoles as Anti-microbial Agents-

The synthesis and biological activity of novel pyrazoline and pyrazolidine derivatives were reported by Salem.A. Basaif et al. [10] in 1997. 5-Anthracen-9-yl-3-aryl-1-(p-sulfamylphenyl)pyrazoles and other pyrazole derivatives were created from chalcones and p-sulfanyl phenylhydrazine. Every synthetic pyrazole analogue's antimicrobial activity activity was tested[10].



4. Pyrazoles as Anticancer Agent-

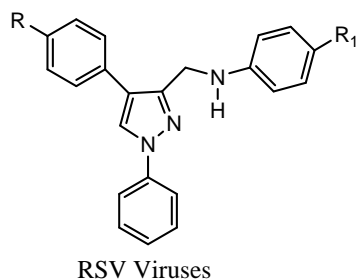
A number of 1,3-disubstituted pyrazoles are active on several cancer cell lines, including MCF-7 (breast cancer), BGC823 (intestinal cancer), K562 (myeloid leukemia), HT1080 (sarcoma), and A549 (lung cancer), according to Yao and colleagues. Additionally, a small number of these compounds—particularly compound below, which had a biphenyl group—were more potent than the medication suberoylanilide hydroxamic acid (SAHA) at inhibiting histone deacetylase enzymes (iHDAC) (Fig. 15). These iHDAC inhibitors are a novel family of anticancer medicines that have efficacy against a range of cancer types and have significant impacts on tumor cell proliferation, differentiation, angiogenesis, and programmed death of cells both in vitro and in vivo[11].



5. Pyrazole as a antiviral agent

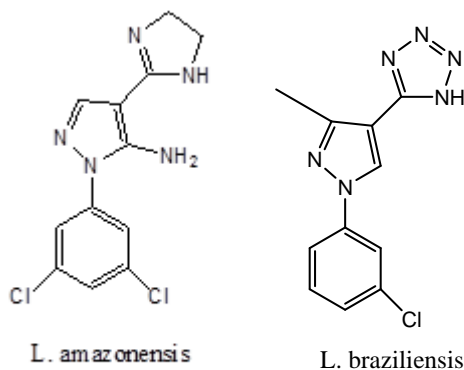
Many viruses are present now a days which create problem like Hepatitis B, hepatitis C and HIV are three examples of viruses which common chronic infections with high rates of morbidity and mortality. Pyrazole

moieties containing a pyrazole core have been highlighted in the search for new antiviral agents. Pyrazole derivatives gives activity against H1N1, HIV, hepatitis C, HSV-1, RSV have been reported in the literature [12].



6. Antileishmanial activity of pyrazole derivatives.

Numerous compounds featuring the pyrazole core have been assessed for their antileishmanial properties. The research team led by Bernardino developed a range of pyrazole derivatives that exhibited significant antileishmanial effects[13]. Bernardino and his team evaluated various pyrazole-tetrazole hybrids for their efficacy against *L. amazonensis* and *L. braziliensis*. Among these, following Compound demonstrated the highest potency against *L. braziliensis*.



II. CONCLUSION

In the conclusion Pyrazole derivatives are a versatile class of compounds with a wide range of biological activities and uses. Pyrazole moiety has been utilized for creating numerous compounds with biological effects and can be investigated further for potential application in treating various diseases.

III. REFERENCES

- [1]. Davies, D.T. Aromatic Heterocyclic Chemistry, Oxford, 1997, pp. 28, 29.
- [2]. Keter, K.F.; Darkwa, J. Biometals 2012, 25, 9-21.
- [3]. Fustero, S.; Sanchez-Rosello, M.; Barrio, P.; Simon-Fuentes, A. Chem. Rev. 2011, 111, 6984-7034
- [4]. Kurz T, Widyan K, Elegemeie GH. The vilsmeier-haack reaction–III cyclization of hydrazones to fluoro substituted pyrazoles. Phosphorous sulfur and silicon of pharmaceutical sciences., 2006; 1(2): 181-299.
- [5]. Kohli P, Steg PG, Cannon CP, et al. NSAID use and association with cardiovascular outcomes in outpatients with stable atherothrombotic disease. Am J Med. 2014;127:53–60.

- [6]. El-Sehemi AG, Bondock S, Ammar YA. Transformations of naproxen into pyrazolecarboxamides: search for potent anti-inflammatory, analgesic and ulcerogenic agents. *Med Chem Res.* 2014; 23:827–838.
- [7]. Kadam P, Karpoormath R, Omondi B, Chenia H, Ramjugernath D, Koorbanally NA. Stereo-selective synthesis, structural and antibacterial studies of novel glycosylated b2,3-amino acid analogues. *Med Chem Res.* 2015;24:3174–3193.
- [8]. Hassan GS, Abou-Seri SM, Kamel G, Ali MM. Celecoxib analogs bearing benzofuran moiety as cyclooxygenase-2 inhibitors: design, synthesis and evaluation as potential anti-inflammatory agents. *Eur J Med Chem.* 2014;76:482–493
- [9]. Aggarwal R, Bansal A, Rozas I, et al. P-Toluenesulfonic acid-catalyzed solventfree synthesis and biological evaluation of new 1-(40,60-dimethylpyrimidin-20-yl)-5-amino-4H-3-arylpyrazole derivatives. *Med Chem Res.* 2014;23:1454–1464.
- [10]. Basaif SA, Faidallah HM, Hassan SY. Synthesis and biological activity of new pyrazoline and pyrazole derivatives. *J. King Abdul. Uni.*, 1997; 9(2): 83-90.
- [11]. Yao Y, Liao C, Li Z, et al. Design, synthesis, and biological evaluation of 1,3 disubstituted-pyrazole derivatives as new class I and IIb histone deacetylase inhibitors. *Eur J Med Chem.* 2014;86:639–652.
- [12]. Anuradha S. Antiviral agents and treatment of viral infections. *J Int Med Sci Acad.* 2014;27: 191.
- [13]. Santos MS, Oliveira MLV, Bernardino AMR, et al. Synthesis and antileishmanial evaluation of 1-aryl-4-(4,5-dihydro-1H-imidazol-2-yl)-1H-pyrazole derivatives. *Bioorg Med Chem Lett.* 2011;21:7451–7454.

Medicinal Properties and Health Benefits of Giloy Plant (*Tinospora Cordifolia*)

Dr. Deepak Devilal Pardhe

Research Guide and Associate Professor, Department of Botany, Sant Dnyaneshwar Mahavidyalya, Soegaon,
Chhatrapati Sambhaji Nagar, Maharashtra, India

ARTICLE INFO

Article History:

Published : 27 January 2025

Publication Issue :

Volume 12, Issue 10

January-February 2025

Page Number :

06-14

ABSTRACT

Medicinal plants are the natural reservoirs of bioactive and therapeutic components that play vital role in the prevention of diseases and improvement of human health. The widely used modern synthetic drugs are associated with some undesirable side effects which may lead to other patho-physiological complications. Medicinal herbs are being widely accepted as alternative remedies for preventing various diseases especially in India and other Asian countries. "*Tinospora cordifolia* (Willd.) Miers ex Hook.F. & Thomson", one of the most promising plant species of *Tinospora* known as "Giloy" or Guduchi that is used in several traditional medicines in treating diseases. *Tinospora cordifolia* is a popular medicinal plant which is used in several traditional medicines to cure various diseases. It is considered an essential herbal plant of Indian system of medicine (ISM) and has been used in the treatment of fever, urinary problem, dysentery, skin diseases leprosy, diabetes, and many more diseases. The plant reported containing chemical compound including Alkaloids, Terpenoids, Lignans, Steroids and others that establish the phytochemistry and pharmacological activity of *Tinospora cordifolia*. The main pharmacological importance of giloy is antioxidant activity, antimicrobial activity, antibacterial activity, antifungal activity, anti-diabetic activity, anti-stress activity, hypolipidaemic effect, hepatic disorder, anti-cancer, anti-HIV potential, antio-steoporotic effects, antitoxic effects, wound healing, anti-complementary activity, and immunomodulating activity, systemic infection and Parkinson's disease. As an alternate source of medication, medicinal herbs are continuously showing better compatibility with the human body with minimal side effects than other therapies. Keeping this in mind, the present review mainly focusing on medicinal properties and health benefits of *Tinospora cordifolia* against various diseases.

Keywords: Giloy Plant, *Tinospora cordifolia*, Medicinal properties, Health benefits etc.

I. INTRODUCTION

Tinospora cordifolia (synonym: *Tinospora sinensis* (Lour.) Merr.) is also known as Guduchi/Amrita and its names in Latin: *Tinospora cordifolia* (Wild) Hook. f. & Thomson, English: *Tinospora* Gulancha/Indian *Tinospora*, Hindi: Giloya. It belongs to the family of Menispermaceae and is found in Myanmar, Sri Lanka, and China (Singh *et al.*, 2003). *Tinospora cordifolia* (Thunb.) Miers has long been a part of Ayurvedic medicine in India. This perennial, herbaceous vine belongs to the family Menispermaceae with many common names viz., Giloy, Guduchi, Gurucha, Amrita or heart-leaved moonseed.

The species is common throughout tropical and subtropical zones at an altitude of 600 m. It is found in India, Bangladesh, Sri Lanka, Myanmar, China, Thailand, Philippines, Indonesia, Malaysia, Borneo, Vietnam, North Africa, and South Africa. Giloy is a large climbing shrub with elongated twining branches spreading extensively. A special feature is the presence of wiry aerial roots arising from the branches. Stems are rather succulent, creamy white to grey, deeply cleft, papery bark and rosette-like pores (lenticels). Leaves are simple, alternate, cordate-ovate, and very thin with long leaf stalks bulged at the base and apex. Inflorescence, called racemes is both axillary and terminal; flowers tiny, greenish yellow, unisexual dioecious. Fruits are of three shortly stalked sub-globose drupes, scarlet coloured when ripe. The plant flowers during the summer and fruits during the winter. The plant is genetically diverse, containing different active components, including steroids, aliphatics, alkaloids, glycosides, and diterpenoid lactones. These active compounds are distributed over all parts of the plant, such as the root and stem. *Tinospora cordifolia* has tremendous therapeutic medicinal properties showing anti-diabetic, anti-inflammatory, anti-arthritic, antioxidant, hepatoprotective, cardioprotective, anti-allergic, anti-stress and many more (Bala M. *et al.*, 2015; Mishra *et al.*, 2013; Sharma P. *et al.*, 2019). The root of Giloya (*Tinospora cordifolia*) is used as potent emetic and for bowel obstruction. The starch of this plant serves a beneficial household remedy for chronic fever, relieves burning sensation, increases energy and appetite.

II. CHEMICAL CONSTITUENT

The chemical constituents of *Tinospora cordifolia* belong to different classes such as alkaloids, glycosides, steroids, phenolics, aliphatic compounds, poly-saccharides, leaves are rich in protein (11.2%), calcium and phosphorus (Chaudhari N. *et al.*, 2014). The stem contains clerodane furono diterpene glucoside (amritoside A, B, C, and D) and the structure has been established by different spectroscopic studies (Mayura R. *et al.* 2004; Abhijeet R. & Mokhat D., 2018; Sumran G. & Aggarwal A., 2019). Almost all the parts of the plant are used in ayurvedic formulation. Fresh plant is more efficacious than dried plant. The plant mainly contains alkaloids, glycosides, steroids, sesquiterpenoid, aliphatic compound, essential oils, mixture of fatty acids and polysaccharides. The alkaloids include berberine, bitter gilonin, non-glycoside gilonin and gilosterol. The main alkaloid and secondary metabolites of giloy are tinosporine, tinosporide, tinosporaside, cordifolide, cordifol,

heptacosanol and tinosporidine, which are effective in removing body toxins and improving immune system (Singh *et al.*, 2003). Phytochemical investigation of the methanol extract of *Tinospora cordifolia* aerial parts led to the isolation of four new and seven known compounds. The two new aporphine alkaloids, N-formylasimilobine 2-O-β-D-glucopyranosyl- (1→2)-β-D-glucopyranoside (tinoscorside A) and N-acetyl asimilobine 2-O-β-D-glucopyranosyl- (1→2)-β-D-glucopyranoside (tinoscorside B), a new clerodane diterpene, tinoscorside C, and a new phenylpropanoid, sinapyl 4-O-β-D-apiofuranosyl-(1→6)-O-β-D-glucopyranoside (tinoscorside D) (Upadhyay *et al.*, 2011). Besides its therapeutic properties, the plant also provides multiple essential minerals, such as iron, copper, manganese, calcium, zinc, and phosphorus. *Tinospora cordifolia* contains with high fibre (15.8%), protein (4.5% - 11.2%), carbohydrate (61.66%), and low fat (3.1%). *Tinospora cordifolia* nutritive value is 292.54 calories per 100 grams.

1) Pharmacological activities

Phytochemical Profile of Various Parts of *Tinospora cordifolia*

Leaves are rich in protein, calcium, and phosphorus (Singh *et al.*, 2003; Sinha *et al.*, 2004). Methanol extract of leaves is rich in flavanoids, alkaloids and glycosides (Soni H.P. *et al.*, 2011). A post harvest experiment has revealed that mechanical drying of the herb at 40°C provides the highest alkaloid (tinosporin) content (0.045%). However, the content decreases (0.033%) with drying at 60 °C or in direct sunlight. Further, the dried stem bits packed in polyethylene lined gunny bag retain the highest alkaloid content (0.042%) as compared to storage under ambient conditions (Padmapriya S. *et al.*, 2009).

Several studies published on *Tinospora cordifolia* revealed that it has numerous uses in Ayurvedic medicinal systems. *T. cordifolia* is renowned for its immunomodulatory properties. It is used to enhance the body's natural defense mechanisms and is often recommended to boost the immune system (Nair P. K. *et al.*, 2006). It has been traditionally used to manage various types of fever, including viral and bacterial infections (Gupta *et al.*, 2016). It is believed to help reduce fever symptoms and support the body's fight against pathogens. The plant is known for its antioxidant and anti-inflammatory effects. It is used to alleviate inflammation-related conditions such as arthritis and to counter oxidative stress in the body. *Tinospora cordifolia* is used to improve digestion, reduce acidity and promote overall digestive wellness. It also supports liver health and protect the liver from damage (Kaushik A. *et al.*, 2017). *Tinospora cordifolia* is used to manage diabetes too. It is believed to help regulate blood sugar levels and improve insulin sensitivity. The plant's anti-inflammatory and anti-microbial properties make it useful for managing skin conditions like eczema, psoriasis, and various skin infections. It also alleviates respiratory problems such as asthma, bronchitis, and coughs. It is thought to have bronchodilator and anti-asthmatic effects (Zalawadia R. *et al.*, 2009). In Ayurveda, *Tinospora cordifolia* is classified as an adaptogen, or Rasayana, which means it is believed to enhance vitality, reduce stress, and promote overall well-being. There is growing interest in its anticancer properties (Ahmad R. *et al.*, 2015). Research suggests that it may have cytotoxic effects on cancer cells and could be explored further for cancer therapy. Some traditional uses include *Tinospora cordifolia* for cognitive health and its neuroprotective effects (M. Mathew & S. Subramaniam, 2014). It may be used to enhance memory and protect the nervous system (A. Agarwal *et al.*, 2022). *Tinospora cordifolia* is often used as a general health tonic in traditional medicine. It is believed to promote longevity, improve vitality and enhance overall health.

2) Pharmacological activities of *Tinospora cordifolia*

Antioxidant activity

Antioxidant plays a major role in normal physiological functions by protecting against cell damage by ROS and reducing the adverse effects of free radicals. Total flavonol and phenolic phytochemicals isolated from the

formulation of the *Tinospora cordifolia* plant showed potent antioxidant activity measured by using 1-diphenyl-2-picrylhydrazyl (DPPH) (Mehra R. *et al.*, 2013). *Tinospora cordifolia* has been reported to increase GSH levels and gamma-glutamylcysteine ligase gene expression.

It also exhibited strong free radical-scavenging properties (Rawal A. *et al.*, 2004). This happened because it improved the enzymatic system by controlling ROS production and normalizing the oxidative load (Rawal A. *et al.*, 2004; Gupta A. *et al.*, 2024).

Antimicrobial activity

Antimicrobial activity of the *Tinospora cordifolia* with different solvents on different micro-organism, showed good antifungal and antibacterial activity (Duraipandiyan V. *et al.*, 2012). Jeyachandran *et al.*, reported the antimicrobial activity of stem extracts by *in-vitro* analysis against both gram-positive and gram-negative bacteria and showed good therapeutic activity on the infectious disease. It has taken a methanolic extract of *Tinospora cordifolia* against both bacteria group (Jeyachandran R. *et al.*, 2003). Narayanan *et al.*, have reported antibacterial activity of *plants* to extract against *Escherichia coli*, *Proteus vulgaris*, *Salmonella typhi*, *Salmonella paratyphi*, *Salmonella typhimurium*, *Klebsiella pneumoniae* *Pseudomonas aeruginosa*, *Enterobacter aerogene*, *Shigella flexneri*, *Staphylococcus aureus* and *Serratia marcescens* (Gram-positive bacteria) (Narayanan A. *et al.*, 2011). The aqueous, ethanol and acetone extract of *T. cordifolia* inhibited the activity on clinical isolates of urinary pathogens *Klebsiella pneumoniae* and *Pseudomonas aeruginosa* (Shanthi V. *et al.*, 2013). Singh *et al.*, has reported silver nanoparticles from the stem of *T. cordifolia*, which possess antibacterial activity against the different strains of bacterias (Singh *et al.*, 2014). Allemailem *et al.*, have reported the antifungal activity of *T. cordifolia*, which was determined using the agar well plate diffusion method. The aqueous extract of *T. cordifolia* showed potent activity against *A. fumigatus*, *Aspergillus flavus*, and *Aspergillus nigar* (fungus) in the study (Allemailem *et al.*, 2019). Prasad *et al.*, studied the anti-oxidant and antimicrobial properties phenolic extract of *T. cordifolia* stem and root. Total reducing power, hydrogen peroxide scavenging activity assay, and hydroxyl radical scavenging activity were checked using different *in-vitro* assays. The ethanolic extract showed maximum 87.2% and 91.0% free radical scavenging activity concerning H₂O₂ scavenging and hydroxyl free radical scavenging assay (Prasad B. *et al.*, 2019).

Anti-toxic effects

Gupta *et al.*, reported the extract to scavenge free radicals generated during aflatoxicosis. It showed protective effects of *T. cordifolia* on thiobarbituric acid reactive substances (TBARS) levels and increase the level of GSH, ascorbic acid, protein, and the activities of anti-oxidant enzymes *viz.*, Superoxide Dismutase (SOD), Catalase (CAT), GPx enzyme, Glutathione S-transferase (GST) and glutathione reductase (GR) in kidney. The alkaloids such as choline, tinosporin, isocolumbin, palmatine, tetrahydropalmatine, and magnoflorine present in the plant of *T. cordifolia* showed protection against aflatoxin-induced nephrotoxicity (Gupta *et al.*, 2011). Sharma *et al.*, studied the stem and leaves extract of the plant has shown hepatoprotective effect in Swiss albino male mice against lead nitrate induced toxicity (Sharma *et al.*, 2010).

Antidiabetic activity

One of the world's major health issues, diabetes mellitus is increasing in prevalence and mortality. The health consequences of inadequate blood sugar regulation are severe.

Despite their effectiveness, conventional antidiabetic medications come with undesirable side effects. On the other hand, medicinal plants may be able to substitute for other sources of antidiabetic drugs. In Ayurveda,

Giloy is referred to as "Madhunashini," which means "destroyer of sugar." The production of insulin is helped by this activity. Giloy slows down digestion due to its high fiber content (Prince *et al.*, 2003). From Guduchi, Prasant *et al.*, isolated alkaloids, cardiac glycosides, saponins, flavonoids, tannins, and steroids that contains anti-diabetic property. Alkaloids from this plants showed insulin-mediated actions due to insulin hormone (Patel *et al.*, 2016). Gestational diabetes can increase the GSH content and other reactive species that can act as a threat to the mother as well as the fetus. The study based upon the pregnant rat using *T. cordifolia* was incorporated in the daily diet to a diabetic-pregnant rat (streptozocin-induced diabetes), which showed a protective effect by reducing the oxidative load thereby preventing the relative incidence of diseases and any birth defect. In a diabetic rat model, *T. cordifolia* root extracts of Guduchi attenuated the brain mediated lipid level and down-regulated the blood glucose and urinary glucose level emphasizing its anti-diabetic and lipid-lowering activity (Shivnanjappa *et al.*, 2011). The root extract of Guduchi showed an antihyperglycemic effect in the alloxan-induced diabetic model by decreasing its excess glucose level in urine as well as in normal (Singh *et al.*, 2017). Certain herbal preparation, including Guduchi like Ilogen-Excel, Hyponidd, and Dihar have been tested in diabetic rat models, the anti-diabetic activity of *T. cordifolia* was observed. The effects by Ilogen Excel down the level of excess glucose in the blood and enhance the insulin efficiency by increasing its amount in the systemic circulation. Hyponidd is reported, and it maintained the oxidative load by decreasing reactive species and reduced the glucose-mediated hemoglobin count. when the tested of 'Dihar' for one and a half month in streptozotocin-induced diabetic model decreased the urea as well as creatinine amount in the blood with an increase in enzyme activities (Prince *et al.*, 2003; Patel *et al.*, 2009).

Anti-stress activity

Sarma *et al.*, reported ethanolic extract of *Tinospora cordifolia* at the dose of 100 mg/kg gives significant anti-stress activity in all parameters compared with standard drug diazepam (dose of 2.5 mg/kg) (Sarma *et al.* 1996). The plant extract gives a moderate degree of behavior disorders and mental deficit response. The clinical research showed the improved I. Q level of patients. In Ayurveda, it acts as Medhya Rasayana or brain tonic by increasing mind power like memory and recollection (Baghel P. 2017).

Hypolipidemic effect

Stanely *et al.*, studied the hypolipidemic effect of an aqueous extract of the root on the rats weighing 2.5 and 5.0 g/kg body weight on sixth weeks, that resulted in decrease tissue cholesterol, reduction in serum, phospholipids, and free fatty acid in alloxan diabetic rats. The dose of root extract 5.0 g/kg body weight showed the highest hypolipidaemic effect. When the level of serum lipids in diabetes increased, they represented coronary heart disease, lower the serum lipids level decreased the risk of vascular disease. The ability of *T. cordifolia* root extract to reduce the level of serum or tissue lipids in diabetics animals have never been studied before till then (Stanely M. 1999).

Anti-cancer activity

Ali *et al.*, studied the anticancer activity of *T. cordifolia* palmatine extract in animal models, alkaloid using response surface methodology (RSM). The extract indicates the anticancer potential in 7,12-dimethylbenz(a)anthracene DMBA induced skin cancer model in mice (Ali H. *et al.*, 2013). Rahul *et al.*, prepared the extract of 200, 400, 600 mg/kg dry weight in a dose depend upon manners. 50% methanolic extract of *cordifolia* to C57 BI mice for 30 days at a dose of 750 mg/kg body weight the tumor size reduced life span (Verma R. *et al.*, 2011). Mishra *et al.*, showed the anti-brain cancer potential, 50% ethanolic

extract of *T. cordifolia* (TCE) using C6 glioma cells significantly induced differentiation in C6 glioma cells, and reduced cell proliferation (Mishra R. *et. al.*, 2013).

III. ANTI-HIV POTENTIAL

Kalika *et al.*, showed that the root extract of *T. cordifolia* affects the immune system of HIV positive patient. The stem extract of *Tinospora cordifolia* reduces the ability of eosinophil count, stimulation of B lymphocytes, macrophages, level of hemoglobin, and polymorphonuclear leucocytes (Kalika M.V. *et. al.*, 2008).

Wound healing

Shanbhag T *et al.*, The present study was aimed at evaluating the wound healing profile of alcoholic extract of *T. cordifolia* and its effect on dexamethasone suppressed healing. Incision, excision, and dead space of the wound models were employed to investigate the wound healing potential of the plant increased tensile strength extract of *T. cordifolia* may be attributed to the promotion of collagen synthesis. The extract of *T. cordifolia* did not reverse dexamethasone suppressed wound healing (Shanbhag T. *et. al.*, 2019).

Parkinson's disease

Birla *et al.*, reported *T. cordifolia* extract is highly attractive against the Parkinsonism. They observed the anti-inflammatory activity of aqueous extract in 1-methyl-4-phenyl-1,2,3,6-tetra hydroxyridine (MPTP)-intoxicated Parkinsonian mouse model. The extract reversed the behavior of the target MPTP-intoxicated mice and it suggests that *T. cordifolia* protected dopaminergic neurons by suppressing neuroinflammation in MPTP-induced Parkinsonian mouse model (Birla H. *et. al.*, 2019). The plant exhibited multiple biological activities due to diverse chemical constituents present in it. The biologically active chemical molecules are present in different parts of the *Tinospora cordifolia*.

IV. CONCLUSION

The plant, *Tinospora cordifolia*, exhibited multiple biological activities due to diverse chemical constituents present in it. The biologically active chemical molecules are present in different parts of the *Tinospora cordifolia*. Giloy is not just a plant; it is considered one of the best medicines in Ayurveda, used to treat various fevers and other inflammatory conditions.

Tinospora cordifolia is good for the digestive system and helps to improve digestion.

It also helps to reduce burning sensation, pain, and excessive thirst because of its Tridosha balancing property. It also shows antifungal activity, antioxidant activity, antimicrobial activity, antibacterial activity, hypolipidaemic effect, hepatic disorder, anticancer, Anti HIV potential, Antiosteoporotic effects, Antitoxic effects, Wound healing, anticomplementary activity and Parkinson's disease. In this regard, further studies need to be carried out to explore *Tinospora cordifolia* for its potential in preventing and treating diseases.

V. REFERENCES

- [1]. Singh S.S., Pandey S.C., Srivastava S., Gupta V.S., Patro B., Ghosh A.C., Chemistry and medicinal properties of *Tinospora cordifolia* (Guduchi). Indian Journal of Pharmacology. 2003; 35:83-91.

- [2]. Bala M., Pratap K., Verma P.K., Singh B., Padwad Y., Validation of ethnomedicinal potential of *Tinospora cordifolia* for anticancer and immunomodulatory activities and quantification of bioactive molecules by HPTLC. *J. Ethnopharmacol.* 2015;175:131–137.
- [3]. Mishra A., Kumar S., Pandey A.K., Scientific validation of the medicinal efficacy of *Tinospora cordifolia*. *Sci. World J.* 2013.
- [4]. Sharma P., Dwivedee B.P., Bisht D., Dash A.K., Kumar D., The chemical constituents and diverse pharmacological importance of *Tinospora cordifolia*. *Heliyon.* 2019.
- [5]. Chaudhary N., Siddiqui M.B., Khatoon S., Pharmacognostical evaluation of *Tinospora cordifolia* (Willd) Meers and identification of biomarkers. *J. Res. Indian Med.* 2014; 13:543–550.
- [6]. Maurya R., Manhas L.R., Gupta P., Mishra P.K., Singh G., Yadav P.P., Amritosides A, B, C and D: clerodane furano diterpene glucosides from *Tinospora cordifolia*. *Phytochemistry.* 2004;5:2051–2055.
- [7]. Abhijeet R., Mokhat D., On vegetative propagation through stem cuttings in medicinally lucrative *Tinospora* species. *J. Pharmacogn. Phytochem.* 2018; 2:2313–2318.
- [8]. Sumran G., Aggarwal A., Prospect of Indian herbs as sources of antioxidants in combating oxidative stress. *Chem. Biol. Interface.* 2019;9:1–20.
- [9]. Singh S.S., Pandey S.C., Srivastava, S., Gupta V.S., Patro, B., 2003. Chemistry and medicinal properties of *Tinospora cordifolia*. *Indian J. Pharmacol.*, 35:83.
- [10]. Upadhyay P.R., Sharma V., Anita K.V., 2011. Assessment of the multifaceted immunomodulatory potential of the aqueous extract of *Tinospora cordifolia*. *Res J Chem Sci.*, 1:71-79.
- [11]. Singh S.S., Pandey S.C., Srivastava S., Gupta V.S., Patro B., Ghosh A.C. Chemistry and medicinal properties of *Tinospora cordifolia* (Guduchi). *Indian Journal of Pharmacology.* 2003; 35:83-91.
- [12]. Sinha K, Mishra NP, Singh J, Khanuja SS., *Tinospora cordifolia* (Guduchi), a reservoir plant for therapeutic applications: A review. *Indian Journal of Traditional Knowledge.* 2004; 3:257-70.
- [13]. Soni HP, Nayak G, Patel SS, Mishra K, Singh RP. Pharmacognostic studies of the leaves of *Tinospora cordifolia*. *IJPI's Journal of Pharmacognosy and Herbal Formulations.* 2011; 1:1-6.
- [14]. Padmapriya S, Kumanan K, Rajamani K. Optimization of post-harvest techniques for *Tinospora cordifolia*. *Academic Journal of Plant Sciences.* 2009; 2:128-31.
- [15]. P.K. Nair, S.J. Melnick, R. Ramachandran, E. Escalon, C. Ramachandran, Mechanism of macrophage activation by (1,4)- α -D-glucan isolated from *Tinospora cordifolia*, *Int. Immunopharm.* 6 (2006) 1815–1824.
- [16]. P.K. Gupta, P. Chakraborty, S. Kumar, P.K. Singh, M.G. Rajan, K.B. Sainis, S. Kulkarni, G1-4A, a polysaccharide from *Tinospora cordifolia* inhibits the survival of *Mycobacterium tuberculosis* by modulating host immune responses in TLR4 dependent manner, *PLoS One* 11 (2016) .
- [17]. Kaushik, A. Husain, H. Awasthi, D.P. Singh, R. Khan, D. Mani, Antioxidant and hepatoprotective potential of Swaras and Hima extracts of *Tinospora cordifolia* and *Boerhavia diffusa* in Swiss albino mice, *Phcog. Mag.* 13 (2017) S658–S662.
- [18]. R. Zalawadia, C. Gandhi, V. Patel, R. Balaraman, The protective effect of *Tinospora cordifolia* on various mast cell mediated allergic reactions, *Pharmaceut. Biol.* 47 (2009) 1096–1106.
- [19]. R. Ahmad, A.N. Srivastava, M.A. Khan, Evaluation of in-vitro anticancer activity of stem of *Tinospora cordifolia* against human breast cancer and Vero cell lines, *J. Med. Plants Studies.* 3 (2015) 33–37.
- [20]. M. Mathew, S. Subramanian, In-vitro screening for anti-cholinesterase and antioxidant activity of methanolic extracts of ayurvedic medicinal plants used for cognitive disorders, *PLoS One* 9 (2014).

- [21]. Agarwal, S. Malini, K.L. Bairy, M.S. Rao, Effect of *Tinospora cordifolia* on learning and memory in normal and memory deficit rats, *Indian J. Pharmacol.* 34 (2002) 339–349.
- [22]. Mehra R., Naved T., Arora M., Madan S. Standardization and evaluation of formulation parameters of *Tinospora cordifolia* tablet. *J. Adv. Pharm. Educ. Res.* 2013;3:440–449.
- [23]. Rawal A., Muddeshwar M., Biswas S. Effect of *Rubia cordifolia*, *Fagonia cretica* linn, and *Tinospora cordifolia* on free radical generation and lipid peroxidation during oxygen-glucose deprivation in rat hippocampal slices. *Biochem. Biophys. Res. Commun.* 2004;324:588–596.
- [24]. Jayaprakash R., Ramesh V., Sridhar M.P., Sasikala C. Antioxidant activity of ethanolic extract of *Tinospora cordifolia* on N-nitrosodiethylamine (diethyl nitrosamine) induced liver cancer in male wister albino rats. *J. Pharm. BioAllied Sci.* 2015;7:40–45.
- [25]. Gupta A., Gupta P., Gunjan B., *Tinospora cordifolia* (Giloy): An insight on the multifarious pharmacological paradigms of a most promising medicinal ayurvedic herb, *PMC Heliyon.* 2024 Feb 15;10(4):e26125.
- [26]. Singh N. Scientific output on *Azadirachta indica indica* (neem): A bibliometric study. *SRELS journal of information Management.* 2006;53(6):479–485.
- [27]. Singh SS, Pandey SC, Srivastava S, Gupta VS, Patro B. Chemistry and medicinal properties of *Tinospora cordifolia*. *Indian J Pharmacol.* 2003;35:83.
- [28]. Duraipandiyar V., Ignacimuthu S., Balakrishna K., Aaharbi N.A. Antimicrobial activity of *Tinospora cordifolia*: an ethnomedicinal plant. *Asean J. Trad. Knowldge.* 2012;7:59–65.
- [29]. Jeyachandran R., Xavier T.F., Anand S.P. Antibacterial activity of stem extracts of *Tinospora cordifolia* (willd) hook. *Anc. Sci. Life. Res.* 2003;25:40–43.
- [30]. Narayanan A.S., Raja S.S., Ponmurugan K., Kandekar S.C., Natarajaseenivasan K., Maripandi A., Mandeel Q.A. Antibacterial activity of selected medicinal plants against multiple antibiotic resistant uropathogens. *Benef. Microbes.* 2011;2:235–243. Shanthi V., Nelson R. Antibacterial activity of *Tinospora cordifolia* (Willd) Hook. F. Thoms on urinary tract pathogens. *Int. J. Curr. Microbiol. App. Sci.* 2013;2:190–194.
- [31]. Singh K., Panghal M., Kadyan S., Chaudhary U., Yadav J.P. Antibacterial activity of synthesized silver nanoparticles from *Tinospora cordifolia* against multi-drug resistant strains of *pseudomonas aeruginosa* isolated from burn patients. *J. Nanomed. Nanotechnol.* 2014;5:1–6.
- [32]. Allemailem K.S., Almatroudi A., Alsahli M.A., Khan A., Khan M.A. *Tinospora cordifolia* aqueous extract alleviates cyclophosphamide-induced immune suppression, toxicity and systemic candidiasis in immunosuppressed mice: in vivo study in comparison to antifungal drug fluconazole. *Curr. Pharmaceut. Biotechnol.* 2019;20:1–5.
- [33]. Prasad B., Chauhan A. Anti-Oxidant and antimicrobial studies of *Tinospora cordifolia* (Guduchi/Giloy) stems and roots under in-vitro condition. *Int. J. Adv. Microbiol. Health. Res.* 2019;3:1–10.
- [34]. Gupta R., Sharma V. A meliorative effects of *Tinospora cordifolia* root extract on histopathological and biochemical changes induced by aflatoxin-b in mice kidney. *Toxicol. Int.* 2011;18:94–98.
- [35]. Gupta R., Sharma V. A meliorative effects of *Tinospora cordifolia* root extract on histopathological and biochemical changes induced by aflatoxin-b in mice kidney. *Toxicol. Int.* 2011;18:94–98.
- [36]. Sharma V., Pandey D. Beneficial effects of *Tinospora cordifolia* on blood profiles in male mice exposed to lead. *Toxicol. Int.* 2010;17:8–11.
- [37]. Prince S.M., Menon V.P. Hypoglycaemic and hypolipidaemic action of alcohol extract of *Tinospora cordifolia* roots in chemical induced diabetes in rats. *Phytother Res.* 2003;17:410–413.

- [38]. Patel M.B., Mishra S. Hypoglycemic activity of alkaloidal fraction of *Tinospora cordifolia*. *Pharma Innovation*. 2016;5:104.
- [39]. Patel M.B., Mishra S.M. Magnoflorine from *Tinospora cordifolia* stem inhibits α -glucosidase and its antihyperglycemic in rats. *J. Funct. Foods*. 2012;4:79–86.
- [40]. Shivananjappa M.M., Muralidhara M. Abrogation of maternal and fetal oxidative stress in the streptozotocin-induced diabetic rat by dietary supplements of *Tinospora cordifolia*. *Phytomedicine*. 2011;18:1045–1052.
- [41]. Singh D., Chaudhuri P.K. Chemistry and pharmacology of *Tinospora cordifolia*. *Nat. Prod. Commun*. 2017;12:299–308.
- [42]. Patel S.S., Shah R.S., Goyal R.K. Antihyperglycemic, antihyperlipidemic, and antioxidant effects of Dihar, a polyherbal ayurvedic formulation in streptozotocin-induced diabetic rats. *Indian J. Exp. Biol*. 2009;47:564–570.
- [43]. Sarma D.N.K., Khosa R.L., Chaurasia J.P.N., Sahai M. Antistress activity of *Tinospora cordifolia* and *Centella asiatica* extracts. *Phytother Res*. 1996;10:181–184.
- [44]. Baghel P. Plant of versatile vroperties of *Tinospora cordifolia* (Guduchi) *IJAIR*. 2017;5:751–753.
- [45]. Stanely P.P.M., Menon V.P., Gunasekharam G. Hypolipidaemic action of *Tinospora cordifolia* roots in alloxan-induced diabetic rats. *J. Ethnopharmacol*. 1999;64:53–57.
- [46]. Ali H., Dixit S. Extraction optimization of *Tinospora cordifolia* and assessment of the anticancer activity of its alkaloid palmatine. *Sci. World J*. 2013;28:1–10.
- [47]. Verma R., Chaudhary H.S., Agrawal R.C. Evaluation of antcarcinogenic and antmutagenic effect of *Tinospora cordifolia* in experimental animals. *J. Chem. Pharm. Res*. 2011;3:877–881.
- [48]. Mishra R., Kaur G. Aqueous ethanolic extract of *Tinospora cordifolia* as a potential candidate for differentiation based therapy of glioblastomas. *PLoS One*. 2013.
- [49]. Kalikaer M.V., Thawani V.R., Varadpande U.K., Santakke S.D., Singh R.P., Khiyani R.K. Immunomodulatory effect of *Tinospora cordifolia* extracts in HIV positive patients. *Indian J. Pharmacol*. 2008;40:107–110.
- [50]. Shanbhag T., Shenoy S., Rao M.C. Wound healing profile of *Tinospora cordifolia*. *Indian Drugs*. 2005;42:217–221.
- [51]. Birla H., Rai S.N., Singh S.S., Zahra W., Rawat A., Tiwari N., Singh R.K., Pathak A., Singh S.P. *Tinospora cordifolia* suppresses neuroinflammation in Parkinsonian mouse model. *NeuroMolecular Med*. 2019;21:42–53.

Facile Synthesis and Characterization of NiO Nanoparticles by Ultrasound Assisted Sol-Gel Method

Dr. Sharada D. Shirole*¹, Dr. Yogesh S. Suryawanshi²

*¹Assistant Professor, S. S. M. M. Arts, Science and Commerce College, Pachora, Dist- Jalgaon, Maharashtra, India

²Assistant Teacher, D. D. S. P. Arts, Science and Commerce College, Erandol, Dist: Jalgaon, Maharashtra, India

ARTICLE INFO

Article History:

Published : 27 January 2025

Publication Issue :

Volume 12, Issue 10

January-February 2025

Page Number :

15-19

ABSTRACT

Nikel oxide (NiO) nanoparticles were synthesized by ultrasound assisted sol-gel precipitation method using nikel nitrate as a precursor and sodium hydroxide as a reducing and stabilizing agent. Synthesized NiO nanoparticles were studied by field emission scanning electron microscopy (FE-SEM), E.D.A.X., X-ray diffraction (XRD) and FTIR. The XRD pattern confirms the very good crystalline of the material and the average crystallite size was found to be about 18.2 nm. FE-SEM shows NiO nanoparticles found to be dispersed uniformly with an average diameter of ~35-55 nm. FT-IR shows absorption bonds at 470 and 522 cm^{-1} are associated to Ni-O vibration bond, and 619 cm^{-1} is assigned to Ni-O-H stretching bond. The presence of Ni and O peaks in the EDAX spectrum indicated the presence of NiO phase with other impurities such as C, N, and Fe.

Keywords- nikel nitrate, Sol-gel precipitation, Ultrasonication, nikel oxide nanoparticles, Morphology

I. INTRODUCTION

Nanotechnology is one of the most exciting and rapidly developing fields of science and engineering, combining expertise from chemistry, biotechnology and other industries in one field. NPs are widely used in a variety of industries, including food, cosmetics, farming, medicinal products, the diagnosis/recovery of cancer, and cancer treatments, among others [1]. In recent years, researchers from all over the world have been studying nanotechnology for its unique characteristics [2], [3], and nanomaterials are superior to bulk materials in terms of properties [4][5]. Nickel oxide is an antiferromagnetic transition metal oxide, which is a wide gap p-type semi-conductor [6]. It is an interesting material because of its chemical stability as well as optical, electrical and magnetic properties. Its nanoparticles are used in electrochromic devices [7], smart windows [8], optical fibers [9], gas sensors [10], solar thermal absorbers [11], batteries [12], transparent conducting layers

[13]. Numerous techniques, such as chemical precipitation [14, 15], magnetron sputtering [15], and sol-gel [16] have been used to fabricate NiO nanoparticles. Among different techniques for controlled synthesis, ultrasound assisted sol-gel technique was used to synthesize crystalline and impurity free NiO nanoparticles.

The present work, nano-nickel oxide was successfully prepared in an environmentally friendly manner by combining the nickel nitrate salt with the sodium hydroxide. Ultrasound assisted sol-gel synthesis is a system that is environmentally friendly, cheap, socially acceptable, safe and cost-effective. The nickel nitrate was utilized as a precursor, while the sodium hydroxide was utilized as a reducing agent.

II. EXPERIMENTAL

2.1 Materials

The chemicals required for the synthesis of NiO nanoparticles were of analytic grade such as nickel nitrate and sodium hydroxide were procured from Merck, India.

2.2 Synthesis of NiO nanoparticles

0.5 M Sodium hydroxide was added drop wise under controlled ultrasound in 0.1 M nickel nitrate solution. This process of ultrasound assisted sol-gel precipitation technique was carried out at 60 °C. Even though the addition was completed, the mixture was sonicated for next one hour at 5 seconds on/off pulse and at intensity of 20 KHz to achieve homogeneous dispersion. During the reaction, mixture of copper nitrate and sodium hydroxide shows formation of bluish greenish colour indicates the formation of NiO nanoparticles. The precipitate was filtered through nylon mesh followed by washing to remove the impurities from the surface. The obtained precipitate was dried and crushed into powder form. This powder was calcinated at 450 °C in muffle furnace for 2 hours.

III.CHARACTERIZATION OF NANOPARTICLES

3.1. Fourier transform infrared spectroscopy (FTIR)

FTIR spectra in the range of 400-4000 cm⁻¹ of as-synthesized nanoparticles, were recorded (Shimadzu FTIR-8400 spectrophotometer Tokyo, Japan).

3.2. X-ray diffraction (XRD)

X-ray study was conducted on Brukers D8 Advance X-ray diffractometer (Brukers, Germany) with CuK α 1 radiation ($\lambda=1.5404$ Å) within the 2 θ range of 20-80°. The crystallite size of the metal and metal oxide nanoparticles was calculated using Scherer's formula.

$$\tau = \frac{0.9\lambda}{\beta\cos\theta} \dots\dots\dots 3.1$$

where, τ is crystallite size, λ is wavelength, (β) is full width at half maxima (FWHM) (in radians) and θ is diffraction angle.

3.3. Field emission scanning electron microscopy (FE-SEM)

Field emission scanning electron microscope (Hitachi S-4800,Tokyo, Japan) was used to assess the surface morphology of nanoparticles. The samples were of gold coated and mounted on a specimen stub prior to

viewing under the microscope. Energy dispersive X-ray (EDAX) analysis of nanoparticles was also studied to know the elements present into the material.

IV. CONFIRMATION OF NiO NANOPARTICLES

4.1. FT-IR of NiO nanoparticles

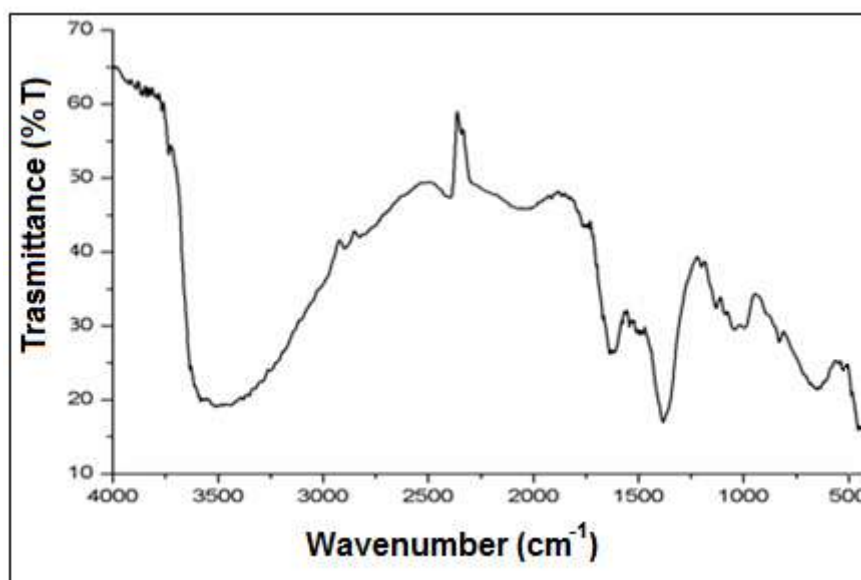


Figure 1 FT-IR spectra of NiO nanoparticles

Figure 1 shows the FT-IR spectra of NiO nanoparticles. The peak around 3480 cm^{-1} on the FT-IR spectrum is related to O-H bond. The absorption at 1630 cm^{-1} attributed to hydroxyl groups. The absorption bands at 1410 and 1115 cm^{-1} indicates the existence of carbonates. The absorption bands at 470 and 522 cm^{-1} are associated to Ni-O vibration bond, but absorption band at 619 cm^{-1} is assigned to Ni-O-H stretching bond [10]. The above information confirmed formation of pure NiO nanoparticles.

4.2. XRD of NiO nanoparticles

Figure 2 shows the XRD spectra of NiO nanoparticles. The XRD spectrum consists of four dominant diffraction peaks centered at 37.1 , 43.2 , 62.8 and 75.2° . All of the peaks are consisted of NiO phase, indicating the existence of NiO particles. The four peaks are corresponding to 111, 200, 220 and 311 crystal planes indicate the formation of cubic nickel oxide. In addition, the XRD spectrum shows clearly, the formation of a dominant phase, face centered cubic (FCC) nickel oxide [11]

The high peak intensity indicates that the NiO nanoparticles are of high crystallinity. No peaks from other phases are detected, indicating that the product is of high purity. The average crystallite size calculated using the Scherrer equation based on the half-width of the (111) peak is about 18.2 nm .

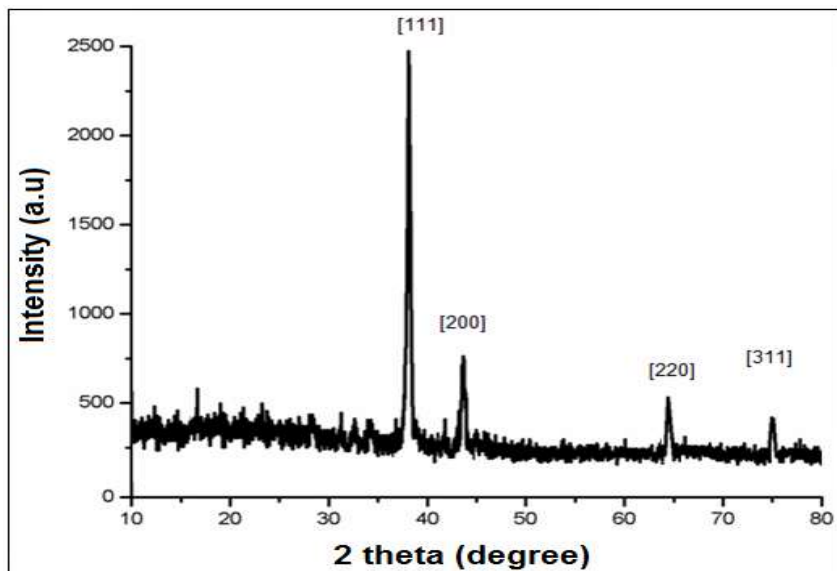


Figure 2 XRD of nNiO nanoparticles

4.3. FE-SEM and EDAX spectra of NiO nanoparticles

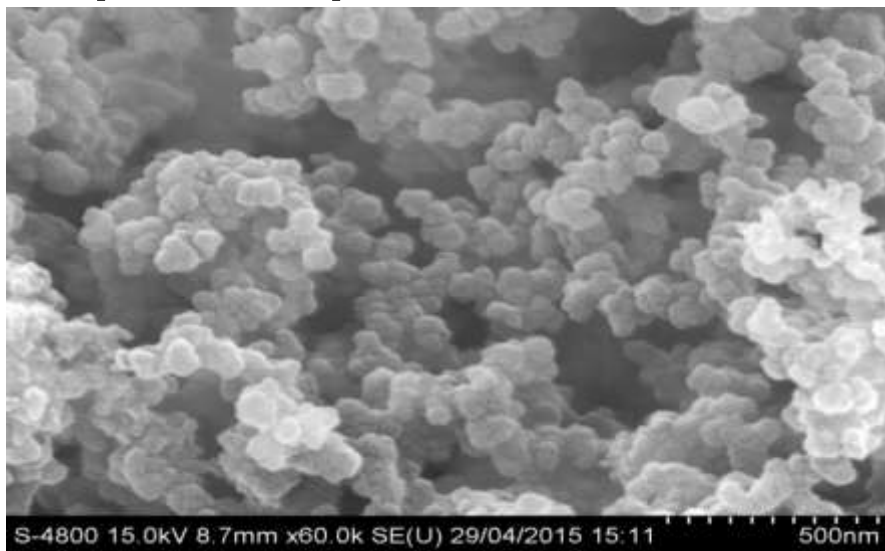


Figure 3(a) FE-SEM of NiO nanoparticles

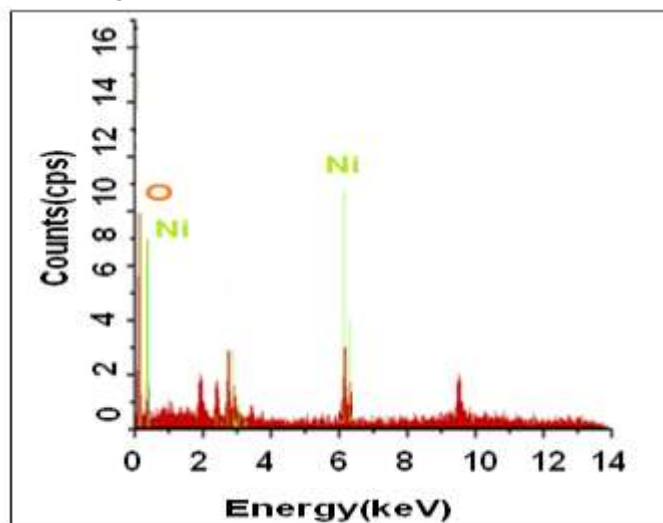


Figure 3(b) EDAX of NiO nanoparticles

Figure 3(a) represents the FE-SEM image of NiO nanoparticles. It was observed that NiO nanoparticles found to be dispersed uniformly with an average diameter of ~35-55 nm. This uniformity in size distribution was due to effective ultrasound, which allows the solution to get dispersed uniformly with formation, growth and collapsing of bubbles. During ultrasonic process the de-aggregated structure was observed due to formation of stable latex even though encapsulating agent was absent. FE-SEM images also shows that NiO nanoparticles are of spherical in shape having minimal aggregation. The results of FE-SEM are in line with XRD.

Figure 3(b) shows elemental spectra of the NiO nanoparticles and found that elemental signals of nickel and oxide ions are present with other impurities such as C, N, and Fe.

V. CONCLUSION

Nanocrystalline nickel oxide nanoparticles were synthesized by inexpensive ultrasound assisted sol-gel method. the XRD spectrum shows clearly, the formation of a dominant phase, face centered cubic (FCC) nickel oxide. So the ultrasound assisted sol gel synthesis of NiO nanoparticles is safe, cost effective and easy way of synthesis of nanoparticles.

VI. REFERENCES

- [1]. Navinchandra G. Shimpil, Mujahid Khan, Sharda Shirole And Shriram Sonawane Materials Science Journal, 2018, 12, 29-39
- [2]. Navinchandra G. Shimpi, Sharada Shirole And Satyendra Mishra Micro And Nanosystems, Volume 7, Issue 1, Feb 2015, P. 49 – 54
- [3]. N. G Shimpi, S Mishra, SD Shirole - J Nanosci Nanoeng Appl, 2016
- [4]. Navinchandra Shimpi, Sharada Shirole, Satyendra Mishra <https://doi.org/10.1002/Pc.23692> 2015
- [5]. Navinchandra G. Shimpi, Sharada Shirole, Yogesh Suryawanshi And Satyendra Mishra Advances In Polymer Technology Vol -36, No. 2 21594-21599 2015
- [6]. Kamal H., Elmaghraby K.E., Ali A.S., Abdelhady K., J. Cryst. Growth, 262 (2004), 424.
- [7]. He J., Lindstrom H., Hagfeldt A., Lindquist E.S., J. Phys. Chem. B, 103 (1999), 8940.
- [8]. Yoshimura K., Miki T., Tanemura S., Jpn. J. Appl.Phys., 34 (1995), 2440.
- [9]. Liu K., Anderson M., J. Electrochem. Soc., 143 (1966), 124.
- [10]. Hotovy I., Rehacek V., Siciliano P., Capone S., Spiess L., Thin Solid Films, 418 (2002), 9.
- [11]. Cook G.J., Koffyberg P.F., Sol. Energ. Mater., 10 (1984), 55.
- [12]. Makkus C.R., Hemmes K., Wit D.W.H.J., J. Electrochem. Soc., 141 (1994), 3429.
- [13]. Chan M.I., Hsu Y.T., Hong C.F., Appl. Phys. Lett., 81 (2002), 1899.
- [14]. Derakhshi M., Jamali T., Elyasi M., Bijad M., Sadeghi R., Kamali A., Niazazari K., Shahmiri R.M., Bhari A., Mokhtari S., Int. J. Electrochem. Sc., 8 (2013), 8252.
- [15]. Khansari A., Enhessari M., Niasari S.M., J.Clust. Sci., 24 (2013), 289
- [16]. Alagiri M., Ponnusamy S., Muthamizhchelvan C., J. Mater. Sci. Mater. El., 23 (2012), 728.



Mesoporous Al-SBA-15 Zeolite: An Efficient and Reusable Heterogeneous Catalyst for Green Synthesis of Pyrimido [4, 5-d] Pyrimidine Derivatives

Ganesh T. Pawar^{*1}, Rameshwar R. Magar², Bhagwat B. Nagolkar³, Machhindra K. Lande³

¹Department of Chemistry, School of Basic and Applied Sciences, MGM University Aurangabad-431003, Maharashtra, India

²Department of Chemistry, Sant Dnyaneshwar Mahavidyalaya, Soegaon, Aurangabad-431120, Maharashtra, India

³Department of Chemistry, Dr. Babasaheb Ambedkar Marathwada University, Aurangabad-431004, Maharashtra, India

ARTICLE INFO

Article History:

Published : 27 January 2025

Publication Issue :

Volume 12, Issue 10

January-February 2025

Page Number :

20-30

ABSTRACT

Mesoporous Al-SBA-15 zeolite catalyst was prepared by sole-gel method and studied by powder X-Ray diffraction, SEM-EDS, FT-IR spectroscopic techniques and BET surface area analysis. The catalytic activity of prepared Al-SBA-15 zeolite was tested for one pot synthesis of Pyrimido [4, 5-d] Pyrimidine derivatives, via Biginelli type multicomponent cyclocondensation reaction between substituted benzaldehyde, barbituric acid and urea/thiourea. Al-SBA-15 zeolite show excellent catalytic activity and reusability and offer excellent yield of Pyrimido [4, 5-d] Pyrimidine derivatives under mild reaction condition.

Keywords: Mesoporous Al-SBA-15, Biginelli reaction, Pyrimido-pyrimidine.

I. INTRODUCTION

Nowadays, development of sustainable and green catalytic methods for synthesis heterocyclic molecules by one pot synthesis has gained an importance in organic synthesis because of their advantages such as, minimum steps, short reaction time, high yield of desired product, and fewer byproducts as compared to classical multistep synthetic organic synthesis [1]. The Biginelli reaction is well known multicomponent reaction that yields various bioactive scaffolds such as dihydropyrimidine, tetrahydropyrimidines and pyrimidopyrimidine derivatives via one pot condensation reaction between benzaldehyde, active methylene compounds and urea/thiourea in acidic medium using strong acid as catalyst [2]. Nitrogen containing heterocyclic compounds such as 1,4, dihydropyridine, acridine and pyrimidines are the building blocks of natural alkaloids which possess

biological and pharmaceutical activities such as cytotoxic[3], anticancer [4], antibacterial [5], antifungal [6] and antiallergic [7, 8].

In view of pharmacological importance of pyrimidine derivatives various synthetic methods were developed catalysts like $\text{Fe}_3\text{O}_4@\text{NCs}/\text{Cu}(\text{II})$ [8] $\text{Zn}(\text{BDC})$ MOF [9], 7-aminonaphthalene-1,3-disulphonic acid functionalized $\text{Fe}_2\text{O}_3@\text{SiO}_2$ [10], PEG- SO_3H [11], sulphonic acid functionalized SBA-15 [12], p-TSA [13], Al_2O_3 [14], $\text{Bi}(\text{OTf})_3$ [15], $\text{Fe}_3\text{O}_4@\text{TiO}_2$ immobilized Ionic Liquids [16] However, some of the methods are suffered from some problems such as acid fictionalization of catalyst and solvents, high temperature, maximum reaction time, low yield of desired product, some methods requires irradiation of microwave/sonication. Therefore, there is still need of efficient method for synthesis of pyrimidine derivatives. Which is sustainable efficient and green method with heterogeneous reusable catalyst for synthesis of Pyrimido [4, 5-d] Pyrimidine derivatives.

Heterogeneous solid acids catalysts such metal oxides, supported clays, mesoporous zeolites are playing an important role in development of green organic synthesis. Mesoporous zeolites possess suitable pore size and provide high surface area for organic molecules and provide microreactor type environment during reaction. During past decades, many efforts have been made to synthesize the mesoporous ordered silica such as SBA-15, MCM-41, MCM-22 due to their tuneable properties and applications in the field of advanced drug delivery, fluid catalytic cracking and ketalization reaction [17] and supports for active transition oxide nanoparticles which shows superior catalytic activity and reusability in organic reactions [18-21]. Furthermore Co-Fe-SBA-15 is utilized for degradation of rhodamine dye in water, recently Zn-SBA-15 is reported as effective sorbent for removal of hydrogen sulphide (H_2S) gas [22, 23].

Structurally, SBA-15 is two dimensional ordered hexagonal siliceous materials with mesopores and possess better hydrothermal stability as compared to MCM-41-zeolites. However, such material shows weak Lewis acidity. Several reports were available for tailoring acidity of SBA-15 by isomorphous substitution of trivalent metal ion in SBA-15, which generates strong Lewis acidity in his framework [24]. Trivalent Al^{+3} cation can be incorporated in framework of SBA-15 either by co-precipitation (direct) method or post synthetic grafting to improve the acidity of SBA-15.

To address these problems in conventional synthesis of heterocyclic molecules our research group is working on development of heterogeneous solid acid catalyst their physicochemical study and utilization as design and development of green protocol for synthesis of heterocyclic organic compounds [25-27]. In present work, we have prepared Al-SBA-15 zeolite catalyst by sol-gel hydrothermal method and studied by powder-X ray diffraction, SEM-EDAX, FT-IR spectroscopic techniques and BET surface area analysis for characterization. The prepared Al-SBA-15 zeolite was utilized as heterogeneous solid acid catalyst for one pot synthesis of Pyrimido [4, 5-d] Pyrimidine derivatives, via Biginelli type multicomponent condensation of substituted benzaldehyde, malononitrile, and barbituric/thiobarbituric acid. The present method is green and efficient as compared to the reported one and offers several advantages such as reusability of Al-SBA-15 zeolite catalyst, minimum reaction time, easy separation of catalyst, mild reaction condition simple work-up procedure, excellent yield of desired product Pyrimido [4, 5-d] Pyrimidine derivatives.

II. EXPERIMENTAL

2.1. Chemicals and instruments

The chemicals were synthetic grade and procured from Merck, Loba-chem and S-d fine chemicals and used as such. Melting points were taken in an open capillary in melting point apparatus and are uncorrected. FT-IR spectrum was recorded on Bruker FT-IR Spectrometer, TLC was performed on Merck pre-coated silica

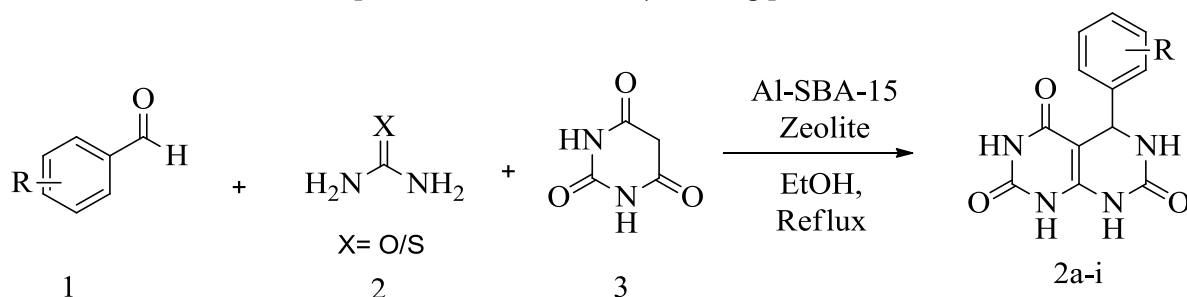
plates. $^1\text{H-NMR}$ and $^{13}\text{C-NMR}$ spectra were recorded on Bruker Avance 500 MHz FT-NMR spectrometer in CDCl_3 as solvent and chemical shifts values are recorded in δ (ppm) relative to tetramethyl silane (Me_4Si) as an internal standard. LCMS was recorded on Quadrupole-ToF MS equipped with ESI APcI source mass spectrometer. The X-ray diffraction patterns were recorded on Bruker 8-D advance X-ray diffractometer using monochromatic $\text{Cu-K}\alpha$ radiation ($\lambda=1.5405\text{\AA}$). SEM with EDS was performed on JSM - 6390LV6330 LA operated at 30.0 kV. The Surface area, pore volume, pore diameter was calculated by using Brunauer-Emmer-Teller N_2 adsorption desorption method on Quantachrome CHEMBET 3000 instrument.

2.2. Synthesis of Al-SBA-15 Zeolite catalyst.

Sol-gel hydrothermal method was adopted with direct addition of Aluminium source during hydrolysis of silica source to form gel. The typical procedure consists of slow and dropwise addition of tetraethylorthosilicate (20.8 g 100 mmol) in the stirred solution of 4 % aqueous solution of tetrapropylammonium bromide as a surfactant this will set hydrolysis reaction and form silica sole. Aluminium nitrate $\text{Al}(\text{NO}_3)_3 \cdot 3 \text{H}_2\text{O}$. 1.2498 g, (3.33 mmol) was dissolved in 50 ml of deionised water and added dropwise in silica sole solution with constant stirring. The viscous gel is formed after hydrolysis. The pH of the gel was maintained to about 12 by adding 0.1 M aqueous solution of NaOH. A white precipitate was formed which was vigorously stirred for 2 h at 30 °C temperature. The homogeneous gel was formed which was transferred in Teflon lined stainless steel autoclave for hydrothermal crystallization under autogenous pressure at 150 °C temperature for 12 h. After hydrothermal treatment solid product is obtained which was filtered, dried in an oven at 100 °C for 5 hours and calcined in muffle furnace at 550 °C for 5 hours under air atmosphere. The resulting porous material was pulverized to obtain fine powder of Al-SBA-15 Zeolite.

2.3. Typical reaction procedure for the synthesis of Pyrimido[4,5-d]Pyrimidine derivatives.

In typical reaction procedure, mixture of aromatic aldehyde (1 mmol), urea/thiourea (1 mmol) and barbituric acid (1 mmol), and catalytic amount of Al-SBA-15 Zeolite (0.1g) was refluxed in ethanol (20 ml) at temperature 80 °C for the time shown in (Table. 2). The progress of the reaction was monitored by TLC (petroleum ether: ethyl acetate=7:3 as eluent). After completion of the reaction, as indicated by TLC the reaction mixture was filtered to recover the Al-SBA-15 Zeolite catalyst and the filtrate was poured on crushed ice. The crude solid product was obtained which was filtered, dried and recrystallized from ethanol to afford pure product (Table 2 entry 2a-2i). All the derivatives are reported and confirmed by melting point.



Scheme-1. Synthesis of synthesis of Pyrimido[4,5-d]Pyrimidine derivatives catalysed by Al-SBA-15 Zeolite

2.4. Spectroscopic data of representative pyrimido [4, 5-d] pyrimidine derivative.

5-(4-methoxyphenyl)-5,6-dihydropyrimido[4,5-d]pyrimidine-2,4,7(1H,3H,8H)-trione (2b)

Yellow Solid: FT-IR(cm^{-1}): 3268, 3190(-NH), 1667(-CONH), 1613, 1541(-NH). $^1\text{H NMR}$ (400 MHz, DMSO-d_6): δ (ppm) 10.00(s, 1H, NH), 6.67 (d, $J = 8.7$ Hz, 2H), 7.14 (d, $J = 8.7$ Hz, 2H), 5.85 (s, 3H, NH), 5.41 (s, 1H, CH),

3.67 (s, 3H, OCH₃). ¹³C NMR (400 MHz, DMSO-d₆): 54.85, 91.19, 112.79, 127.54, 136.5, 150.66, 156.47, 159.59.
LC-MS: m/z (%): 291 (M⁺)

III.RESULT AND DISCUSSION

3.1. Powder X-ray diffraction analysis of Al-SBA-15 Zeolite:

X-ray diffraction patterns of uncalcined and calcined Al-SBA-15 Zeolite are given in Figure 1. Which shows high intense peaks at $2\theta = 6.834, 7.180, 21.052, 29.324, 43.402, 45.171$ with corresponding planes (100), (100), (111), (400) (600), (430) respectively, the plane (100) indicate the presence of ordered hexagonal structure of Al-SBA-15 type material. A broad peak between 20-25° is due to presence of amorphous mesoporous silica.²⁸ The reflection plane (400) is due to the formation of nanocrystalline Al₂O₃ [29]

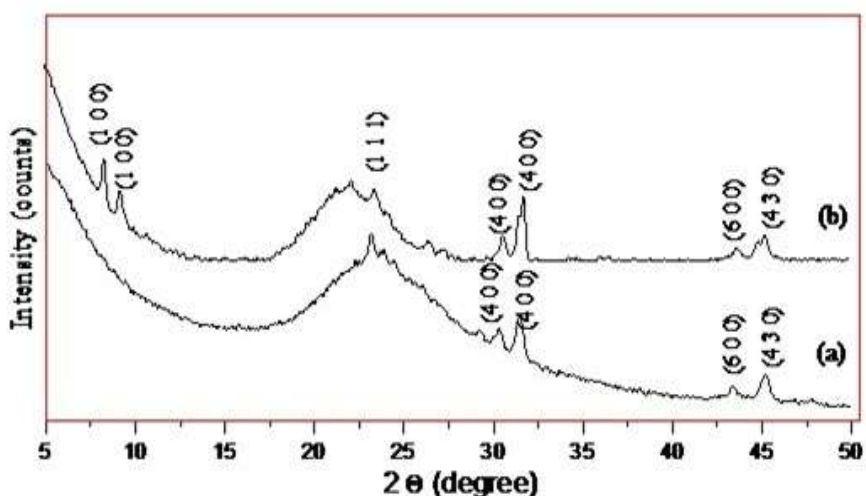


Figure-1 Powder XRD pattern of (a) Uncalcined Al-SBA-15 Zeolite (b) Calcined Al-SBA-15 Zeolite.

3.2. Scanning Electron Microscopy-Energy Dispersive Spectroscopy (SEM-EDS) analysis of Al-SBA-15 Zeolite:

In order to study the surface morphology and chemical composition of synthesized catalyst it was analyzed by SEM-EDS spectroscopy. The Fig.2 (a) shows sponge like morphology for uncalcined Al-SBA-15. This may be due to presence of surfactant inside the pores or channels of Al-SBA-15 framework. The same catalyst was calcined at 550°C and it shows nano rod shaped crystals with size 170.88 - 226.27 nm along with mesoporous silica (Fig.2 (b) the Al-SBA-15). These rod shaped crystals may be grows during calcinations process. The elemental composition of calcined Al-SBA-15 is shown in Fig 3 which confirms the presence of Si, Al, O and Na on the basis of atomic wt% 43.17, 3.82, 50.16 and 2.86 respectively.

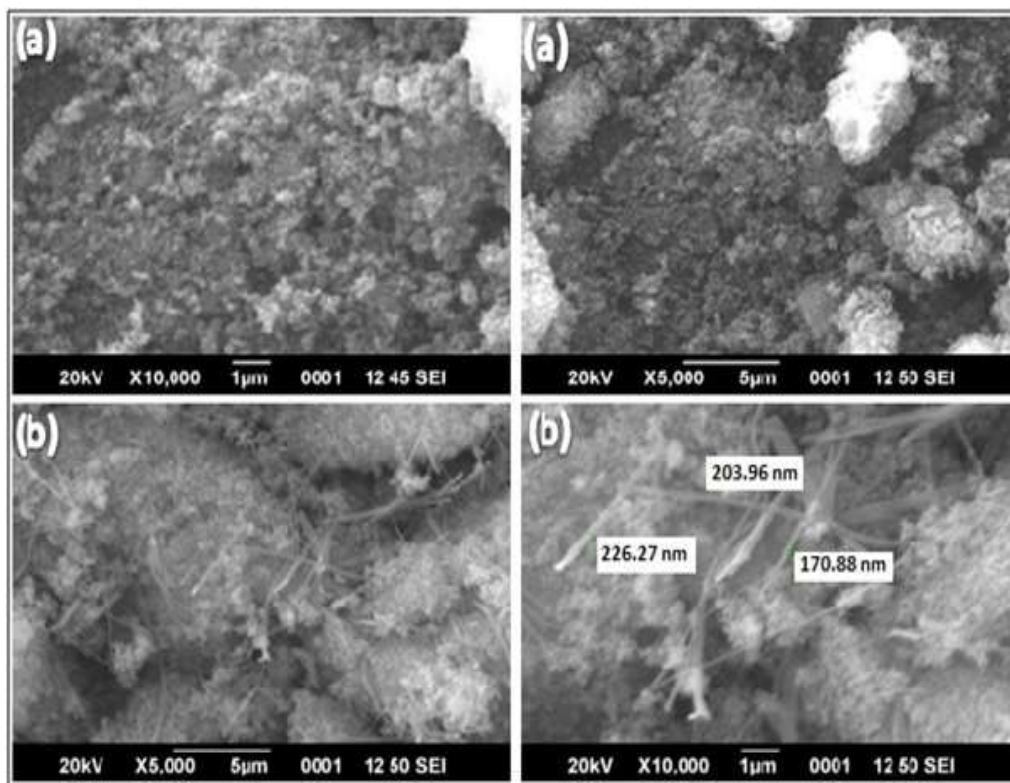


Figure-2. SEM image of (a) Uncalcined Al-SBA-15 Zeolite (b) Calcined Al-SBA-15 Zeolite.

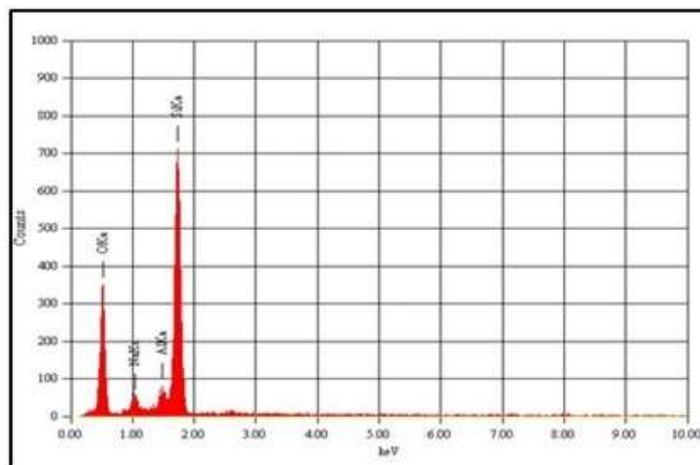


Figure-3 EDSS spectrum of Calcined Al-SBA-15 Zeolite.

3.3. Brunauer-Emmer-Teller (BET) surface area analysis of Al-SBA-15 Zeolite:

Surface area, average pore diameter and pore volumes were calculated by N₂ adsorption and desorption isotherm method. The BET surface area, average pore diameter and pore volume of calcined Al-SBA-15 was found to be 31.792 m²/g, 51.1753 Å and 0.04047 cm³/g which suggest mesoporous nature of Al-SBA-15.

3.4. Fourier Transform Infrared (FT-IR) spectroscopy analysis of Al-SBA-15 Zeolite:

Figure 4 (a-b) shows peak at 468, 471, 795, 802, 1099, 1103 cm⁻¹ due to the symmetric stretching of T-O-T unit which assigned for Si-O-Si or Al-O-Si bond form tetrahedron unit inside the framework. Stretching vibration of O-Si-O bond is observed in the range 1099-1103 cm⁻¹ in present work confirm formation of characteristic ordered Al-SBA-15 framework [30]. The peak at 1627-1631 cm⁻¹ is attributed to bending

vibration of adsorbed water molecule. The broad band appear between 3437-3442 cm^{-1} confirms presence of bridged and surface hydroxyl group which act as Bronsted acid site [31].

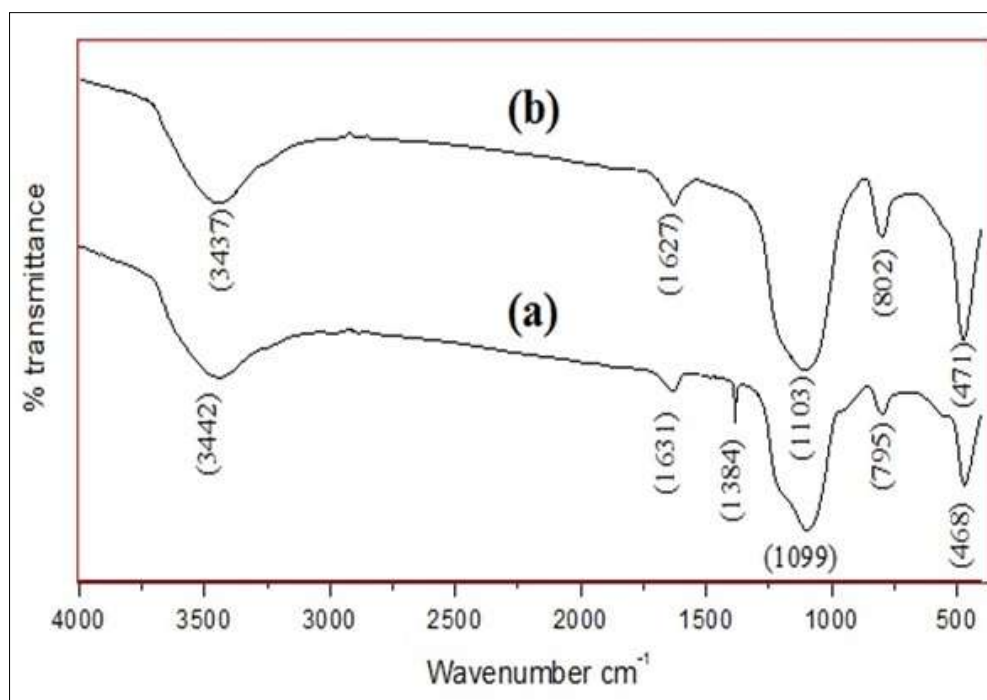


Figure-4 (a) FT-IR Spectrum of (a) Uncalcined Al-SBA-15 Zeolite (b) Calcined Al-SBA-15 Zeolite.

3.5. Optimization of reaction conditions for synthesis of Pyrimido [4,5-d] Pyrimidine derivatives:

To find the optimum loading of Al-SBA-15 Zeolite catalyst, and suitable solvent for one pot efficient synthesis of Pyrimido[4,5-d]Pyrimidine derivatives. The reaction between 4-OCH₃-benzaldehyde (1mmol), urea (1mmol) and barbituric acid (1mmol) was selected as model reaction. Initially model reaction was carried in ethanol without loading Al-SBA-15 Zeolite catalyst under reflux condition gives very less yield of desired product (2b) which indicate important role of catalyst. The same reaction when carried out with loading of Al-SBA-15 Zeolite as catalyst under same condition the yield of desired product increases significantly and reaction takes less time for completion (Table 1). It has been found that the 0.10 g of Al-SBA-15 Zeolite is suitable to catalyze reaction smoothly. The various solvents at reflux condition has been also checked with loading optimum amount of Al-SBA-15 Zeolite catalyst and results are summarized in (Table 1). It has been found that the reaction proceeds faster in polar protic solvent such as water and ethanol with maximum yield in minimum time as compare to less polar and aprotic solvent which gives lower yield (Table 1)

Table 1. Optimization of catalyst loading with different solvents for the synthesis of (2b).

Entry	Solvent	Amount of Al-SBA-15 Zeolite (g)	Time (min)	Yield(%) ^a
1	Solvent free	0.00	120	10
2	Ethanol	0.00	120	40
3	Ethanol	0.05	60	80
4	Ethanol	0.10	60	85
5	Ethanol	0.15	60	85
6	Ethanol	0.20	60	85

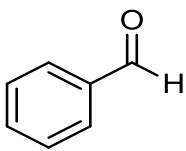
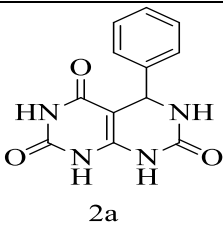
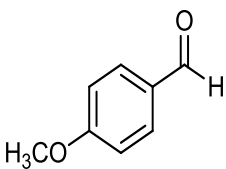
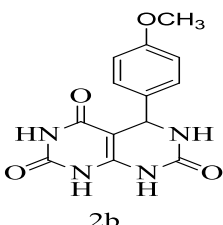
Entry	Solvent	Amount of Al-SBA-15 Zeolite (g)	Time (min)	Yield(%) ^a
7	Water	0.10	120	30
8	Methanol	0.10	120	25
9	Acetonitrile	0.10	120	23
10	1,4-dioxane	0.10	120	20
11	Tetrahydrofuran	0.10	120	20

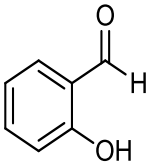
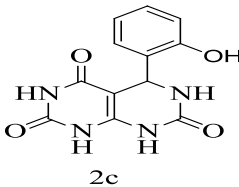
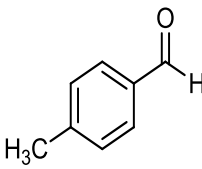
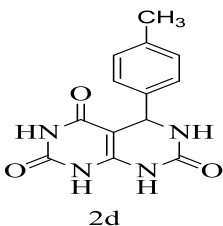
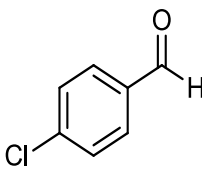
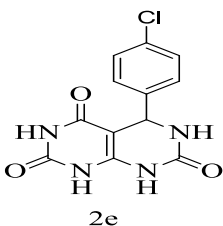
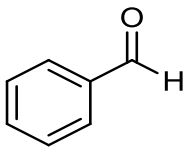
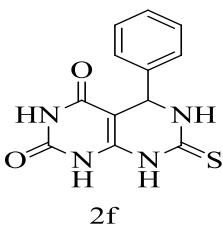
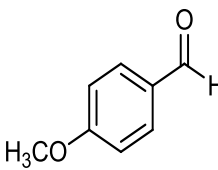
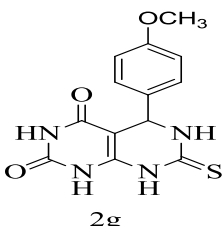
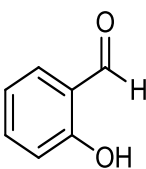
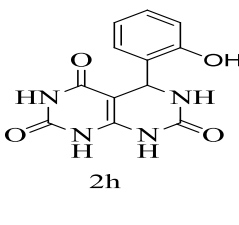
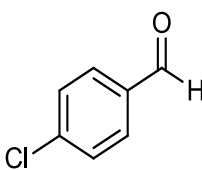
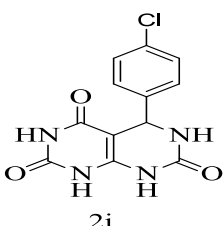
Reaction conditions 4-OCH₃-benzaldehyde (1mmol), urea (1mmol), and barbituric acid (1mmol), different solvents (20 ml) under reflux condition.

^aIsolated yields.

After optimizing loading of Al-SBA-15 Zeolite catalyst and finding suitable solvent for model reaction. The various derivatives of pyrimido[4,5-d]pyrimidine was prepared under optimum reaction condition with different aromatic aldehydes, urea/thiourea and barbituric acid which gives corresponding Pyrimido[4,5-d]Pyrimidinederivatives in stipulated time with in excellent yield (Table 2). After completion of reaction reusability of the Al-SBA-15 Zeolite catalyst was tested thrice on the model reaction (Table-2, entry-2) in which catalyst was separated and recovered from reaction mixture by dissolving the reaction mixture in hot ethanol followed by filtration. The recovered Al-SBA-15 Zeolite catalyst was washed 3-4 times with ethyl acetate and acetone then dried in a hot air oven at 150°C for 6 h before reuse. It was found that Al-SBA-15 Zeolite catalyst retain its catalytic activity and yields of desired product (2b) with excellent yield in successive catalytic cycle (Table-2, entry-2).

Table 2. Al-SBA-15 Zeolite catalyzed cyclocondensation of aromatic aldehyde, urea/thiourea and barbituric acid.

Entry	Aldehydes (R)	(X) O/S	Derivative	Time (min)	Yield (%) ^a	Melting point (°C) (Observed)	Melting point (°C) (Ref.) [14]
1		O	 2a	60	84	248-250	247-250
2		O	 2b	60	85 (82, 80, 79) ^c	285-287	285-287

3		O		60	86	218-220	218-220
4		O		60	87	248-250	248-250
5		O		60	82	294-295	294-295
6		S		60	85	294-295	294-295
7		s		60	87	>300	>300
8		S		60	86	218-220	218-220
9		S		60	82	280-282	280-282

Reaction conditions benzaldehyde (1mmol), urea/thiourea (1mmol), Barbituric acid (1mmol) and (0.10 g) calcined Al-SBA-15 catalyst in ethanol 20 ml. ^aIsolated yields. ^cYield after consecutive cycle.

To specify the advantages of newly developed method for one pot efficient and green synthesis of Pyrimido[4,5-d] Pyrimidine derivatives the results of present work is compared with different reported

methods in literature and summarized in (Table 3). It is been found from tabulated results that, Al-SBA-15 Zeolite catalyst promotes reaction more effectively than other reported methods.

Table 3. Catalytic performance of different catalysts for the synthesis of Pyrimido[4,5-d]Pyrimidine derivatives

Entry	Catalyst	Condition	Time (min)	Yield (%)	References
1	Zn-(BDC) MOF	Ultrasound irradiation, Solvent Free	05	98	[9]
2	PEG-SO ₃ H	H ₂ O, Reflux.	50	90	[11]
3	p-TSA	MeOH, Reflux.	180	80	[13]
4	Al ₂ O ₃	Microwave, 600 watt.	01	95	[14]
5	Bi(OTf) ₃	Reflux, Ethanol	360	86	[15]
6	Fe ₃ O ₄ @TiO ₂ Immobilized IL	80 °C, Reflux, Ethanol	40	97	[16]
7	Al-SBA-15 Zeolite	reflux in ethanol	60	85	Present work

IV. CONCLUSION

In summary, we have synthesized Al-SBA-15 mesoporous zeolite by hydrothermal method. The Powder X-ray diffraction analysis confirmed hexagonal phase of Zeolite framework. SEM images show nano roads ranging from 170.88 to 226.27 nm and prorousmorphology of Al-SBA-15 zeolite. The FT-IR analysis shows presence of bridge and surface hydroxyl group which is Bronsted acidic site framework. BET surface area analysis shows high surface area mesoprous nature of framework. The Al-SBA-15 Zeolite shows excellent catalytic activity and reusability for one post synthesis of Pyrimido [4,5-d]Pyrimidine derivatives via Biginelli type multicomponent condensation reaction between substituted benzaldehyde, barbituric acid and urea/thiourea. The present method offers significant advantages over the reported one such as high yield of desired product, complete separation of catalyst, mild reaction condition simple work-up procedure, and reusability of catalyst without significant loose in catalytic activity.

V. ACKNOWLEDGEMENT

The authors are grateful to the Head, Department of Chemistry, Dr. Babasaheb Ambedkar Marathwada University, Aurangabad-431004 (MS), India for providing the laboratory facility. The authors are also thankful to STIC Cochin and SAIF Chindigarh and CSMCRI Bhavnagar for providing characterization facilities.

VI. REFERENCES

- [1]. R. C. Cioc, E. Ruijter, V. A. Romano, Green Chem.16 (2014) 2958-2975. <https://doi.org/10.1039/C4GC00013G>
- [2]. P. Biginelli Gazz, Chim. Ital.23 (1893) 360-41.
- [3]. Feng Shi, Jie Ding, Shu Zhang, Wen-Juan Hao, Chuang Cheng, Shujiang Tu, Bioorg. Med. Chem. Lett. 21 (2021) 1554-1558.

- [4]. P. Sharma, N. Rane, V. K. Gurram, *Bioorg. Med. Chem. Lett.* 14 (2004) 4185-4190. <https://doi.org/10.1016/j.bmcl.2004.06.014>
- [5]. R. Santosh, P. Paul, M. K. Selvam, C. Raril, P. M. Krishna, J. G. Manjunatha, G. K. Nagaraja, *ChemistrySelect*, 4 (2019) 990-996. <https://doi.org/10.1002/slct.201803416>
- [6]. W. Wu, W. Lan, C. Wu, Q. Fei, *Front. Chem.* 9 (2021) 695628. <https://doi.org/10.3389/fchem.2021.695628>
- [7]. J. J. Wade, C. B. Toso, C. J. Matson, V. L. Stelzer, *J. Med. Chem.* 26, 4 (1983) 608-611. <https://doi.org/10.1021/jm00358a031>
- [8]. A. Kumar, K. K. Bhagat, A. K. Shing, H. Singh, T. Angre, A. Verma, H. Khaliullah, M. Jaremko, A. H. Emwase, P. Kumar, *RSC Adv.* 13, (2023) 6872-6908. <https://doi.org/10.1039/D3RA00056G>
- [9]. M. H. Abdollahi-Basir, F. Shirini, H. Tajik, M. A. Ghasemzadeh, *Polycycl. Aromat. Compd.* 41, 7 (2019) 1580-1589. <https://doi.org/10.1080/10406638.2019.1689404>
- [10]. R. G. Vaghei, N. Sarmast, *Appl. Organometal. Chem.* 32, 2 (2017) 8-9. <https://doi.org/10.1002/aoc.4003>
- [11]. S. Badvel, R. R. Gopireddy, T. B. Shaik, S. Hasti, V. R. Tummaluru, N. R. Chamarthi, *Chem. Heterocycl. Compd.* 51, 8, (2015) 749-753. <https://doi.org/10.1007/s10593-015-1769-3>
- [12]. G. M. Ziarani, N. H. Nasab, M. Rahimifard, A. A. Soorki, *J. Saudi Chem. Soci.* 19, 6 (2015) 676-681. <https://doi.org/10.1016/j.jscs.2014.06.007>
- [13]. M. R. Khodabakhshi, M. Kiamehr, F. M. Moghaddam, A. Villinger, P. Langer, *ChemistrySelect*, 3, 41 (2018) 11671-11676. <http://dx.doi.org/10.1002/slct.201801869>
- [14]. A. H. Kategaonkar, S. A. Sadaphal, K. F. Shelke, B. B. Shingate, M. S. Shingare, *Ukr. Bioorg. Acta.* 1 (2009) 3-7. https://www.bioorganica.org.ua/UBAdenovo/pubs_7_1_09/Shingare.pdf
- [15]. D. Saglam, Z. Turgut, *Int. J. Org. Chem.* 12 (2022) 11-27. <http://dx.doi.org/10.4236/ijoc.2022.121002>
- [16]. M. A. Ghasemzadeh, R. B. Dehkordi, *ChemistrySelect*, 5, 29, (2020) 9097-9104. <https://doi.org/10.1002/slct.202002085>
- [17]. (a) E. T. C. Vogt, B. M. Weckhuysen, *Chem. Soc. Rev.* 44, (2015) 7342-7370. <https://doi.org/10.1039/C5CS00376H> (b) K. N. Tayade, M. Mishra, K. Munsamy, R. S. Somani, *Catal. Sci. Technol.* 5 (2015) 2427-2440. <https://doi.org/10.1039/C4CY01396D>
- [18]. (a) M. A. Alibeik, Z. Ramazani, *J. Chem. Sci.* (2022) 134:77. <https://doi.org/10.1007/s12039-022-02066-w> (b) R. P. Kisomi, F. Shirini, M. Golshekan, *Appl. Organomet. Chem.* 35 (2021) e6212. <https://doi.org/10.1002/aoc.6212> (c) Y. Li, Y. Guan, R. A. Van Saten, P. J. Kooyman, I. Dugulan, C. Li, E. J. M. Hensen, *J. Phy. Chem. C.* 113 (2009) 21831-21839. <https://doi.org/10.1021/jp908059y>
- [19]. M. Ojeda, M. Balu, A. V. Brron, A. Pineda, A. G. Coletto, A. A. Romero, R. Luque, *J. Mater. Chem. A.* 42 (2011) 387-393. <https://doi.org/10.1039/C4GC01354A>
- [20]. G. M. Ziarani, S. Rohani, A. Ziarati, A. Badiei, *RSC Adv.* 8 (2018) 41048-41100. <https://doi.org/10.1039/C8RA09038F>
- [21]. H. Yu, C. Wu, S. Wang, T. Li, H. Yin, *ACS Appl. Nano Mater.* 2021, 4, 7, 7213-7220. <https://doi.org/10.1021/acsnm.1c01164>
- [22]. L. Hu, F. Yang, L. Zou, H. Yuan, X. Hu, *Chin. J. Cat.* 36, 10 (2015) 1785-1797. [https://doi.org/10.1016/S1872-2067\(15\)60939-1](https://doi.org/10.1016/S1872-2067(15)60939-1)
- [23]. M. Mureddu, I. Ferino, E. Rombi, M. G. Cutrufello, P. Deiana, A. Ardu, A. Musinu, G. Piccaluga, C. Canna, *Fuel*, 102 (2012) 691-700. <https://doi.org/10.1016/j.fuel.2012.05.013>
- [24]. B. Dragoi, E. Dumitriu, C. Guimon, *Miro. Meso. Mater.* 121 (2009) 7-17. <https://doi.org/10.1016/j.micromeso.2008.12.023>

- [25]. G. T. Pawar, R. R. Magar, M. K. Lande, *Polycycl. Aromat. Compd.* 38, 1 (2018) 75-84. <https://doi.org/10.1080/10406638.2016.1159584>
- [26]. R. R. Magar, G. T. Pawar, S. P. Gadekar, M. K. Lande, *Iran. J. Catal.* 7, 1 (2017) 1-9. <https://oiccpres.com/ijc/article/view/3945>
- [27]. V. N Rathod, G.T. Pawar, S. T. Gaikwad, M.K. Lande, *J. Chem. Technol. Biotechnol.* 97 (2022) 2005-2012. DOI 10.1002/jctb.7071
- [28]. Y. C. Hsu, Y. T. Hsu, H. Y. Hsu, C. M. Yang, *Chem. Mater.* 19, (2007) 1120-1126. <https://doi.org/10.1021/cm062167i>
- [29]. V. K. Das, R. R. Devi, P. K. Raul, A. J. Thakur, *Green. Chem.* 14 (2011) 847-854. <https://doi.org/10.1039/C2GC16020J>
- [30]. O. Aktas, S. Yasyerli, G. Dogu, I. Dogu, *Ind. Eng. Chem. Res.* 49 (2010) 6790-6802. <https://doi.org/10.1021/ie800192t>
- [31]. F. Jin, Y. Li, *Catl. Today*, 145 (2009) 101–107 <https://doi.org/10.1016/j.cattod.2008.06.007>

A Review on Biological Routes to Palladium Nanoparticle Synthesis: A Path toward Sustainable Nanomaterials

M. B. Suwarnkar¹, G. V. Shitre², S. N. Sinkar^{3*}

¹Department of Chemistry, Baburaoji Adaskar Mahavidyalaya, Kaij, Dist. Beed, Maharashtra, India

²Department of Chemistry, Vaishnavi Mahavidyalaya, Wadvani, Dist. Beed, Maharashtra, India

³Department of Chemistry, MSS'S Arts Science & Commerce College, Ambad, Dist. Jalna, Maharashtra, India

ARTICLE INFO

Article History:

Published : 27 January 2025

Publication Issue :

Volume 12, Issue 10

January-February 2025

Page Number :

31-36

ABSTRACT

Biogenic synthesis of palladium nanoparticles (PdNPs) has emerged as an eco-friendly and sustainable alternative to conventional chemical and physical synthesis methods. This green approach utilizes biological entities such as bacteria, fungi, algae, and plant extracts, which act as reducing and stabilizing agents through biomolecules like proteins, enzymes, and metabolites. Biogenic PdNPs exhibit unique physicochemical properties, including high catalytic activity, biocompatibility, and enhanced stability, making them promising for applications in catalysis, biomedicine, environmental remediation, and energy storage. This review provides a simple overview of the biological methods used for PdNP synthesis, their key properties, and potential applications. Additionally, challenges in large-scale production and future research directions are discussed to enhance the efficiency and applicability of biogenic PdNPs.

Keywords: Nanoparticles, Biomolecules, Catalysis.

I. INTRODUCTION

Nanobiotechnology is the technology that deals with the nanosized material within biogenic formations, which is more popular for the formation of nanoparticles for the protection of the environment from hazardous chemicals within emerging research [1,2]. Therefore, different nanomaterials have been formed such as carbons, metals, polymers, composites, chalcogenides, and are being investigated for much utilization [3]. Nanotechnology allows scientists to manipulate the characteristics of materials through manipulating molecular scale, which has led to a slew of new applications for nanostructures.

Palladium can manufacture different kinds of geometrical shapes due to its face-centered cubic metal structure, and for crystalline production, it achieves rapid reduction rates through manipulating thermodynamics, a shift in the amount of palladium seed aggregation caused by slower reduction changes the formation to a kinetically mediated phase [4]. The crystallinity of palladium seeds plays a major role in the controlling of structure and

form of the final product [5]. The investigations of nanoparticles, and in particular nanomaterials clusters in terms of physical and chemical properties as a function of size and structure [6]. Palladium nanoparticles made up from plants [7], fungi [8], bacteria [9]. Nanotechnology has revolutionized various scientific disciplines, with PdNPs playing a crucial role due to their exceptional catalytic, electronic, and antimicrobial properties. However, conventional PdNP synthesis methods pose environmental hazards and high costs. Palladium nanoparticles have different energetic applications such as catalytic degradation, cancer therapy, drug delivery, chemical, and biological sensors, bioimaging, methane combustion, hydrogen generation and storage, and lithium-ion batteries and are widely covered with the catalytic ability [10, 11]. The quest for eco-friendly alternatives has led to the exploration of biological routes, which leverage the reducing and stabilizing properties of biomolecules found in microbes, plants, and other biological entities. Nanoparticles may be used to increase chemical performance and play an essential role in nanocatalysis, but maybe extra importantly. The initial necessities of good electric and thermal conductivity for proper support resources are produced electrochemically and have great stability and surface area.

II. BIOLOGICAL SYNTHESIS OF PALLADIUM NANOPARTICLES

The biological synthesis of palladium nanoparticles (PdNPs) is an eco-friendly and sustainable alternative to conventional chemical and physical synthesis methods. This green approach utilizes microorganisms, plants, and biomolecules to reduce palladium ions (Pd^{2+}) into stable PdNPs under mild conditions, eliminating the need for toxic chemicals and high-energy inputs. The synthesis methods can be broadly classified into microbial, plant-mediated, and biomolecule-assisted synthesis.

2.1. Microbial Synthesis

Microorganisms such as bacteria, fungi, and algae possess biomolecules (e.g., proteins, enzymes, and polysaccharides) that can act as reducing and stabilizing agents for PdNPs. Bacteria, fungi, and algae possess metabolic pathways that facilitate Pd(II) reduction into PdNPs. Some notable microbial systems include:

- **Bacteria:** *Shewanella oneidensis*, *Escherichia coli*, and *Bacillus subtilis* have been reported to reduce Pd(II) into PdNPs through enzymatic processes involving hydrogenases and NADH-dependent mechanisms.
- **Fungi:** *Aspergillus niger* and *Fusarium oxysporum* mediate nanoparticle formation by secreting extracellular enzymes.
- **Algae:** Marine and freshwater algae produce PdNPs via intracellular bioaccumulation and extracellular reduction.

2.2. Plant-Mediated Synthesis

The biological fabrication of palladium nanoparticles during the aforementioned process required complex experimental techniques in the physical method, a large amount of reducing agents, and a medium in the chemical method. As a result, a simple approach for selecting artificial processing that uses environmentally beneficial resources must be developed. Furthermore, biological approaches offer a wider range of resources, such as reducing agents and better control over the size and form of the nanoparticles.

Palladium Nanoparticles are Phyto-Fabricate Using a Variety of Plants

In biological methods, synthesis of metallic nanoparticles in various shapes and sizes from diverse plant parts such as flower, leaves, roots, fruit, and bark [12]. The sizes and shapes of nanoparticles can be changed through

a broad variety of concentration of metal, and concentration of plant extracts in the reaction mixture [13]. In the biology method there are different plant parts used for the synthesis of palladium nanoparticles such as flower, leaves, stem, root, bark, etc.

2.2.1. Flower Extract Mediated Palladium Nanoparticles

A green synthesis of palladium nanoparticles from *Moringa oleifera* flower extract. The SPR peak of synthesized palladium nanoparticles was observed at 460 nm. Palladium nanoparticles are used in a variety of applications, including the reduction of 4-nitrophenol and methylene blue, as well as the Suzuki-coupling reactions in water. Plant extracts containing poly-phenols act as stabilizers of the smaller dimensions of the PdNPs examined by transmission electron microscopy [14].

A green synthesis of palladium nanoparticles from *Hibiscus sabdariffa* flower extract has been developed. When flower extract was added to the palladium ions medium, the color changed gradually from light brown to dark brown, which suggested the palladium nanoparticles production on SPR peak at 420 nm [15]. Under moderate circumstances, TEM analysis of palladium nanoparticles revealed that nanoparticles were spherical in shape with a diameter of around 10 nm and were employed as a heterogeneous catalyst for Suzuki coupling processes [16].

2.2.2. Leaf Extract Mediated Palladium Nanoparticles

Soybean leaf extract used for the production of a green synthesis of palladium nanoparticles. When soybean leaf extract is added to a palladium ion solution, the color of the solution shifts from light orange to dark brown. The existence of palladium ions in the reaction mixture is shown by a peak at 420 nm. HRTEM was used to analyze the size and SAED patterns of palladium nanoparticles. HRTEM pictures of PdNPs show that an evenly dispersed spherical shape with a diameter of 15 nm has formed. These biological syntheses of PdNPs can be employed as catalysts, particularly for the breakdown of azo dyes [17].

2.2.3. Root Extract Mediated Palladium Nanoparticles

The use root extract of *Euphorbia condylocarpa* as reducing agents and stabilizers in the biological synthesis of palladium nanoparticles and their catalytic uses in ligand and copper free Sonogashira and Suzuki coupling reactions high yield, simple approach, and reused several times without losing substantial catalytic activity. The UV-Vis spectrum shows a band at 387 nm, which is caused by a transition inside the B ring of the cinnamoyl system. For the phosphine-free Sonogashira and Suzuki coupling processes, *Euphorbia condylocarpa* root extract employed as a reducing agent and stabilizer is a highly efficient, magnetically recoverable, and recyclable catalyst [18].

2.2.4. Dried Fruit Extract Mediated Palladium Nanoparticles

Using the aqueous fruit extract of *Couroupita guianensis* as a powerful biological reducing agent, manufacture palladium nanoparticles. The production of a black precipitate, which has a lower absorbance in UV-Vis spectroscopy, indicated the reduction of PdCl₂ solution into their nanoscale. The activity of phenolic components from *C. guianensis* in nanoparticles reduction and surface functionalization is revealed by the FTIR spectrum. HRTEM micrographs of nanoparticles show well- distributed, spherical nanoparticles with an average size of 6 nm. Synthesized palladium nanoparticles have demonstrated outstanding antibacterial efficacy against both gram-negative and gram-positive bacteria. The experiment shows that manufactured nanoparticles are safe to use in biological applications such as in vitro cell viability, anticancer capability and hemocompatibility [19].

2.2.5. Bark Extract Mediated Palladium Nanoparticles

The biological synthesis of palladium nanoparticles used *Terminalia arjuna* bark extract. Palladium chloride PdCl₂ used as a precursor for synthesis of palladium nanoparticles. The absorption band at 234 nm of aqueous

solution of palladium chloride is caused by charge transfer from the precursor ion to the palladium nanoparticles. The SPR band in the UV-Vis spectrum was found after the addition of bark extract and palladium ions. The SPR band showed the synthesis of palladium nanoparticles. HRTEM analysis of synthesized PdNPs showed was spherical in shape and ranging sizes ~ 16 nm. Synthesized palladium nanoparticles showed excellent catalytic activity for reductive degradation [20].

III. ADVANTAGES OF BIOLOGICAL SYNTHESIS

Biological synthesis offers a sustainable and environmentally friendly alternative to traditional chemical and physical synthesis methods for nanomaterials, pharmaceuticals, and industrial compounds. It avoids hazardous chemicals commonly used in chemical synthesis (e.g., reducing agents like sodium borohydride). Generates minimal toxic byproducts, reducing environmental pollution. Biodegradable biomolecules act as natural stabilizers, eliminating the need for synthetic surfactants. Operates at ambient temperature and pressure, unlike chemical methods that require high temperatures and energy-intensive processes. Utilizes biological materials such as plant extracts, microbial cultures, and enzymes, which are renewable and naturally replenished. Follows the principles of green chemistry by minimizing waste generation and optimizing resource efficiency. Produces biocompatible materials, making them suitable for biomedical and pharmaceutical applications. Reduces risks of toxicity and environmental harm associated with chemically synthesized nanoparticles. Prevents contamination of water bodies and soil by eliminating harmful solvents and heavy metal residues. Can be used in eco-friendly bioremediation strategies to remove pollutants from the environment [21]. Biological synthesis represents a cleaner, safer, and more sustainable method for producing nanomaterials and industrial compounds. By reducing environmental impact and conserving natural resources, it aligns with global efforts toward green technology and eco-friendly industrial practices.

IV. APPLICATIONS OF BIOSYNTHESIZED PDNPS

- **Catalysis:** Palladium nanoparticles (PdNPs) are widely utilized in catalysis due to their exceptional catalytic efficiency, stability, and surface reactivity. They play a key role in organic synthesis, facilitating hydrogenation, cross-coupling reactions (e.g., Suzuki, Heck, and Sonogashira), and carbon-carbon bond formation with high selectivity [22]. In environmental catalysis, PdNPs aid in pollutant degradation and water purification by promoting redox reactions. Their electrocatalytic properties enhance fuel cell performance, particularly in hydrogen oxidation and oxygen reduction reactions. Additionally, PdNPs contribute to sustainable energy by catalyzing CO₂ reduction and hydrogen production, making them valuable for green chemistry, energy conversion, and industrial catalytic processes.
- **Biomedical Applications:** Palladium nanoparticles (PdNPs) have diverse biomedical applications due to their excellent catalytic, photothermal, and biocompatible properties [23]. They are used in targeted drug delivery systems, enabling controlled and responsive drug release. In cancer therapy, PdNPs facilitate photothermal therapy (PTT) and photodynamic therapy (PDT) for selective tumor destruction. Their catalytic activity enhances bioorthogonal reactions for in vivo drug activation. PdNPs also improve biosensing technologies for detecting disease biomarkers with high sensitivity. Additionally, their antimicrobial properties make them effective against bacterial and viral infections, while their role in regenerative medicine aids wound healing and tissue repair, offering promising advancements in healthcare.

- **Environmental Remediation:** Palladium nanoparticles (PdNPs) play a vital role in environmental remediation due to their outstanding catalytic properties and high surface reactivity. They are widely used in wastewater treatment for the degradation of organic pollutants, such as dyes, pesticides, and pharmaceutical residues, through advanced oxidation and reduction processes [24]. PdNPs also facilitate the catalytic reduction of toxic heavy metals like hexavalent chromium (Cr^{6+}) and lead (Pb^{2+}), converting them into less harmful forms. In air purification, PdNPs serve as efficient catalysts in automobile exhaust treatment, helping to remove carbon monoxide (CO), nitrogen oxides (NO_x), and volatile organic compounds (VOCs). Their role in hydrogenation and dechlorination reactions further supports the removal of environmental contaminants, such as chlorinated hydrocarbons and persistent organic pollutants. Additionally, PdNPs contribute to sustainable energy solutions by promoting CO_2 reduction and hydrogen production, making them valuable for both pollution control and green energy applications.

V. CONCLUSION

In conclusion, biological routes for palladium nanoparticle (PdNP) synthesis offer a sustainable and eco-friendly alternative to conventional chemical and physical methods. By leveraging biomolecules from plants, microorganisms, and other natural sources, these green synthesis approaches minimize toxic byproducts, reduce energy consumption, and enhance biocompatibility. Additionally, biologically synthesized PdNPs exhibit remarkable catalytic, biomedical, and environmental remediation potential, further reinforcing their significance in sustainable nanotechnology. Despite challenges such as scalability and precise control over nanoparticle properties, ongoing research and advancements in bioengineering hold promise for optimizing these methods. Embracing biological synthesis pathways can drive the development of greener, more efficient nanomaterials for diverse applications.

VI. REFERENCES

- [1]. Kanchi, S.; Ahmed, S. (Eds.) Green Metal Nanoparticles: Synthesis, Characterization and Their Applications; Wiley-Scrivener: Hoboken, NJ, USA, 2018.
- [2]. Mousavi, Seyyed Mojtaba, et al. "Green synthesis of silver nanoparticles toward bio and medical applications: review study." *Artificial cells, nanomedicine, and biotechnology* 46.sup3 (2018): S855-S872.
- [3]. Vajtai, Robert. "Science and engineering of nanomaterials." *Springer Handbook of Nanomaterials*. Springer, Berlin, Heidelberg, 2013. 1-36.
- [4]. Agostini, Giovanni, et al. "Effect of different face centered cubic nanoparticles distributions on particle size and surface area determination: a theoretical study." *The Journal of Physical Chemistry C* 118.8 (2014): 4085-4094.
- [5]. Wang, Yi, et al. "Shape-controlled synthesis of palladium nanocrystals: a mechanistic understanding of the evolution from octahedrons to tetrahedrons." *Nano letters* 13.5 (2013): 2276-2281.
- [6]. Zhao, Hong, et al. "Fabrication of a palladium nanoparticles/graphene nanosheets hybrid via sacrifice of a copper template and its application in catalytic oxidation of formic acid." *Chemical Communications* 47.7 (2011): 2014-2016.

- [7]. Vinodhini, S., B. Scholastica Mary Vithiya, and T. Augustine Arul Prasad. "Green synthesis of palladium nanoparticles using aqueous plant extracts and its biomedical applications." *Journal of King Saud University- Science* (2022): 102017.
- [8]. Yong, P., Rowson, N. A., Farr, J. P. G., Harris, I. R., Macaskie, L. E. Bioreduction and biocrystallization of palladium by *Desulfovibrio desulfuricans* NCIMB 8307. *Biotechnol Bioeng.* 2002, 80 (4), 369-379.
- [9]. Lengke, Maggy F., Michael E. Fleet, and Gordon Southam. "Synthesis of palladium nanoparticles by reaction of filamentous cyanobacterial biomass with a palladium (II) chloride complex." *Langmuir* 23.17 (2007): 8982-8987.
- [10]. Adams, Brian D., and Aicheng Chen. "The role of palladium in a hydrogen economy." *Materials today* 14.6 (2011): 282-289.
- [11]. Anderson, S.D.; Gwenin, V.V.; Gwenin, C.D. Magnetic Functionalized Nanoparticles for Biomedical, Drug Delivery and Imaging Applications. *Nanoscale Res. Lett.* 2019, 14, 188.
- [12]. Dubey, Shashi Prabha, et al. "Bioprospective of *Sorbus aucuparia* leaf extract in development of silver and gold nanocolloids." *Colloids and Surfaces B: Biointerfaces* 80.1 (2010): 26-33.
- [13]. Makarov, V. V., et al. "“Green” nanotechnologies: synthesis of metal nanoparticles using plants." *Acta Naturae (англоязычная версия)* 6.1 (20) (2014): 35-44.
- [14]. Anand, Krishnan, et al. "Biosynthesis of palladium nanoparticles by using *Moringa oleifera* flower extract and their catalytic and biological properties." *Journal of Photochemistry and Photobiology B: Biology* 165 (2016): 87-95.
- [15]. H. Veisi, N. Hajimoradian Nasrabadi, P. Mohammadi, *Appl. Organometal. Chem.* 2016, 30, 890.
- [16]. Hekmati, Malak, et al. "Green synthesis of palladium nanoparticles using *Hibiscus sabdariffa* L. flower extract: Heterogeneous and reusable nanocatalyst in Suzuki coupling reactions." *Applied Organometallic Chemistry* 31.11 (2017): e3757.
- [17]. Petla, Ramesh Kumar, et al. "Soybean (*Glycine max*) leaf extract based green synthesis of palladium nanoparticles." (2011).
- [18]. Nasrollahzadeh, Mahmoud, et al. "Green synthesis of Pd/Fe₃O₄ nanoparticles using *Euphorbia condylocarpa* M. bieb root extract and their catalytic applications as magnetically recoverable and stable recyclable catalysts for the phosphine-free Sonogashira and Suzuki coupling reactions." *Journal of Molecular Catalysis A: Chemical* 396 (2015): 31-39.
- [19]. Gnanasekar, Sathishkumar, et al. "Antibacterial and cytotoxicity effects of biogenic palladium nanoparticles synthesized using fruit extract of *Couroupita guianensis* Aubl." *Journal of Applied Biomedicine* 16.1 (2018): 59-65.
- [20]. Garai, Chhabi, et al. "Green synthesis of *Terminalia arjuna*-conjugated palladium nanoparticles (TA-PdNPs) and its catalytic applications." *Journal of Nanostructure in Chemistry* 8.4 (2018): 465-472.
- [21]. Haleemkhan, A. A., B. Naseem, and B. V. Vardhini. "Synthesis of nanoparticles from plant extracts." *Int J Mod Chem Appl Sci* 2.3 (2015): 195-203.
- [22]. Khan, Mujeeb, et al. "Miswak mediated green synthesized palladium nanoparticles as effective catalysts for the Suzuki coupling reactions in aqueous media." *Journal of Saudi Chemical Society* 21.4 (2017): 450-457.
- [23]. Xiao, J.-W.; Fan, S.-X.; Wang, F.; Sun, L.-D.; Zheng, X.-Y.; Yan, C.-H. Porous Pd nanoparticles with high photothermal conversion efficiency for efficient ablation of cancer cells. *Nanoscale* 6, (2014): 4345-4351.
- [24]. Garole, V. J., et al. "Palladium nanocatalyst: green synthesis, characterization, and catalytic application." *International Journal of Environmental Science and Technology* 16.12 (2019): 7885-7892.

Advanced Chemical Synthesis and Characterization of γ -Fe₂O₃ Nanoparticles

Mugale Y.G¹, Suryawanshi V.S²

¹Research Scholar, Department of Chemistry, P.G. and Research Centre, Shri Chhatrapati Shivaji College, Omerga, Maharashtra, India

²Department of Chemistry, P.G. and Research Centre, Shri Chhatrapati Shivaji College, Omerga, Maharashtra, India

ARTICLE INFO

Article History:

Published : 27 January 2025

Publication Issue :

Volume 12, Issue 10
January-February 2025

Page Number :

37-48

ABSTRACT

At the forefront of nanotechnology, magnetic oxide nanoparticles (MNPs) have exceptional potential for treating hyperthermia and delivering drugs precisely. Through the use of an alternating magnetic field, their special magnetic characteristics allow for precise targeting to certain biological locations, improving therapeutic efficacy. Multifunctional hybrid nanostructures that improve biocompatibility and expand the range of their therapeutic uses have been created as a consequence of the incorporation of MNPs into composite materials including liposomes and magnetic hydrogels. Magnetic nanoparticles may be used in a variety of biological settings by coating them to increase biocompatibility while maintaining their inherent magnetic properties. A range of chemical techniques are used in the manufacture of magnetic oxide nanoparticles, and each one provides exact control over the size, shape, and surface changes of the particles. To create MNPs with the right qualities for particular uses, processes including co-precipitation, sol-gel synthesis, and hydrothermal techniques are frequently used. The chemical production of magnetic oxide nanoparticles is examined in this work, along with their physico-chemical characteristics and possible uses in biomedicine. This study emphasises the importance of MNPs in nanomedicine and pinpoints future prospects for innovation and use in targeted treatments by analysing recent advancements in this quickly developing sector..

Keywords: Magnetic nanoparticles, Chemical synthesis, Physico-chemical properties, Biocompatibility, Drug delivery, Hyperthermia treatment, Hybrid nanostructures

I. INTRODUCTION

Nanotechnology has had a profound impact on a wide range of scientific fields as a result of the unique characteristics and potential applications of the materials produced by this technology. There is a significant amount of importance placed on the structural characteristics and qualities of NMIOPs when it comes to determining their capabilities and applications. The magnetic properties of these materials, such as their saturation magnetization (MS), coercivity (HC), and remanence (MR.), are a significant area of research that is being conducted. Iron-based oxides such as magnetite (Fe₃O₄), hematite (Fe₂O₃), and maghemite (γ -Fe₂O₃) are examples of materials that exhibit superparamagnetic at dimensions that are less than 20 nanometres. In the absence of an external magnetic field, these nanoparticles do not display any magnetization, which makes them very useful for applications that need precise control of magnetic properties. [1–4]

MNPs possess a core and a coated shell, together forming the "typical" architecture of these particles. The core often consists of magnetic elements, including iron (Fe), nickel (Ni), and cobalt (Co), together with their related oxides. The coated shell regulates the interaction of the nanoparticles (NPs) with the medium, hence maintaining their structure and characteristics. MNPs possess a large surface area, facilitating surface changes, hence making them adaptable for many applications. The coating is essential for improving the biocompatibility of MNPs in biological applications while preserving their distinctive magnetic characteristics. Conversely, in the context of biological applications, the characterization of these nanostructures is paramount. Consequently, many approaches for assessing the chemical and physical characteristics of MNPs were devised. Given that MNPs exhibit magnetic properties and confinement effects in all three dimensions, a wider array of unique qualities may be envisioned for practical medical applications and the investigation of basic scientific processes. They may also be used to examine fundamental scientific phenomena. [5]

The goal has been to facilitate the development of synthesis procedures that are not only straightforward but also economical. Chemical transformations are the most efficient means of controlling the size and shape of the object. To the contrary, it is possible to handle some limits that are associated with purity, dispersity, crystalline structure, and variable size by adjusting parameters such as composition and the processing solution. In order to avoid agglomeration and to ensure compatibility with biological systems, it is necessary to limit the size of the particles by careful execution and characterizations. A large amount of impact is exerted on the final features of the nanoparticles by the pH of the solution, the washing process, and the choice of washing solvent. The opposite is true; there is a dearth of comprehensive study on the relationship between pH, the washing solvent, and the eventual structure and features of nanoparticles. (6)–(8)

Applications of magnetic iron oxide nanoparticles in medicine

Magnetic iron oxide nanoparticles, which are often known as MIONs, are nanomaterials that are made of either maghemite (γ -Fe₂O₃) or magnetite (Fe₃O₄). Magnetic and superparamagnetic properties are shown by these particles, in addition to their small size, which ranges from one to one hundred nanometres in diameter. MIONs are used in a variety of biological systems, including the following:

- **Imaging contrast**

The presence of MIONs has the potential to enhance the pictures of tumours obtained by magnetic resonance imaging (MRI). Cells have been found to contain MNPs! Nanoparticles are created to allow the alignment of particles with each other under geomagnetic circumstances. This alignment is made possible by the nanoparticles. In addition, there is a substantial body of scientific literature that contains information on the use of fungi in the production of MNPs. The production of iron oxide nanoparticles, which has significant

potential applications in the fields of biomedicine and cleaning, is carried out by a number of different fungal species. [9]

- **Drug delivery**

Through the use of MIONs, it is possible to facilitate the targeted delivery of therapeutic compounds to certain locations inside the body. MNPs have the potential to act as carriers for the delivery of drugs in a targeted manner due to their magnetic properties. Through the use of an external magnetic field, these characteristics make it possible to deliver specific substances to specific tissues. By using this method, the systemic effects of the drug are reduced, while at the same time, its bioavailability is improved, and focused distribution to the sick tissue is made easier, all in accordance with the specific needs associated with that tissue. It is possible for a pharmaceutical to improve therapeutic efficacy while simultaneously lowering the probability of experiencing adverse effects if it is given correctly.

- **Hyperthermia**

The usage of elevated temperatures on tumours via MIONs may effectively eradicate the cellular composition of tumours. The elevated surface area-to-volume ratio of MNPs is one of its most notable benefits. This ratio allows extensive functionalization and modifications to meet certain biological needs. Adaptability facilitates the mixture of magnetic nanoparticles (MNPs) with specific belongings appropriate for many claims, with molecular detection, cancer therapy, and hyperthermia.

- **Molecular and cellular regulation**

MIONs has the capacity to regulate the cellular and molecular functions of the organism. Fluorescently tagged MNPs provide a diverse and efficient tool for visualising biological processes and structures at the molecular and cellular levels. Several preclinical investigations have shown that the use of MNPs in bioimaging has promise for illness diagnosis, monitoring disease progression, and evaluating therapy effectiveness [10].

The use of MIONs in clinical practices and biological research has been ongoing for an extended period. However, there are certain restrictions on their potential use, notably as:

- **Agglomeration:** It is possible for MIONs to cluster together; however this may be avoided by making surface alterations.
- **Size dependency:** The human body has the ability to eliminate MIONs that are either too big or too tiny.
- **Poor degradation:** MIONs may accumulate in normal tissues, potentially resulting in chronic inflammation. The preparation procedure used in the synthesis of MIONs may significantly affect their magnetic properties, surface chemistry, morphology, and dimensions.

II. OBJECTIVES OF THE STUDY

1. To study on Magnetic iron oxide nanoparticles biomedical applications
2. To study on Chemical synthesis magnetic oxide nanoparticle

Chemical synthesis magnetic oxide nanoparticle

In the expansive and fast evolving domain of nanoparticle production, chemical techniques are mostly used. Chemical synthesis has been the predominant approach, accounting for over ninety percent of the published work to far. Furthermore, the coprecipitation process for creating iron salts is the most often used industrial method nowadays.[11–12]

1. **Together with coprecipitation, precipitation**

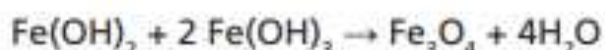
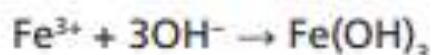
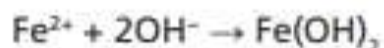
When it comes to the manufacture of magnetic nanoparticles (MNPs) containing magnetic metal oxide cores from suitable salt solutions, the two most common procedures that are used are precipitation and

coprecipitation. It is possible to precisely modify the sizes of these MNPs as well as their magnetic properties thanks to the production processes that are simple, adaptable, and less hazardous.

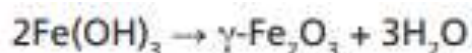
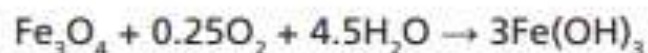
Metal ions are often used in situations where they are dissolved in a solvent, which results in the generation of a solution that is ideal for the synthesis of MNP. Examples of MNPs that may be created by these approaches include the synthesis of Fe₃O₄ or γ -Fe₂O₃ nanoparticles, which serves as an additional example. Following the conclusion of the reaction, a precipitate composed of Fe₃O₄ will be formed in the bottom of the reactor. Magnetic isolation and centrifugation are two other technologies that are beneficial for the recovery of environmental materials. The precipitate that is produced ought to have a pH that falls anywhere between 7.5 and 14. The synthesis of these particular forms of MNPs is very reliant on the sources of metal ions, in addition to the temperature, pH, and ionic strength of the medium in which the reaction takes place. Remember that this is an important factor to take into account [13]

The coprecipitation process is the most promising choice because to its user-friendliness and high output efficiency. Biomedicine applications often use it since it is user-friendly and requires less potentially dangerous materials and processes. The creation of iron oxide particles occurs via the ageing process, including the stoichiometric mixing of ferrous and ferric ions in an aqueous media. [14]

A chemical process that results in the creation of Fe₃O₄ may be expressed as follows:



After doing an analysis of the thermodynamics of this reaction, it is reasonable to anticipate that the entire precipitation of Fe₃O₄ will take place within a pH range of 9 to 14. This is because Fe₃O₄ is an unstable molecule that has the potential to undergo oxidation to γ -Fe₂O₃ when oxygen is present. The response might be communicated in the following manner:



To put a stop to this oxidation that is taking place in the atmosphere, it is necessary to establish an atmosphere that is devoid of oxygen. Through its movement through the solution, nitrogen is responsible for producing this state. The presence of nitrogen in the solution has the potential to lower particle size and impede oxidation. There are two distinct stages that may be distinguished within the process of coprecipitation. Following the formation of the first little nuclei in the medium, which occurs when the concentration of the species exceeds the critical supersaturation level, the crystal then begins to grow. The process is controlled by mass transport during the succeeding stage, which is the diffusion of solutes to the surface of the crystal. In order to successfully produce nanoparticles, it is necessary to differentiate between the two processes that are pertinent. Nucleation is not something that should take place throughout the period of crystal growth.

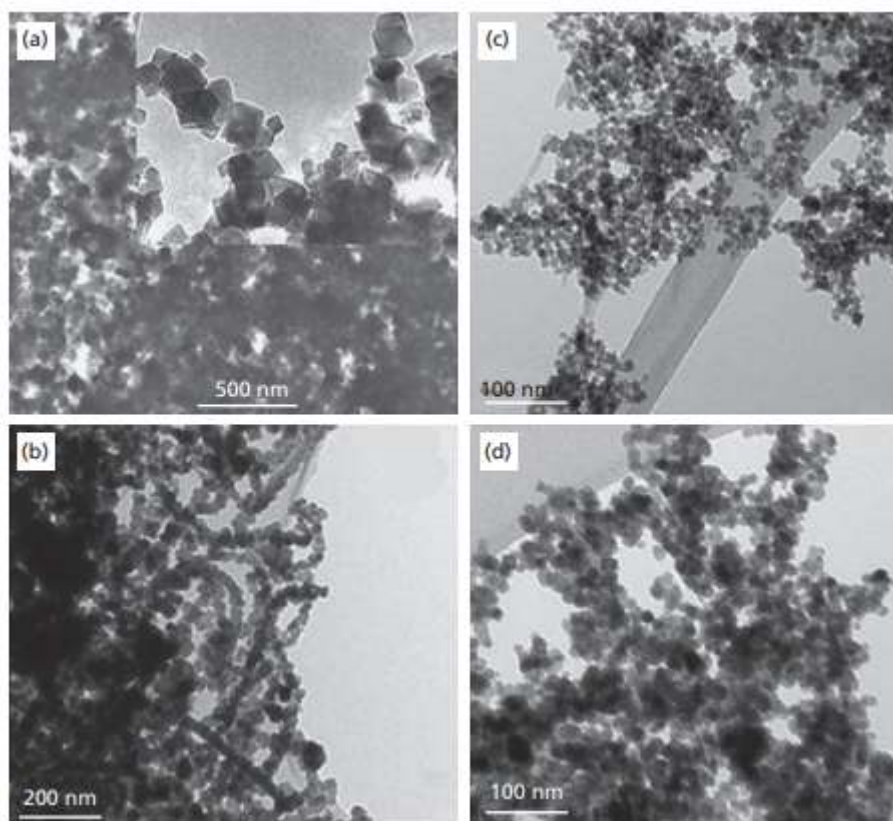


Figure 1. The following are examples of magnetite nanoparticle micrographs that were captured using a transmission electron microscope: (a) Sugimoto's method reaction with excess $[\text{OH}]$; (b) Sugimoto's method reaction without stirring and without excess $[\text{OH}]$ or $[\text{Fe}^{2+}]$; (c) Massart's method reaction with $\text{NH}_4 \text{OH}$; and (d) Massart's method reaction with dispersing agent TMAOH and without $\text{NH}_4 \text{OH}$.

2. Method of Thermal Decomposition

As a means of overcoming the limitations associated with the co-precipitation method, the thermal breakdown technique, which is sometimes referred to as pyrolysis, was developed. It was made easier to carry out this operation successfully by making use of non-aqueous solvents that had higher boiling points. The manufacture of highly crystalline MNPs of uniform sizes is made possible by this method. Decomposition of organometallic compounds in organic solvents is the first characteristic that distinguishes it from other types of reactions. Stabilising compounds, such as surfactants, enable this breakdown to take place at higher temperatures, which in turn facilitates the process. [15].

High-temperature decomposition of organic precursors

A diverse array of organometallic precursors for nanoparticles (NPs) exists, including acylketenes, N-nitroso phenylhydroxylamine, and carbonyls including different metallic centres such as $\text{Fe}^{2+,3+}$, $\text{Mn}^{2+,3+}$, $\text{Co}^{2+,3+}$, and $\text{Ni}^{2+,3+}$. Common stabilizing chemicals include hexadecyl amine, fatty acids, and oleic acids.

Decomposing iron precursors with heated organic surfactants enables the synthesis of iron oxide nanoparticles characterized by precise size control, a limited size distribution, and superior crystallinity. Furthermore, the generated particles are distributed across an extensive region. Besides $\text{Fe}(\text{Cup})_3$, $\text{Fe}(\text{CO})_5$, and $\text{Fe}(\text{acac})_3$, several more examples of iron precursors exist. Iron oleate may be synthesized by the decomposition of iron carbonyl at one hundred degrees Celsius in the presence of octyl ether and oleic acid. Subsequent to permitting the solution to reach room temperature, it is refluxed, and $(\text{CH}_3)_3 \text{NO}$ is incrementally introduced. Magnetite nanoparticles with exceptional crystallinity and a size range of 4–16 nm may be produced by decomposing iron

pentacarbonyl with oleic acid and then ageing the mixture at 300 degrees Celsius. The dimensions and morphology of the particles generated by this process are affected by various factors, including reaction duration, temperature, precursors, concentration, and the ratios of reactants to solvent. The surfactant's presence on particle surfaces aids in preserving the stability of the colloidal solution.

Particles measuring between 4 and 11 nanometres may develop due to the thermal degradation of iron oleate and iron pentacarbonyl in an organic solvent at varying temperatures. The iron oxide nanoparticles produced may dissolve in some organic solvents; however, the bulk remain insoluble in water. It is moreover a solvent. The particles in the report may range in size from 4 to 60 nm, contingent upon the duration of the reflux period. In a specific experiment investigating the breakdown of $\text{Fe}(\text{acac})_3$ in a high-temperature organic solvent, particles measuring 4, 6, 9, and 12 nm were generated. The particle size distribution is highly constrained, and they are encapsulated with 2,3-dimercaptosuccinic acid. Furthermore, these particles may be disseminated in water.

3. Hydrothermal Method

The hydrothermal process, which is sometimes referred to as the solvothermal method, is an example of a "bottom-up" synthesis methodology that may be used for IOMNP materials. In this method, the synthesis is carried out in an aqueous solution at a high temperature and pressure, and it is often carried out with the assistance of autoclaves or reactors. It is defined in the beginning by the fast nucleation and development of freshly synthesised MNPs, which ultimately leads to the creation of pure particles with morphologies that are tailored to the specific needs of the experiment. Micron nanoparticles (MNPs) are produced by a series of processes that take place during the hydrothermal process. These reactions include hydrolysis and oxidation. Several papers highlight the fact that the shape and crystallinity of the MNPs that are synthesised are dependent on the optimal mix of solvent, process time, pressure, and temperature. It is essential that minerals be soluble in water in order for the crystallization process to be successful. In accordance with the reports, it is possible to produce magnetite nanoparticles by the use of hydrothermal techniques. The reactions that are carried out using these techniques take place in an aqueous medium that is contained inside reactors or autoclaves. Furthermore, the pressure must be greater than two thousand pounds per square inch, and the temperature must be higher than two hundred degrees Celsius. In the presence of hydrothermal conditions, the synthesis of ferrites takes place via two primary pathways: hydrolysis and the oxidation or neutralization of mixed metal hydroxides. These two reactions are quite much identical, with the exception of the fact that the first step involves the utilization of ferrous salts. The 24th In this method, the particles are subject to a significant amount of influence from the solvent, temperature, and the amount of time that has passed. The size of the particles that are produced as a consequence of the reaction is increased by both the length of time that the reaction is carried out and the amount of water that is present. The nucleation stage and the crystal development stage are the two steps that are involved in the production of particles. By increasing the temperature, the nucleation process is sped up in comparison to the creation of crystals, which ultimately results in a reduction in the size of the particles. As the duration of the reaction time increases, crystal development becomes more prevalent, which ultimately results in the formation of bigger particles. In order to produce magnetite nanoparticles with a diameter of 27 nanometres, the hydrothermal technique was used, and the sodium salt bis(2-ethylhexyl) sulfosuccinate was utilised as a surfactant.

4. Polyol Method

When it comes to the synthesis of nanoparticles, the polyol approach is often considered to be among the most straightforward procedures. Through the use of this technique, the synthesis of nanoparticles from inorganic materials, such as alloys, sulphides, oxides, and fluorides, may be accomplished in a straightforward manner.

The capability to generate high-crystalline hydrophilic MNPs in a single technique that is both cost-effective and readily scalable is one of the most significant advantages.

5. Sol-Gel Method

The sol-gel method is a wet chemistry approach. This method employs metal alkoxide hydrolysis and polycondensation processes to generate a gel at ambient temperature. Dissolving metallic salts in water or other solvents produces a sol or colloidal solution that is uniformly distributed throughout the medium. Van der Waals forces are formed between the particles inside the system. Elevating the temperature and agitating the mixture both enhance the extent of particle-to-particle contact. Upon heating the combination until the solvent evaporates, the solution will eventually desiccate and transform into a gel.

The sol-gel technique is a wet-chemical method reliant on the hydrolysis and condensation of precursors inside a colloidal solution. This is the foundation of the procedure. individual A metal oxide network (gel) is generated due to a chemical reaction or the removal of a solvent. Acidic catalysis yields a polymeric gel, while basic catalysis produces a colloidal gel. The rates of condensation and hydrolysis are critical process parameters that significantly affect the characteristics of the resulting particles.

A slower and more regulated hydrolysis rate may provide smaller particles. Moreover, temperature, pH, concentration, and the particular solvent influence particle size. Heating the gel to 400 degrees Celsius produces γ -Fe₂O₃ particles measuring between 6 and 15 nanometres. Considering the experimental circumstances, the technique allows the precise prediction of particle structures in advance. This method allows the encapsulation of γ -Fe₂O₃ nanoparticles inside a transparent, inorganic silica matrix that withstands temperature variations.[16]

The majority of approaches for synthesising iron oxide-silica composites need an initial step involving the amalgamation of iron oxide and silica precursors in a solvent to generate a sol. Conversely, the sol-gel process yields more reactive iron oxide-silica aerogel composites compared to the traditional iron oxide technique.

6. Microemulsion Method

A microemulsion consists of three components: an amphiphilic surfactant, water, and oil, forming a thermodynamically stable dispersion. This method involves integrating precursor materials throughout many stages of the microemulsion process to generate nanoparticles (NP). Nanoparticles are generated as a result of chemical processes occurring inside microemulsion droplets, which are distinguished by their close closeness to one other.

Within the framework of water-in-oil microemulsion systems, the microdroplets that are present in the aqueous phase are distributed over the whole of the petroleum phase. In order to protect the microdroplets, surfactant molecules protect them. As a result of the presence of surfactant molecules, the particles are unable to nucleate, mature, or aggregate appropriately. Microdroplets that are composed of water will integrate iron salt into the microemulsion in the event that an iron salt solution is put into the microemulsion. By continuing to collide with one another, these little droplets will eventually combine and break apart. In the event that two reactants are injected into a microemulsion, the result will be the formation of a precipitate. The two processes that support the creation of particles are the aggregation of nuclei and the interchange of particles between droplets. There is no doubt that the precipitate can be eliminated from the surfactants via the process of separation.

Iron oxide nanoparticles with a remarkably uniform size distribution were produced as a result of the integration of an aqueous core containing aerosol-OT/n-hexane reverse micelles into a microemulsion. Through the use of the aqueous core, the reactants are dissolved. An aqueous core that included a solution of Fe³⁺ and

Fe²⁺ salts in a ratio of 4:1 was one of the individual components that comprised this report. The precipitation process is carried out with the assistance of a sodium hydroxide solution that has been deoxygenated. Magnetite nanoparticles were produced as a result of the introduction of nitrogen gas, which resulted in the reduction of their dimensions and the creation of a more uniform size distribution (Figure 5). At lower temperatures, the nanoparticles were created using the synthesis process. Because of the minuscule size of the aqueous core, which is measured in the nanometre range, the particles that are produced are generally less than 15 nanometres and have an extraordinarily narrow size distribution. The capacity of microemulsion technology to control the size of particles by adjusting the diameters of the aqueous core is one of the most significant advantages of this technology.

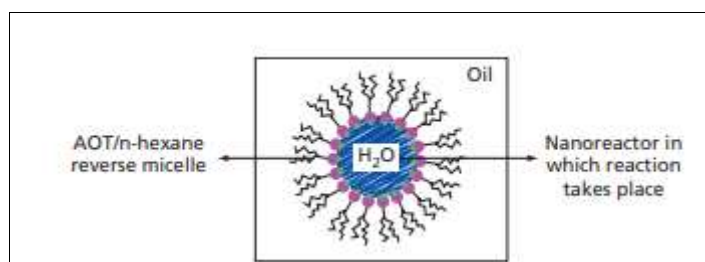


Figure 2. Structure of an aqueous core with aerosol-OT/n-hexane reverse micelles.

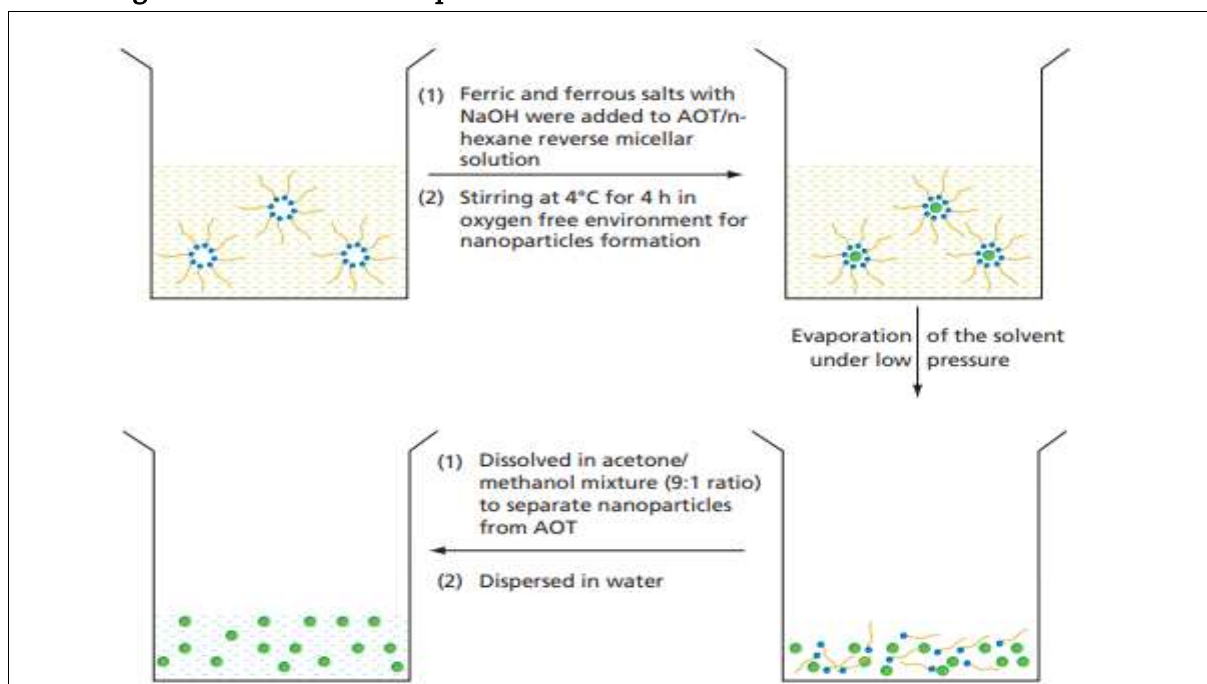


Figure 3. Highly monodispersed iron oxide nanoparticles are produced using the microemulsion technique.

7. Pyrolysis Methods

It is well known that spray pyrolysis is a technique that is used in the production of a wide variety of materials, one of which is magnetic nanoparticles (MNPs). The use of this method includes the production of very minute droplets of precursor solutions, which are subsequently aerosolised into an environment that is heated to a reasonable degree. Following the evaporation of the solvent, the remaining solute is collected on a substrate, and it is then subjected to a series of chemical reactions in order to produce the compound that is required.

The synthesis of iron oxide nanoparticles may also be accomplished by the use of sonolysis, which is the process of degrading organometallic precursors. When structural hosts, polymers, or organic capping agents are present, it is possible that they will hinder the formation of particles. The rapid collapse of holes that are formed by acoustic waves results in the production of a zone with a high temperature, which makes it easier for ferrous salts to be converted into magnetic nanoparticles. The sonolysis of an aqueous solution of $\text{Fe}(\text{CO})_5$, in combination with sodium dodecyl sulphate, has the potential to produce a hydrosol that contains amorphous magnetite nanoparticles.

Through the use of sonolysis, it has been possible to successfully produce superparamagnetic iron oxide nanoparticles that have been accurately characterised. In the course of this inquiry, the particles that have been created are coated with oleic acid, which is a surfactant. This coating prepares the particles for dispersion in a solution of chitosan. This is carried out in order to make the investigation easier. An excellent level of stability is shown by the 65 nm coated particles. Particularly important for a number of applications are the magnetic properties, the diameters of the particles, the size distribution, the particle shape, and the size distribution. It is possible to create a wide variety of particle qualities via the use of a variety of production techniques, and these characteristics may be obtained through a variety of different approaches. The aerosol/vapor method, polyol methods, and electrochemical approaches are some other ways that may be used for deposition.

8. Non-Thermal Methods

The synthesis of MNPs may be accomplished via the use of non-thermal procedures, which are methods that do not need the use of high temperatures during the production process. In order to avoid issues with aggregation or thermal breakdown, these approaches are often used since they have the potential to produce nanoparticles (NPs) that possess unique characteristics.

Common non-thermal methods used for MNP synthesis are:

- **Chemical Reduction**

By reducing metal ions with chemical agents, it is possible to produce magnetic nanoparticles without the need for increased temperatures. This can be accomplished without the need for increasing the temperature. This method is not only simple and cost-effective, but it can also be used to a wide variety of metals. In addition to this, it is often used in the production of metal nanoparticles, which may include those that are made of platinum, silver, and gold.

- **Electrochemical Synthesis**

Electrochemical reactions occur at the electrodes, producing MNPs as a consequence. This technology may be used to achieve simplicity, the ability to scale up, and control over size and form. It's also critical to note that it works well with a variety of materials, including conducting polymers, metals, and metal oxides.

- **Microwave-Assisted Synthesis**

Through the use of microwave radiation, reaction mixtures are heated, which enables the heating process to be both rapid and uniform. When compared to conventional methods of heating, this strategy consumes less energy, results in higher yields, and has reaction rates that are far faster [17]

- **Ultrasound-Assisted Synthesis**

The application of ultrasonic waves to a reaction mixture results in the formation of acoustic cavitation, which prompts the synthesis of particles more often. Better homogeneity, control over particle size, and rapid reaction times are all benefits that come with using this technology.

Physical and chemical properties of magnetic oxide nanoparticles

Magnetic oxide nanoparticles have many physical and chemical properties, including:

- **Magnetism**

A physical property that can be observed by how an object reacts to a magnet.

- **A high ratio of surface area to volume**

A unique property of magnetic nanoparticles that is different from their bulk materials.

- **Size-related magnetism**

A distinctive characteristic of magnetic nanoparticles that differentiates them from their bulk counterparts

- **Colloidal stability**

Magnetic nanoparticles have higher colloidal stability because they don't magnetically agglomerate.

- **Chemical stability**

Magnetic nanoparticles have higher chemical stability, which is important for biomedical applications.

- **Narrow size distribution**

Magnetic nanoparticles have a narrow size distribution, It is crucial for biological applications.

- **Zeta potential**

A physical characteristic of colloidal dispersions, including nanoparticle suspensions. It is the potential difference between the bulk solution and the static fluid layer adhered to the dispersed particle.

Other properties of magnetic oxide nanoparticles include:

- **X-ray diffraction:** Utilised for the purpose of analysing the arrangement of atoms inside the magnetic core, which provides information on the crystalline structure of the atoms.
- **Thermal decomposition:** A widely accepted method for synthesizing high-quality magnetic nanoparticles.
- **Microwave synthesis:** Can be used to generate metal oxides in the nanoscale range.

III. CONCLUSION

The modern techniques that are used to manufacture iron oxide nanoparticles make it possible to customise the surface for a variety of applications, one of which is the production of superparamagnetic particles that have an extremely narrow size distribution. The capacity of magnetic nanoparticles to be effectively targeted to specific regions inside the body by means of an alternating magnetic field is one of the many advantages that they provide. Other advantages include its use in treatments such as hyperthermia. These two advantages are only two of the innumerable advantages that magnetic nanoparticles provide. Magnetic nanoparticles are excellent for drug administration because they give large replacement levels. This is because to the raised surface-area-to-volume ratio that can be achieved with these particles. The incorporation of these nanostructures into composites, such as magnetic hydrogels or liposomes, results in the formation of new classes of multifunctional hybrid nanostructures. In addition to exhibiting improved biocompatibility, these nanostructures have the potential to be used in a wider range of therapeutic applications. The continual presence of a number of problems that need solutions is shown by these systems. Magnetic nanoparticles (MNPs) have a significant impact on their effectiveness due to the size and shape of these particles. As a consequence of this, it is of the utmost importance to develop appropriate synthetic procedures and conduct further research in order to ascertain the optimal performance of the final materials. The aggregation of MNPs is another cause for concern since it has the potential to reduce the effectiveness of these particles and to pose toxicity issues. The fact that iron oxide nanoparticles are often considered to be less hazardous than a great number of other types of nanoparticles is something that should be taken into consideration, despite the fact that toxicity studies are

required. The applications of particles have a considerable impact on the magnetic properties of those particles, and the size of the particles has a substantial impact on the magnetic properties of those particles. For applications, the techniques that are used to produce particles are very important. In the field of biomedicine, magnetic nanoparticles have the potential to enhance diagnostic procedures and treatment choices, ultimately leading to an improvement in the quality of life of individuals.

IV. REFERENCES

- [1]. Habibullah, G.; Viktorova, J.; Ruml, T. Current Strategies for Noble Metal Nanoparticle Synthesis. *Nanoscale Res. Lett.* 2021, 16, 47.
- [2]. Biehl, P.; von der Lühe, M.; Dutz, S.; Schacher, F. Synthesis, Characterization, and Applications of Magnetic Nanoparticles Featuring Polyzwitterionic Coatings. *Polymers* 2018, 10, 91
- [3]. Shin, D.N.; Matsuda, Y.; Bernstein, E.R. On the Iron Oxide Neutral Cluster Distribution in the Gas Phase. II. Detection through 118 Nm Single Photon Ionization. *J. Chem. Phys.* 2004, 120, 4157–4164
- [4]. Kurland, H.-D.; Grabow, J.; Staupendahl, G.; Andrä, W.; Dutz, S.; Bellemann, M.E. Magnetic Iron Oxide Nanopowders Produced by CO₂ Laser Evaporation. *J. Magn. Mater.* 2007, 311, 73–77.
- [5]. Yang, G.W. Laser Ablation in Liquids: Applications in the Synthesis of Nanocrystals. *Prog. Mater. Sci.* 2007, 52, 648–698.
- [6]. Amendola, V.; Meneghetti, M. Laser Ablation Synthesis in Solution and Size Manipulation of Noble Metal Nanoparticles. *Phys. Chem. Chem. Phys.* 2009, 11, 3805.
- [7]. Kawamura, G.; Alvarez, S.; Stewart, I.E.; Catenacci, M.; Chen, Z.; Ha, Y.-C. Production of Oxidation-Resistant Cu-Based Nanoparticles by Wire Explosion. *Sci. Rep.* 2015, 5, 18333.
- [8]. Song, K.; Kim, W.; Suh, C.-Y.; Shin, D.; Ko, K.-S.; Ha, K. Magnetic Iron Oxide Nanoparticles Prepared by Electrical Wire Explosion for Arsenic Removal. *Powder Technol.* 2013, 246, 572–574
- [9]. Kotov, Y.A. Electric Explosion of Wires as a Method for Preparation of Nanopowders. *J. Nanoparticle Res.* 2003, 5, 539–550.
- [10]. Grammatikopoulos, P.; Steinhauer, S.; Vernieres, J.; Singh, V.; Sowwan, M. Nanoparticle Design by Gas-Phase Synthesis. *Adv. Phys. X* 2016, 1, 81–100
- [11]. Hammad, M.; Hardt, S.; Mues, B.; Salamon, S.; Landers, J.; Slabu, I.; Wende, H.; Schulz, C.; Wiggers, H. Gas-Phase Synthesis of Iron Oxide Nanoparticles for Improved Magnetic Hyperthermia Performance. *J. Alloys Compd.* 2020, 824, 153814.
- [12]. Flores-Rojas, G.G.; López-Saucedo, F.; Vera-Graziano, R.; Mendizabal, E.; Bucio, E. Magnetic Nanoparticles for Medical Applications: Updated Review. *Macromol* 2022, 2, 374–390.
- [13]. Hariyani, P.L.; Faizal, M.; Ridwan, R.; Marsi, M.; Setiabudidaya, D. Synthesis and Properties of Fe₃O₄ Nanoparticles by Co-Precipitation Method to Removal Procion Dye. *Int. J. Environ. Sci. Dev.* 2013, 4, 336.
- [14]. Ali, A.; Shah, T.; Ullah, R.; Zhou, P.; Guo, M.; Ovais, M.; Tan, Z.; Rui, Y. Review on Recent Progress in Magnetic Nanoparticles: Synthesis, Characterization, and Diverse Applications. *Front. Chem.* 2021, 9, 629054.
- [15]. Kritika; Roy, I. Therapeutic Applications of Magnetic Nanoparticles: Recent Advances. *Mater. Adv.* 2022, 3, 7425–7444.

- [16]. Slimani, S.; Meneghini, C.; Abdolrahimi, M.; Talone, A.; Murillo, J.P.M.; Barucca, G.; Yaacoub, N.; Imperatori, P.; Illés, E.; Smari, M.; et al. Spinel Iron Oxide by the Co-Precipitation Method: Effect of the Reaction Atmosphere. *Appl. Sci.* 2021, 11, 5433.
- [17]. Ajeesha, T.; Ashwini, A.; George, M.; Manikandan, A.; Mary, J.A.; Slimani, Y.; Almessiere, M.A.; Baykal, A. Nickel Substituted MgFe₂O₄ Nanoparticles via Co-Precipitation Method for Photocatalytic Applications. *Phys. B Condens. Matter* 2021, 606, 412660.



Ecofriendly Natural and Synthetic Approach for Synthesis of Coumarin Derivatives – A Review

A.V.Sonone¹, R.U. Bhagyawant², M.D.Jadhav³, R.D.More*¹

¹Department of Chemistry, Siddharth Arts, Commerce & Science College, Jafrabad, Dist.Jalna-431206, Maharashtra, India

²Department of Botany, Siddharth Arts, Commerce & Science College, Jafrabad, Dist.Jalna-431206, Maharashtra, India

³Department of Microbiology, Siddharth Arts, Commerce & Science College, Jafrabad, Dist.Jalna-431206, Maharashtra, India

ARTICLE INFO

Article History:

Published : 27 January 2025

Publication Issue :

Volume 12, Issue 10

January-February 2025

Page Number :

49-53

ABSTRACT

Coumarin resides to benzopyrone family commonly found in many natural plants. Coumarin is a secondary metabolite, naturally existed in various plants and essential oils. Firstly, Vogel extracted Coumarin from tonka beans in 1820. Due to easy availability and numerous biological activities of coumarin derivatives, many researchers have attracted to synthesized from natural sources, as well as by synthetic route. The present review focused on study of natural and synthetic coumarin derivatives.

Keywords: Coumarin, benzopyrone family, tonka beans, natural, synthetic.

I. INTRODUCTION

Coumarins, an oxygenated heterocyclic polyphenolic composite, widely distributed in plants. Around 1300 chemotypes have been identified as secondary metabolites in plants, bacteria and fungi¹. In 1820, Vogel firstly isolated from the tonka bean (*Dipteryx odorata*). Coumarin (2H-1-benzopyran-2-one) is a member of subgroup of lactones. Generally, these are benzo- α -pyrone compounds referred to as coumarin and benzo- γ -pyrone is chromone, varying by a carbonyl group located at position 1 of the pyrone ring. Coumarin derivatives were found the various parts of plants such as, in the seeds (*tonka bean*), leaves (*Murraya paniculata*) and roots (*Ferulago campestris*). Typically, coumarins are found in the plants in their free form due to their polar nature and display blue fluorescence when exposed to UV light. In addition, their favorable pharmacological properties, coumarin derivatives are extensively utilized for fragrance enhancement in the cosmetic industry. Notably, the extended conjugation in coumarin rings, combined with their electron rich and charge transfer

characteristics, allows this framework to interact with various molecules and ions²⁻⁴. The name “Coumarin” is derived from French word “Coumarou”, which refers to the tonka bean⁵⁻⁶.

The coumarin ring structure found in natural compounds such as anticoagulant warfarin with remarkable pharmacological activity attracts researchers, prompting investigations into natural coumarins and their synthetic analogs for potential drug applications⁷. Their role remains largely unclear, though it has been suggested that they may regulate plant growth, inhibit fungi and bacteria, or even serve as waste products. Naturally occurring coumarin derivatives consist of compounds such as warfarin, umbelliferone (7-hydroxycoumarin), aesculetin (6,7-dihydroxycoumarin), herniarin (7-methoxycoumarin), psoralen and imperatorin⁸⁻¹³.

Present study dealing with synthesis of natural and synthetic coumarin derivatives.

II. NATURAL COUMARIN DERIVATIVES

Coumarins belong to a wide variety of natural compounds classified as secondary metabolites. Furthermore, coumarin found in vascular plants, also, found in bacteria and fungi, including antibiotics like novobiocin and coumermicin synthesized by bacteria. On the contrary, *Aspergillus flavus* serves as a source of aflatoxin, a substance with strong carcinogenic properties containing a coumarin ring within its structure¹⁴⁻¹⁵.

Miglietta A. and his coworker¹⁶ extracted Geiparyarin from the leaves of *Geijera parviflora*, was recognized as a novel drug targeting tubulin. The researchers examined the antimicrotubular and cytotoxic properties of newly synthesized aromatic derivatives of geiparvarin and found that these compounds hindered the polymerization of microtubular proteins.

Six novel coumarins have recently been identified in *Calophyllumdisparis* (Clusiaceae) fruits and stem bark. There are 200 species in the genus *Calophyllum*, which is widely found in tropical rain forests. Several of these species are used in traditional medicine. The marine alkaloids yielded the coumarin derivatives ningalin B and lambellarin D. which have cytotoxicity, immunomodulatory activity, and HIV-1 integrase inhibition¹⁷⁻²⁰.

M. Curini²¹ et. al. developed an alternate and useful method of synthesizing Collin for biological testing is provided by quick and simple three step synthesis of collinin. In order to establish a structure activity relationship profile, research is currently underway to create appropriately functionalized analogues and investigate the biological activity.

The non-nucleoside reverse transcriptase inhibitor (+)-Calanolide A, which was isolated from *Calophyllumlanigerum*, has strong anti-HIV-1 properties. A tetracyclic coumarin called (+)-Cordatolide A was extracted from the leaves *C. Cordatooblangum* in 1985. (+)-Inophyllum B was extracted from *C. inophyllum*. It was discovered that inophyllum was most effective against HIV- reverse transcriptase²²⁻²⁴.

III. SYNTHETIC COUMARIN DERIVATIVES

Benzopyrene, an alpha-pyrene ring, is fused with a benzene moiety to form coumarin. Various synthetic pathways are used to synthesize Coumarin derivatives including metal catalyzed cyclization, perkin condensation, Knoevenagel condensation and Pechmann reaction. These low molecular weight, stable, soluble compounds doesn't have any harmful side effects or toxicity. Coumarins are a promising therapeutic candidate for a variety of bacterial and viral illnesses due to these and other characteristics. In various phases of drug development, numerous natural, synthetic, conjugated and hybrid candidate lead compounds with coumarin scaffolds have been investigated²⁵⁻²⁷.

Farahi²⁸ et. al. synthesized a new sulphonamide-substituted coumarins using N-silfonylaldimines and 5,7-dihydroxy-4-methylcoumarin using NaOH. The reaction of aromatic aldehydes with p-toluenesulfonamide in the presence of AlCl₃ produced the Sulfonylaldimines. In addition, 5,7-dihydroxy-4-methylcoumarin was synthesized by the condensation reaction of phloroglucinol and ethyl aceto acetat using ZrOCl₂/SiO₂ catalyst.

Sharma et. al.²⁹ synthesized 3-cyanocoumarins using 2-hydroxybenzaldehydes with malononitrile in the presence of iodine as a catalyst and DMF as a solvent under microwave irradiation.

Ranjith H. and co-worker³⁰ synthesized a series of new Coumarin-3-carboxamides and tested for their anti-inflammatory and antioxidant properties in vivo. These carboxamide coumarins had strong anti-inflammatory and antioxidant properties. In order to identify the structural characteristics necessary for activity, structure-activity relationships were established based on the findings.

In 1,4-dioxane, Cavaleiro³¹ and co-worker reported synthesizing Coumarinporphyrin conjugates through the hetero-Diels-Alder reaction of 4-hydroxycoumarins with 2-vinyl-meso-tetraphenylporphyrinenatozinc (II) when paraformaldehyde is present.

Dumas et. al.³² explained a multi-component, effective and environmentally friendly method of producing coumarin derivatives in a single pot by mixing heterocyclic bromoacetyl, thiosemicarbazide and substituted 3-(acetoacetyl)-coumarin in anhydrous EtOH.

IV. CONCLUSION

In Coumarin derivatives are important heterocycles in medicinal field. The present review demonstrated the effectiveness of several synthetic and natural coumarin derivatives. Many medicinal chemists are interested in using them to create even more biologically active derivatives due to their low toxicity and good selectivity, because their biological activity has already been extensively studied. Research on these derivatives has demonstrated that the structural alteration makes it possible to enhance the pharmacological range of various biological activities

V. REFERENCES

- [1]. Rawat, A., & Reddy, A. V. B. (2022). Recent advances on anticancer activity of coumarin derivatives. *European Journal of Medicinal Chemistry Reports*, 5, 100038.
- [2]. Stefanachi, A., Leonetti, F., Pisani, L., Catto, M., & Carotti, A. (2018). Coumarin: A natural, privileged and versatile scaffold for bioactive compounds. *Molecules*, 23(2), 250.
- [3]. Bouhaoui, A., Eddahmi, M., Dib, M., Khouili, M., Aires, A., Catto, M., & Bouissane, L. (2021). Synthesis and biological properties of coumarin derivatives. A review. *ChemistrySelect*, 6(24), 5848-5870.
- [4]. Nikhil, B., Shikha, B., Anil, P., & Prakash, N. B. (2012). Diverse pharmacological activities of 3-substituted coumarins: a review. *Int. Res. J. Pharm*, 3(7), 24-29.
- [5]. Lončarić, M., Gašo-Sokač, D., Jokić, S., & Molnar, M. (2020). Recent advances in the synthesis of coumarin derivatives from different starting materials. *Biomolecules*, 10(1), 151.
- [6]. Bairagi, S. H., Salaskar, P. P., Loke, S. D., Surve, N. N., Tandel, D. V., & Dusara, M. D. (2012). Medicinal significance of coumarins: A review. *Int. J. Pharm. Res*, 4(2), 16-19.
- [7]. Musa, M. A., Cooperwood, J. S., & Khan, M. O. F. (2008). A review of coumarin derivatives in pharmacotherapy of breast cancer. *Current medicinal chemistry*, 15(26), 2664-2679.

- [8]. Borges, F., Roleira, F., Milhazes, N., Santana, L., & Uriarte, E. (2005). Simple coumarins and analogues in medicinal chemistry: occurrence, synthesis and biological activity. *Current medicinal chemistry*, 12(8), 887-916.
- [9]. Kostova, I., Raleva, S., Genova, P., & Argirova, R. (2006). Structure-activity relationships of synthetic coumarins as HIV-1 inhibitors. *Bioinorganic chemistry and applications*, 2006(1), 068274.
- [10]. Murray, R. D. H., Méndez, J., & Brown, S. A. (1982). The natural coumarins.
- [11]. Harvey, R. G., Cortez, C., Ananthanarayan, T. P., & Schmolka, S. (1988). A new coumarin synthesis and its utilization for the synthesis of polycyclic coumarin compounds with anticarcinogenic properties. *The Journal of Organic Chemistry*, 53(17), 3936-3943.
- [12]. Lacy, A., & O'kenney, R. (2004). Studies on coumarins and coumarin-related compounds to determine their therapeutic role in the treatment of cancer. *Current pharmaceutical design*, 10(30), 3797-3811.
- [13]. Gottlieb, O. R., Herrmann, K., Murray, R. D. H., Ohloff, G., & Pattenden, G. (2012). *Fortschritte der Chemie Organischer Naturstoffe/Progress in the Chemistry of Organic Natural Products (Vol. 35)*. Springer Science & Business Media.
- [14]. Tomasz Kubrak, T., Rafał Podgórski, R., & Monika Sompór, M. (2017). Natural and synthetic coumarins and their pharmacological activity. *European journal of clinical and experimental medicine*, (2), 169-175.
- [15]. Borges, F., Roleira, F., Milhazes, N., Santana, L., & Uriarte, E. (2005). Simple coumarins and analogues in medicinal chemistry: occurrence, synthesis and biological activity. *Current medicinal chemistry*, 12(8), 887-916.
- [16]. Miglietta, A., Bocca, C., Gabriel, L., Rampa, A., Bisi, A., & Valenti, P. (2001). Antimicrotubular and cytotoxic activity of geiparvarin analogues, alone and in combination with paclitaxel. *Cell Biochemistry and Function: Cellular biochemistry and its modulation by active agents or disease*, 19(3), 181-189.
- [17]. Reddy, S. M., Srinivasulu, M., Satyanarayana, N., Kondapi, A. K., & Venkateswarlu, Y. (2005). New potent cytotoxic lamellarin alkaloids from Indian ascidian *Didemnum obscurum*. *Tetrahedron*, 61(39), 9242-9247.
- [18]. Guilet, D., Séraphin, D., Rondeau, D., Richomme, P., & Bruneton, J. (2001). Cytotoxic coumarins from *Calophyllum dispar*. *Phytochemistry*, 58(4), 571-575.
- [19]. Ridley, C. P., Reddy, M. V. R., Rocha, G., Bushman, F. D., & Faulkner, D. J. (2002). Total synthesis and evaluation of lamellarin α 20-Sulfate analogues. *Bioorganic & medicinal chemistry*, 10(10), 3285-3290.
- [20]. Ajay Kumar, K., Renuka, N., Pavithra, G., & Vasanth, G. (2015). Comprehensive review on coumarins: Molecules of potential chemical and pharmacological interest. *Journal of Chemical and Pharmaceutical Research*, 7(9), 67-81.
- [21]. GonzalesB, S. P., & RodriguezB, J. C. (2003). Synthesis of collinin, an antiviral coumarin. *Aust. J. Chem*, 56, 59-60.
- [22]. Ranjith, H., Dharmaratne, W., Sotheeswaran, S., Balasubramaniam, S., & Waight, E. S. (1985). Triterpenoids and coumarins from the leaves of *Calophyllum Cordato-Oblongum*. *Phytochemistry*, 24(7), 1553-1556.
- [23]. Flavin, M. T., Rizzo, J. D., Khilevich, A., Kucherenko, A., Sheinkman, A. K., Vilaychack, V., ... & Xu, Z. Q. (1996). Synthesis, chromatographic resolution, and anti-human immunodeficiency virus activity of (\pm)-calanolide A and its enantiomers. *Journal of Medicinal Chemistry*, 39(6), 1303-1313.
- [24]. Patil, A. D., Freyer, A. J., Eggleston, D. S., Haltiwanger, R. C., Bean, M. F., Taylor, P. B., ... & Bartus, H. R. (1993). The inophyllums, novel inhibitors of HIV-1 reverse transcriptase isolated from the Malaysian tree, *Calophyllum inophyllum* Linn. *Journal of medicinal chemistry*, 36(26), 4131-4138.

- [25]. Venugopala, K. N., Rashmi, V., & Odhav, B. (2013). Review on natural coumarin lead compounds for their pharmacological activity. *BioMed research international*, 2013(1), 963248.
- [26]. Jadhav, N. H., Sakate, S. S., Rasal, N. K., Shinde, D. R., & Pawar, R. A. (2019). Heterogeneously catalyzed Pechmann condensation employing the tailored ZnO. 925TiO₂. 075O NPs: synthesis of coumarin. *ACS omega*, 4(5), 8522-8527.
- [27]. Hassan, M. Z., Osman, H., Ali, M. A., & Ahsan, M. J. (2016). Therapeutic potential of coumarins as antiviral agents. *European journal of medicinal chemistry*, 123, 236-255.
- [28]. Farahi, M., Karami, B., & Tanuraghaj, H. M. (2015). Efficient synthesis of a new class of sulfonamide-substituted coumarins. *Tetrahedron Letters*, 56(14), 1833-1836.
- [29]. Eddahmi, M., Moura, N. M., Bouissane, L., Faustino, M. A., Cavaleiro, J. A., Paz, F. A., ... & Rakib, E. M. (2019). Synthesis and biological evaluation of new functionalized nitroindazolylacetonitrile derivatives. *ChemistrySelect*, 4(48), 14335-14342.
- [30]. Ranjith, H., Dharmaratne, W., Sotheeswaran, S., Balasubramaniam, S., & Waight, E. S. (1985). Triterpenoids and coumarins from the leaves of *Calophyllum Cordato-Oblongum*. *Phytochemistry*, 24(7), 1553-1556.
- [31]. Cardoso, M. D. C., Gomes, A. T. P. C., Silva, V. L. M., Silva, A. M. S., Neves, M. G. P. M. S., da Silva, F. D. C., & Cavaleiro, J. A. S. (2015). Ohmic heating assisted synthesis of coumarinyl porphyrin derivatives. *RSC Advances*, 5(81), 66192-66199.
- [32]. Chen, Z., Bi, J., & Su, W. (2012). A Novel Method for One-pot Synthesis of Furo [3, 2-c] coumarin Derivatives from 4-Hydroxycoumarin and Arylglyoxal under Microwave Irradiation. *Chinese Journal of Chemistry*, 30(8), 1845-1850.

Review on Synthesis, Characterization, and Properties of Soft Substituted Ferrite Nanoparticles

A.P. Chavan¹, N.D. Chaudhari², G. B. Andhale³, A. M. Kute⁴, A. O. Dhokte¹, P. R. Kute^{1*}

¹Department of Chemistry, Pratishthan Mahavidyalaya, Paithan, Dist.-Chh. Sambhajinagar, Maharashtra, India

²Department of Physics, Pratishthan Mahavidyalaya, Paithan, Dist.-Chh. Sambhajinagar, Maharashtra, India

³Department of Chemistry, Shri Shivaji Arts, Commerce and Science College Akot, Maharashtra, India

⁴Department of Chemistry, Shankarrao Patil Mahavidyalaya, Bhoom, Maharashtra, India

ARTICLE INFO

Article History:

Published : 27 January 2025

Publication Issue :

Volume 12, Issue 10

January-February 2025

Page Number :

54-57

ABSTRACT

Ferrite nanoparticles have a large interest due to their wide range of applications in various fields such as sensors, biosensors, energy storage systems, recording media, data storage, drug delivery, wastewater treatment. This present review paper is focused on the various synthesis techniques for ferrite nanoparticles, characterization techniques and their application in various fields.

Keywords: Ferrites, Synthesis methods, Characterization techniques

I. INTRODUCTION

Ferrites are ceramic materials with a broad range of applications in electronics, magnetics, and energy storage, due to their unique electrical and magnetic properties. Soft ferrites, particularly, are known for their low coercivity and high permeability, making them highly suitable for applications such as inductors, transformers, and magnetic storage devices. The substitution of metal ions (such as Zn^{2+} , Mn^{2+} , Cu^{2+} , or Mg^{2+}) into the ferrite structure can improve properties like magnetic behavior, conductivity, and catalytic activity. This literature review explores the various synthesis techniques, characterization methods, and key properties of soft substituted ferrite nanoparticles.

1. Synthesis Methods

The synthesis of soft substituted ferrites is a crucial step that influences their size, shape, crystallinity, and overall properties. Several methods are used to synthesize ferrite nanoparticles, with different approaches leading to distinct material characteristics.

1. Co-precipitation Method

- One of the most widely used methods for synthesizing ferrite nanoparticles is co-precipitation. In this method, metal salts such as iron salts (Fe^{2+} , Fe^{3+}) and other metal salts are dissolved in water, and a precipitant (e.g., NaOH) is added to control the pH, leading to the formation of ferrite nanoparticles (Ravindran et al., 2016). By controlling pH, temperature, and metal ion concentration, uniform nanoparticles with well-defined sizes can be synthesized.
- Research indicates that the substitution of ions like Zn^{2+} , Mn^{2+} , and Cu^{2+} in the ferrite structure enhances its magnetic properties (Cao et al., 2017).

2. Sol-gel Process

- The sol-gel process uses metal alkoxides, which undergo hydrolysis and polymerization to form a gel. This method allows for the preparation of ferrite nanoparticles at relatively low temperatures and can produce ferrites with a high degree of purity and homogeneity. The substitution of metal ions during the gel formation process enables precise control over the particle size and crystal structure (Niu et al., 2020).
- Sol-gel synthesized Ni-Zn ferrites have shown excellent soft magnetic properties, which can be tuned by varying the substitution level of the ions (Gómez et al., 2022).
- Studies have shown that hydrothermal synthesis results in ferrites with improved catalytic and magnetic properties, such as Mn-substituted ferrites showing enhanced ferromagnetic behaviour (Ramesh et al., 2018).

3. Mechanochemical Synthesis

- Mechanochemical methods involve grinding metal oxides in a ball mill, which induces chemical reactions through mechanical energy. This technique allows for the synthesis of ferrites without requiring high temperatures (Kaczmarek et al., 2020). The mechanical activation during the milling process facilitates ion substitution and the formation of ferrites.
- Ferrites synthesized by this method often exhibit fine particle sizes and improved magnetic properties due to the high energy imparted to the material during synthesis (Gundiah et al., 2019).

4. Microemulsion Method

- The microemulsion method involves the formation of nanosized droplets in a water-in-oil emulsion system. These droplets act as micro-reactors for the formation of ferrite nanoparticles. This technique allows precise control over the size and morphology of the nanoparticles and can be used to incorporate various metal ions into the ferrite matrix (Zhao et al., 2021).

2. Characterization Techniques

Characterization techniques are essential for understanding the physical, chemical, and magnetic properties of ferrite nanoparticles. The following methods are commonly used:

1. X-ray Diffraction (XRD)

- XRD is a powerful tool for determining the crystalline structure and phase purity of ferrite nanoparticles. The diffraction patterns can reveal the type of ferrite phase (e.g., spinel ferrite) and provide insights into the effects of ion substitution on the crystal lattice (Ravindran et al., 2016).

2. Transmission Electron Microscopy (TEM)

- TEM provides high-resolution images of the morphology, size, and internal structure of ferrite nanoparticles. This technique is especially useful for studying the size distribution of nanoparticles and assessing their aggregation behavior (Li et al., 2019).

3. Scanning Electron Microscopy (SEM)

- SEM is used to study the surface morphology and particle distribution. It provides insight into the microstructure and potential aggregation of the particles (Ali et al., 2020).

4. Fourier Transform Infrared Spectroscopy (FTIR)

- FTIR is used to study the chemical bonding and functional groups present in ferrite nanoparticles. It is an important technique for confirming the substitution of metal ions and understanding the interaction between the metal ions and the oxygen atoms in the ferrite matrix (Niu et al., 2020).

5. Vibrating Sample Magnetometer (VSM)

- VSM is used to measure the magnetic properties of ferrite nanoparticles. It provides information on saturation magnetization, coercivity, and remanence. The magnetic behaviour of soft substituted ferrites depends significantly on the type of metal substitution, as certain ions can reduce coercivity and improve magnetic performance (Cao et al., 2017).

6. Brunauer–Emmett–Teller (BET) Surface Area Analysis

- BET analysis measures the surface area and porosity of ferrite nanoparticles. A higher surface area enhances properties like adsorption and catalytic activity, which are important for applications in sensors and energy storage (Zhao et al., 2021).

3. Properties of Soft Substituted Ferrite Nanoparticles

The substitution of metal ions in ferrites has a profound effect on their magnetic, electrical, and catalytic properties. Key findings from the literature include:

1. Magnetic Properties

- Soft ferrites exhibit low coercivity and high permeability, essential for high-frequency applications. Substituting metal ions like Zn^{2+} , Cu^{2+} , and Mn^{2+} leads to enhanced magnetization and reduced hysteresis losses. For example, Cu-substituted ferrites show a decrease in coercivity and a significant increase in magnetic saturation, making them suitable for low-power applications (Cao et al., 2017).

2. Electrical Properties

- The electrical conductivity and dielectric properties of ferrites can be tailored through ion substitution. For instance, Zn^{2+} and Mg^{2+} substitution increases conductivity due to a reduction in grain boundary resistance and improved ionic mobility (Gómez et al., 2022).

3. Catalytic Properties

- Substituted ferrites exhibit improved catalytic properties, particularly for oxidation and reduction reactions. For instance, Fe^{3+} -substituted ferrites show enhanced catalytic performance in the degradation of organic pollutants (Ramesh et al., 2018). This is due to the enhanced surface area and the presence of additional reactive sites introduced by ion substitution.

4. Thermal Stability

- The thermal stability of ferrites is also influenced by ion substitution. For example, Ni-substituted ferrites exhibit improved thermal stability and sintering properties, which are beneficial for high-temperature applications (Wang et al., 2015).

5. Optical Properties

- Some soft substituted ferrites show promising optical properties. Zn^{2+} and Cu^{2+} substitutions have been found to enhance the photoluminescent properties of ferrite nanoparticles, making them useful for optoelectronic applications (Li et al., 2019).

4. Applications of Soft Substituted Ferrite Nanoparticles

Due to their unique properties, soft substituted ferrites have numerous applications:

- **Magnetic Storage and Sensors:** Used in memory devices, inductors, and sensors due to their magnetic responsiveness (Ali et al., 2020).
- **Energy Storage:** Ferrites, particularly when substituted, are used in supercapacitors and rechargeable batteries, where high surface area and conductivity are beneficial (Ravindran et al., 2016).
- **Environmental Remediation:** Ferrites are used in catalytic applications for environmental cleanup, such as the removal of heavy metals from wastewater (Gundiah et al., 2019).

II. CONCLUSION

Soft substituted ferrite nanoparticles offer exciting possibilities in advanced technological applications. By carefully selecting the metal ions to be substituted, their magnetic, electrical, and catalytic properties can be finely tuned. Continued research into synthesis methods, such as sol-gel and co-precipitation, and improved characterization techniques will enhance the scalability and performance of these materials.

III. REFERENCES

- [1]. Ali, S., et al. (2020). "Synthesis and characterization of Cu-substituted ferrite nanoparticles for gas sensor applications." *Journal of Magnetism and Magnetic Materials*, 498, 166223.
- [2]. Cao, M., et al. (2017). "Magnetic properties of Zn-substituted nickel ferrite nanoparticles." *Journal of Applied Physics*, 122(16), 164308.
- [3]. Gómez, F., et al. (2022). "Electrical and dielectric properties of Ni-Zn ferrites synthesized by sol-gel process." *Journal of Alloys and Compounds*, 869, 159280.
- [4]. Gundiah, G., et al. (2019). "Mechanochemical synthesis of substituted ferrites for catalytic applications." *Materials Science and Engineering B*, 242, 1–7.
- [5]. Kaczmarek, M., et al. (2020). "Mechanochemical synthesis of Cu-substituted ferrites and their magnetic properties." *Materials Chemistry and Physics*, 243, 122527.
- [6]. Li, X., et al. (2019). "Photoluminescent properties of ferrite nanoparticles: Effect of substitution with Zn and Cu." *Journal of Luminescence*, 208, 452–458.
- [7]. Niu, H., et al. (2020). "Synthesis of metal-substituted ferrite nanoparticles by sol-gel method and their magnetic properties." *Journal of Materials Science*, 55(16), 6973–6983.
- [8]. Ravindran, A., et al. (2016). "Co-precipitation method for synthesis of ferrite nanoparticles and their applications." *Journal of Nanoscience and Nanotechnology*, 16(8), 8331–8338.
- [9]. Ramesh, R., et al. (2018). "Catalytic applications of substituted ferrites in environmental remediation." *Applied Surface Science*, 441, 560–568.
- [10]. Wang, X., et al. (2015). "Hydrothermal synthesis of ferrite nanoparticles: Effect of substitution on magnetic and structural properties." *Journal of Magnetism and Magnetic Materials*, 397, 125–130.
- [11]. Zhao, H., et al. (2021). "Synthesis of ferrite nanoparticles by microemulsion method and their characterization." *Materials Science and Engineering C*, 118, 111392.

Synthesis and Characterization of Copper Doped TiO₂ Nanoparticles

Sandip B. Deshmukh^{1*}, Kalyani H. Deshmukh², Appasaheb W. Suryawanshi², Maheshkumar L. Mane³

¹Department of Chemistry, Ramkrishna Paramhansa Mahavidyalaya, Dharashiv 413 501, Maharashtra, India

²Department of Chemistry, Shri Madhavrao Patil Mahavidyalaya, Murum Tq. Omerga Dist. Dharashiv 413 605, Maharashtra, India

³Department of Physics, S.G.R.G. Shinde Mahavidyalaya, Paranda Tq. Paranda Dist. Dharashiv 413 502, Maharashtra, India

ARTICLE INFO

Article History:

Published : 27 January 2025

Publication Issue :

Volume 12, Issue 10

January-February 2025

Page Number :

58-69

ABSTRACT

Titanium dioxide (TiO₂) is an n-type of semiconductor, which has important applications such as H₂ generation, defogger, self-cleaning, air purification, water purification, sterilization and etc. TiO₂ is a semiconducting metal oxide with a wide band gap and it requires an excitation light with a wavelength lower than 400 nm (UV light) ($E_g = hc/\lambda \cong 1240/\lambda$) to begin a photocatalytic activity. When surface of TiO₂ is irradiated with UV light irradiation, electrons (e^- CB) and holes (h^+ VB) are created in conduction (CB) and valence bands (VB), respectively. The produced electrons and holes are consequently trapped and recombined with each other. However, TiO₂ is inactive and inappropriate in visible light. Many efforts have been taken to overcome such limitations and improve the photocatalytic activity of TiO₂, through surface modification/complexation, impurity doping, sensitization, hetero-junction with semiconductors of similar band gap, etc. The impurity of metal doping was focused in this study. Among different metallic doping elements, copper has been proven as potential dopant to improve visible light absorption. For example, Park et al. modified TiO₂ through Co²⁺, Ni²⁺, Zn²⁺, Cu²⁺ incorporations and reported that Cu-doped TiO₂ was a potential photocatalyst in photo-decomposition of methylene blue. However, in the present study the copper selected as a dopant to tune the band gap of TiO₂. Optimum compositions (0.0 mole % , 1 mole % , 3 mole% and 5 mole %) of Cu doped TiO₂ nanoparticles were prepared by sol-gel method at room temperature. The prepared powder samples were characterized by XRD, FTIR, filed emission Scanning Electron Microscopy (FE-SEM) with EDAX,

HR-TEM and UV–Visible diffuse reflectance spectra. With a bigger surface area, a reduced optical energy band gap, a lower charge transfer resistance, and a lower charge recombination rate, the synthesized mole% of Cu-doped TiO₂ NPs improved overall absorption in the visible spectrum..

Keywords: Dopant, Transition metal, photocatalyst, Surface area, Band gap

I. INTRODUCTION

Titanium dioxide (TiO₂) is an n-type of semiconductor, which has important applications such as H₂ generation, defogger, self-cleaning, air purification, water purification, sterilization and etc [7-14]. TiO₂ is abundantly available, cheap, non-toxic, versatile, and stable semiconducting metal oxide [15-18]. Generally, TiO₂ is a semiconducting metal oxide with a wide band gap and it requires an excitation light with a wavelength lower than 400 nm (UV light) ($E_g = hc/\lambda \cong 1240/\lambda$) to begin a photocatalytic activity [19,20]. When surface of TiO₂ is irradiated with UV light irradiation, electrons (e^- CB) and holes (h^+ VB) are created in conduction (CB) and valence bands (VB), respectively [20]. The generated electrons and holes are subsequently trapped and recombined with each other [27]. However, TiO₂ is inactive and inappropriate in visible light. Many efforts have been taken to overcome such limitations and improve the photocatalytic activity of TiO₂, through surface modification/complexation, impurity doping, sensitization, hetero-junction with semiconductors of similar band gap, etc. The impurity doping was focused in this study.

In the process of doping, the fast charge recombination is impeded and visible light absorption is enabled by producing defect states in the band gap. In the first case, the recombination is inhibited and the interfacial charge transfer is enhanced by trapping the VB holes or CB electrons in the defect sites. In the second case, the electronic transitions from the defect states to the CB or from the VB to the defect states are allowable under sub-band gap irradiation. There are the two main categories of dopants; Metal ions (noble metals and transition metals) and non-metal ions [20,21]. Generally, the metals having the potential to transfer electron and decrease the band gap energy level are preferred for the doping [22-27]. For doped catalysts, metal ions are activated in the incidence of light source, generating electron and holes. Therefore, the existence of metal ion dopants in the photocatalyst matrix enhanced the interfacial electron-transfer rates and charge carrier recombination rates extensively, followed by greater photo reactivity. Among different metallic doping elements, copper has been proven as potential dopant to improve visible light absorption. For example, Park et al. [25] modified TiO₂ through Co²⁺, Ni²⁺, Zn²⁺, Cu²⁺ incorporations and reported that Cu-doped TiO₂ was a potential photocatalyst in photo-decomposition of methylene blue. However, in the present study the copper selected as a dopant to tune the band gap of TiO₂.

II. METHODS AND MATERIAL

A. MATERIALS

Various mole % of Cu doped TiO₂ NPs were synthesized by using the sol-gel technique. In this work Analytical grade titanium(IV)tetraisopropoxide (TTIP) (TiOCH(CH₃)₂)₄ 97% Sigma Aldrich), Copper Sulfate

(CuSO₄.5H₂O), Oleic acid (C₁₈H₃₄O₂), ammonia (NH₃) and absolute ethyl alcohol (C₂H₅OH) were used for the synthesis.

B. SYNTHESIS OF CU DOPED TiO₂ NANOPARTICLES

Optimum compositions (0.0 mole %, 1 mole %, 3 mole % and 5 mole %) of Cu doped TiO₂ nanoparticles were prepared by sol-gel method at room temperature.

5ml Oleic acid were taken in a 250 mL round-bottom flask. The content was stirred at 120°C for 10 min. followed by the addition of 10 mL TTIP and 200 mL distilled water (DW); white precipitate of titanium hydroxide was formed. The content was stirred at room temperature for 1 h. Then, the content was filtered and reslurred in 200 mL DW and pH of solution was adjusted to 10 by using ammonia solution. After that, the content was stirred at 60°C for 3 h. The stoichiometric quantity of copper sulfate (CuSO₄.5H₂O) was added into the above solution. The content was again stirred for 3 h at 60°C. Then, the content was filtered and washed with 50 mL DW and 10 mL ethyl alcohol. After that, the residue was dried at 100°C and annealed in air at 500°C for 5 h. After annealing, the residue was resulted into the greenish coloured Cu doped TiO₂ nanoparticles.

C. CHARACTERIZATION

The prepared powder samples were characterized by powder X-ray diffraction technique. XRD data of the samples were collected in the 2θ range of 100 – 900 in step scan mode at a rate of 0.20/min using ULTIMA IV, Rigaku Corporation, Japan diffractometer with source Cu Kα (Kα₁ = 1.5406 and Kα₂ = 1.5444 Å) radiation. Nicolet iS10, Thermo Scientific, USA Fourier Transform Infrared spectrometer was used to record FTIR spectra of the nanoparticles in the range of 400 cm⁻¹ to 4000 cm⁻¹ with the transmission mode. The surface morphology of samples was investigated by using field emission Scanning Electron Microscopy (FE-SEM) Hitachi S-4800 system with EDAX analysis was performed to determine the elemental composition of the samples. A JEOL JEM2100F field emission gun-transmission electron microscope (HR-TEM 200kV) operating at 200 kV with resolution (Point: 0.19 nm Line: 0.1 nm) and magnification (50X – 1.5 X) was employed for generating HR-TEM image of the nanoparticles. UV-Visible diffuse reflectance spectra of all the samples were recorded in the range of 200 nm – 800 nm, using an ELICO – SL159 UV-Visible spectrometer.

III. RESULTS AND DISCUSSION

A. X-ray diffraction analysis (XRD)

XRD spectra of *sol-gel* synthesized nanoparticles of bare TiO₂ and doped with 1 mole %, 3 mole % and 5 mole % concentrations of Cu nanoparticles performed at room temperature using Cu-Kα radiations (λ=1.5406 Å) in order to access the information of phase formation and crystalline structure of material is shown in Figure 3.1. The X-ray diffraction peaks (101), (004), (200), (105), (211), (204), (116), (220), and (215) of bare TiO₂ corresponding to diffraction angles at 2θ = 25.4°, 38.02°, 48.14°, 54.12°, 55.18°, 62.81°, 68.71°, 70.28°, and 75.30° could be attributed to the anatase phase TiO₂, respectively (JCPDS 21-1272). Figure 1 reveals that due to small amount of Cu ion doping into TiO₂ lattice no characteristic diffraction peak of Cu was not found, but diffraction peak (101) initially decreases and then increases as doping concentration increases as indicated in inset of Figure 1 and Table 3.3. Further careful analysis shows diffraction peak intensity of planes (105) and (211) increases with Cu doping in TiO₂.

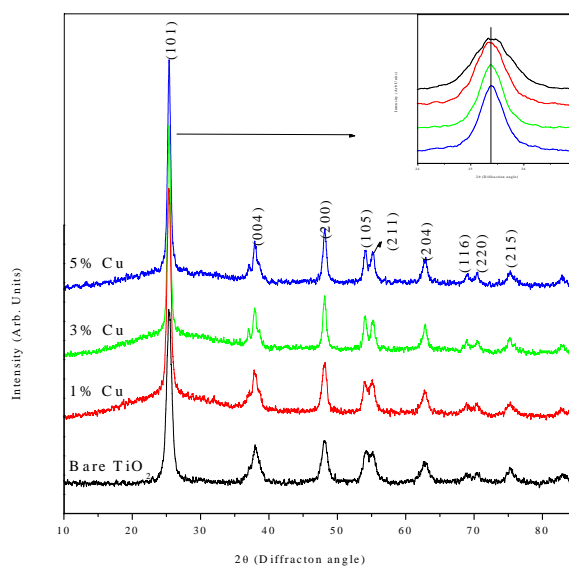


Figure 1: X-ray Diffraction Pattern for bare TiO₂ and Cu-doped TiO₂ nanoparticles

The average crystallite size of all the samples was calculated from the Full Width at Half Maximum (FWHM) (β) of all major diffraction peaks of anatase, using the Debye-Scherer method. The obtained results of the average crystallite size (D) influenced with Cu doping was tabulated in Table - I. The variation of crystallite size with Cu mole% was shown in Figure 2 and it is observed that due to Cu doping crystallite size increases.

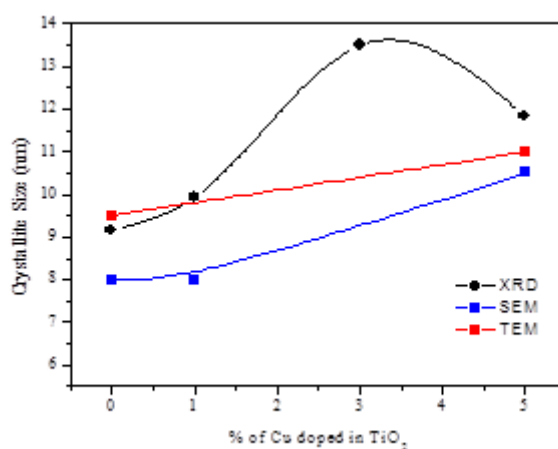


Figure 2: Variation of crystallite size with % of Cu doped in TiO₂ nanoparticles

B. Fourier transform infrared spectroscopy (FTIR)

FTIR spectroscopy mainly used to know the different functional moieties appeared from the bare TiO₂ and 1, 3 and 5 mole% of Cu doped TiO₂; and the results are shown in the figure 3. FTIR spectrum of various mole % of Cu doped TiO₂ shows the frequency regions at 3600 to 2750, and 1635cm⁻¹ corresponding to the O-H stretching, O-H deformation frequency vibrations respectively. All these frequency vibrations originated from the Cu doped into the TiO₂. Also, shows the broad frequency vibrations in the range between 900-400 cm⁻¹, corresponding to the Ti-O, O-Ti-O stretching vibrations from the lattice formation bands of TiO₂ [26] After the stoichiometric addition of Cu into the TiO₂, the insignificant shifting of the peak positions to the higher frequency regions.

Also, it shows the Ti-O peak in the region between 900-400 cm^{-1} border to that of doped TiO_2 , it may be due to the different interfaces of O-Ti-O, Ti-O, Cu-O, and Cu-O-Ti after the incorporation of Cu content.

TABLE -I: The average crystallite size

Bare TiO_2			1 % Cu			3 % Cu			5 % Cu		
2 θ	β	D (nm)	2 θ	β	D (nm)	2 θ	β	D (nm)	2 θ	β	D (nm)
25.41	0.81	10.03	25.37	0.71	11.50	25.38	0.56	14.50	25.40	0.55	14.85
38.03	1.28	6.58	37.92	1.31	6.42	37.95	0.95	8.83	38.00	1.03	8.15
48.14	0.91	9.53	48.11	0.69	12.61	48.14	0.52	16.83	48.16	0.55	15.83
54.13	0.79	11.34	54.65	1.50	5.96	55.12	0.85	10.59	54.87	1.50	5.98
62.81	1.16	8.01	62.79	0.71	13.19	62.82	0.56	16.67	62.83	0.65	14.34
Average D (nm)		9.10			9.94			13.49			11.83

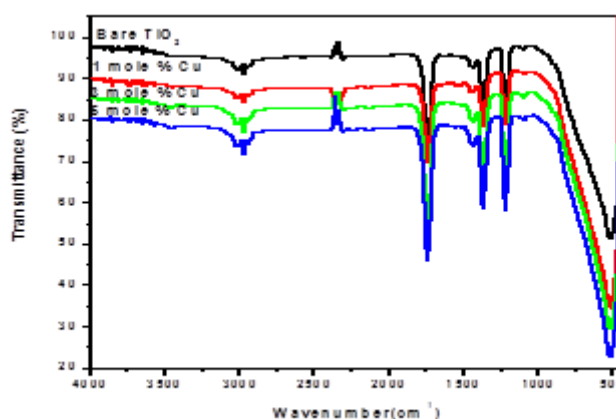


Figure 3: FTIR spectra of bare TiO_2 and Cu-doped TiO_2 nanoparticles

C. Field emission scanning electron microscopy (FESEM)

Figure 4(a), (c) and (e) shows the SEM images of bare TiO_2 and 1, 3 and 5 mole % Cu doped TiO_2 prepared by sol-gel method and calcined at 500°C . It is apparent from these images that the Cu doped TiO_2 NPs having non-spherical shape with an average diameter of 8-9 nm of its particle size. The particle size of these samples was estimated by measuring the diameter of the particles from Gaussian fitting of Histograms. Figure 3.13 (b, d, f) represents the particle size distribution Gaussian fitting of Histograms, and average particle size is determined. The histogram shows an average size distribution is 9 nm. The average particle size determined from Gaussian fitting is in close agreement with the particle size calculated from XRD analysis. After Cu doping, a notable changing for the surface morphology is observed; the surface becomes smooth and lots of grains are homogeneously dispersed onto the catalyst. The tailored surface morphology by Cu doping makes the TiO_2 grains well presenting as the photocatalytic sites, meanwhile the formed micro pores on the surface of doped TiO_2 also result in a large specific surface area which is helpful for adsorbing/degrading the pollutants. The disparity of particle size with mole % of Cu is shown in Figure 4

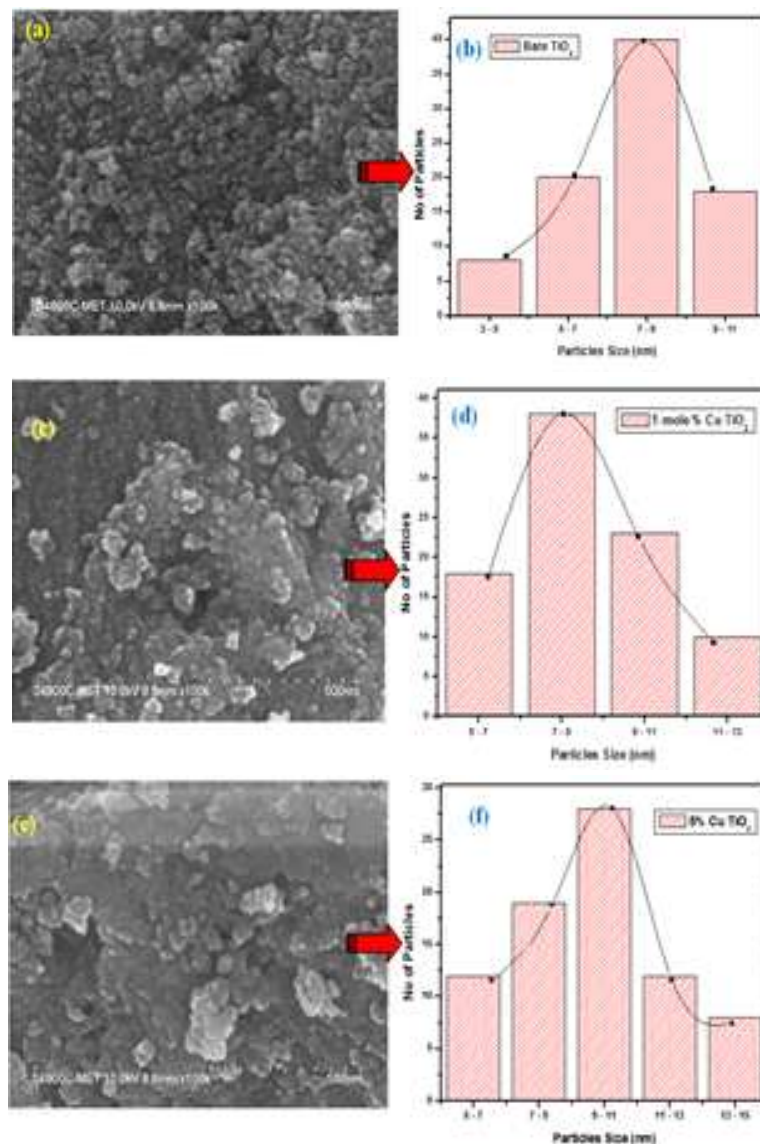


Figure 4: FESEM images of (a) bare TiO₂, (c) 1 mole% and (e) 5 mole% Cu doped TiO₂ and (b), (d) and (f) corresponding histograms of samples

D. EDAX analysis

The elemental composition of Cu doped TiO₂ spheres with varying amounts of Cu loading calcined at 500 °C was analyzed using EDAX. EDAX was used to determine the elemental composition of the nanoparticles and the representative patterns are shown in Figure 5 (a), (b) and (c). These patterns reveal the presence of Ti, Cu, O elements in the doped samples element. It can be observed that the intensity of the Cu peak corresponding to emission lines at 0.9 keV(K α 1), 8.20 keV (L α 1) and 8.9 keV (L α 1) increases with increasing Cu doping by comparing the EDAX spectra of the Cu doped samples with that of bare TiO₂. The presence of a 0.3, 0.4, 0.5, 0.6, 4.5 and 4.9 keV (L α 1) peaks are attributed to the Ti and O. In Figure 5 (a), only Ti and O elements were detected in bare TiO₂ powder, while in Figure 5 (b) and (c), Cu was detected in addition to Ti and O elements in Cu doped TiO₂, indicating that Cu was successfully doped on the TiO₂. Elemental composition in weight% and atomic% is shown in Table-II

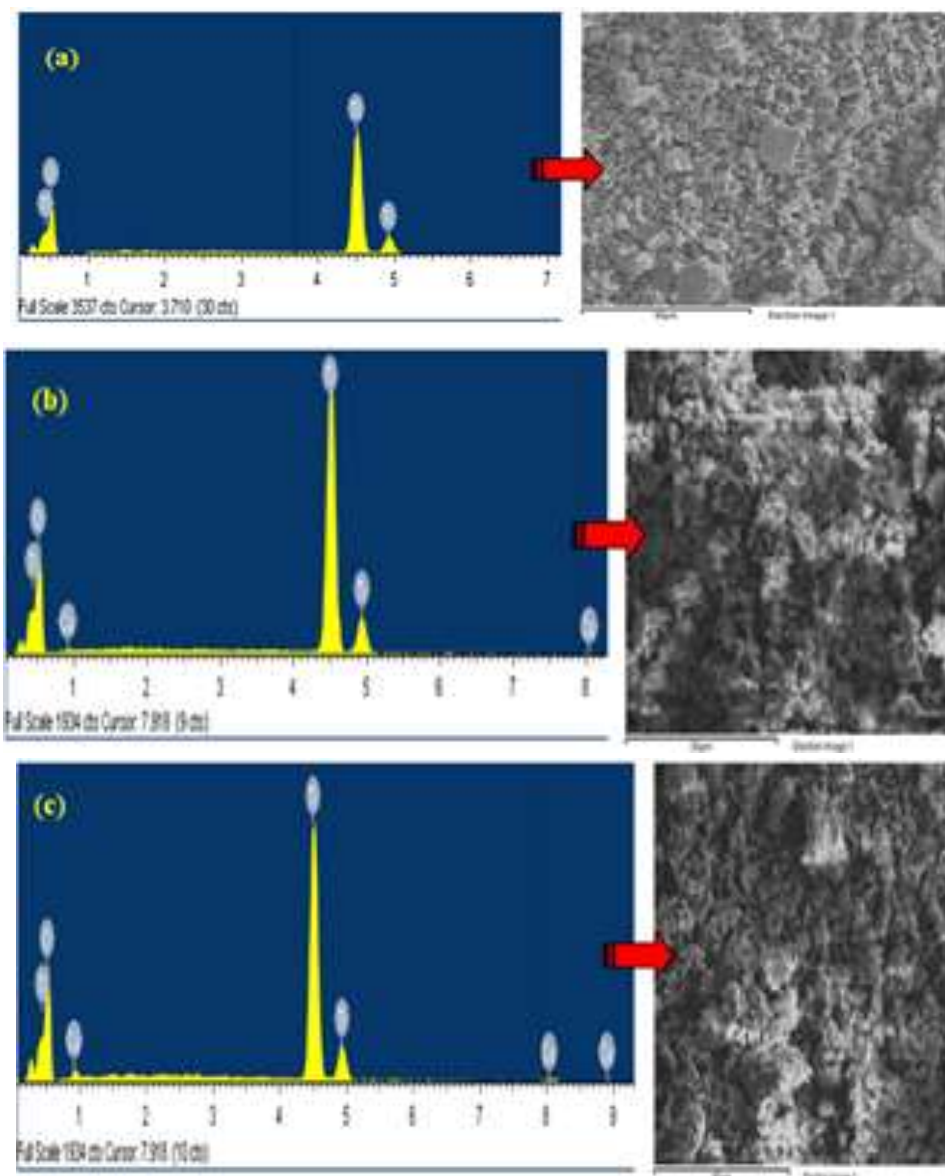


Figure 5: Elemental composition of (a) bare TiO₂, (b) 1mole % Cu, and (c) 5 mole % Cu doped TiO₂ nanoparticles and the representative patterns of EDAX

TABLE - II: Elemental composition in weight% and atomic%

Sample	Element	Weight%	Atomic%
Bare TiO ₂	O K	22.78	46.90
	Ti K	77.22	53.10
	Cu L	0	0
1 mole % Cu	O K	22.94	47.14
	Ti K	76.85	52.75
	Cu L	0.22	0.11
5 mole % Cu	O K	23.56	48.13
	Ti K	74.74	50.99
	Cu L	1.70	0.88
Totals		100%	

D. High resolution transmission electron microscopy (HR-TEM)

Surface morphology and particle structure of bare and 5 mole % Cu doped TiO₂ nanoparticles was analyzed by using HR-TEM. The representative HR-TEM images of the bare TiO₂ are shown Figure 6 (a) to (d) shows the TEM, high-resolution TEM (HR-TEM), histogram of particle size and selected area electron diffraction (SAED) pattern. These images substantiate that the bare TiO₂ particles show a spherical-like structure with a size distribution from 9 to 11 nm. While images of 5 mole % Cu doped TiO₂ shown in Figure 7(a) to (d) confirm that the nanoparticles are non uniform in shape with an average size of 10-11 nm. The nanoparticles are noticeably observed in all the images, which signify the high degree of crystallinity. The particle size of 5 mole % Cu doped TiO₂ nanoparticles are slightly higher to that of bare TiO₂ NPs, which is analogous with the crystallite size obtained from XRD. Moreover, observation by SAED Figure 6 (d) and in Figure 7 (d) confirmed that the nanoparticles are well crystalline in nature with tetragonal anatase structure.

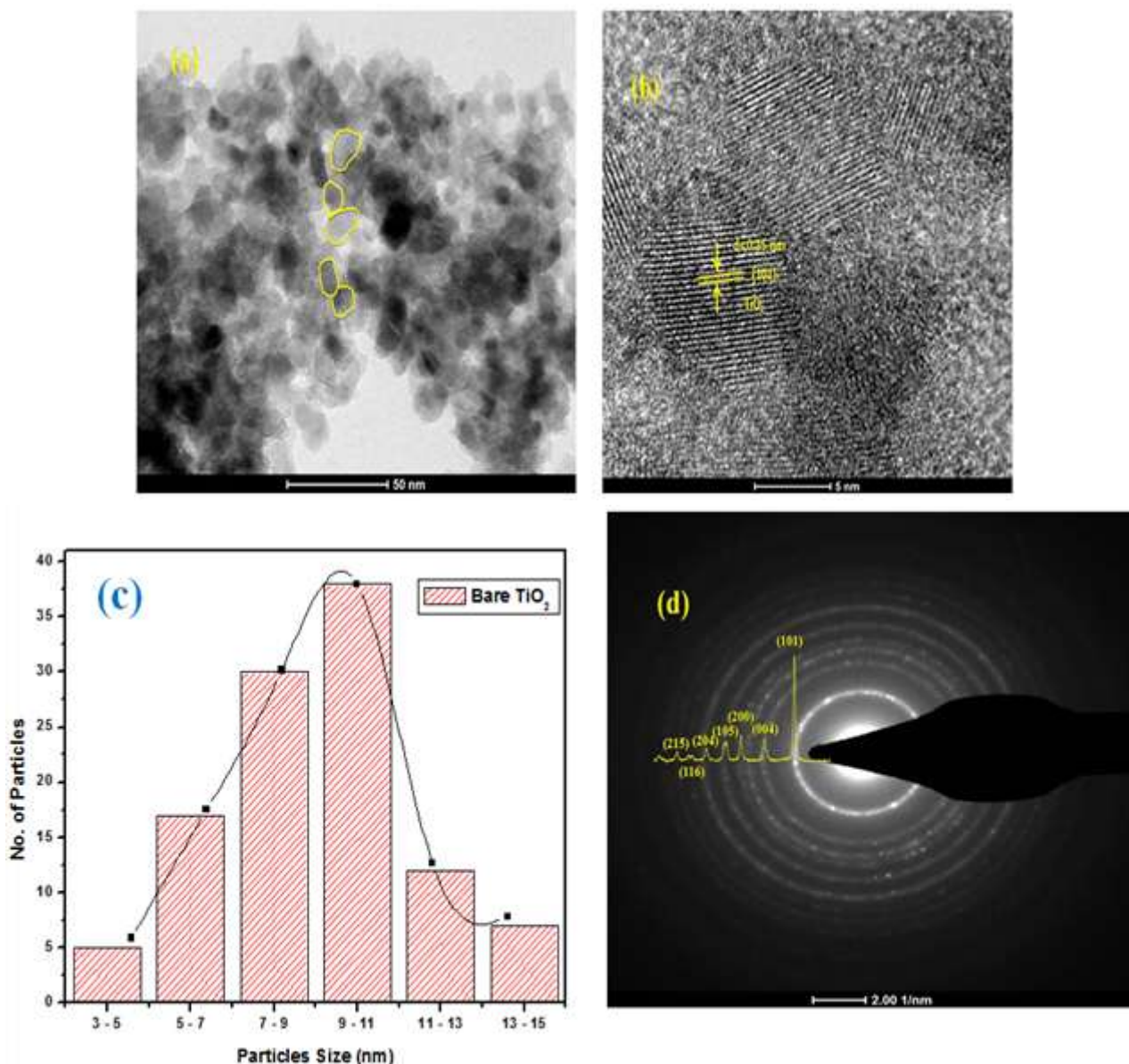


Figure 6 : (a, b, c, d) shows the TEM, High-resolution TEM (HR-TEM), Histogram of particle size and selected area electron diffraction (SAED) pattern for bare TiO₂

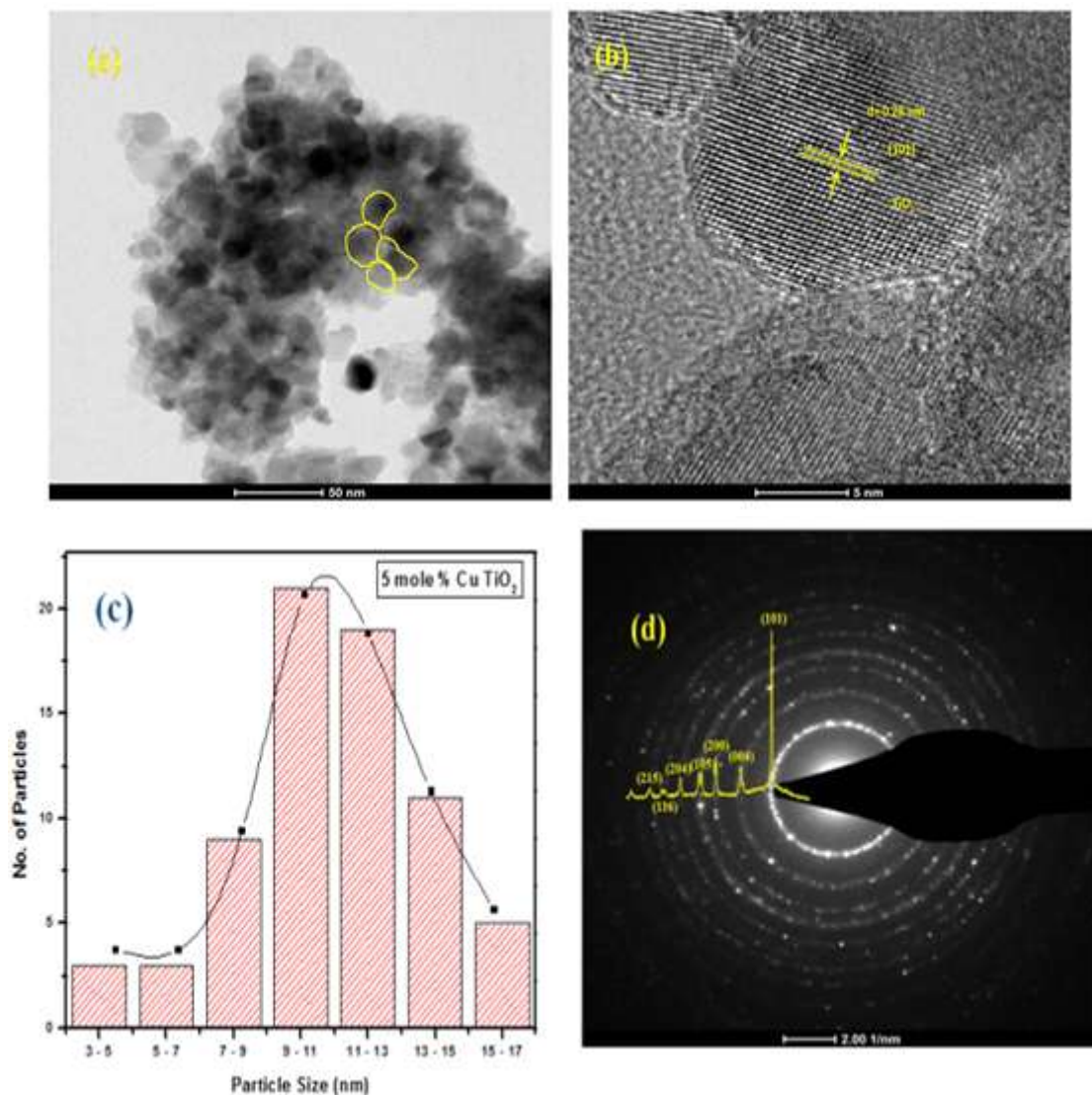


Figure 7: (a, b, c, d) shows the TEM, High-resolution TEM (HR-TEM), Histogram of particle size and selected area electron diffraction (SAED) pattern for 5 mole % Cu doped TiO₂

E. UV-Visible diffuse reflectance spectroscopy

UV-Visible diffused reflectance spectroscopy (DRS) was used for the investigation of the optical properties and band gap energies of the synthesized materials. Figure 8(a) shows the UV-Visible DRS (absorption mode) spectra of bare TiO₂ NPs shows the optical absorption edge in the wavelength region between 250 to 390 nm [1], while compared to Cu doped TiO₂ (1, 3 and 5 mole % Cu) shows the shifting its absorption edge from UV to visible region, indicates doping of Cu in the TiO₂ lattice [2]. As the mole% of Cu increases in the TiO₂, the visible absorption edge shifted towards higher absorbance as well as higher wavelength region; this is reflected through decrease in the optical band gap [3]. The Cu-doped TiO₂ samples indicated a red shift extending up to 500 nm. This is attributed to the characteristic surface Plasmon resonance of Cu nanoparticles. The successful doping of Cu is also evident from the change in the color observed in the samples, shifting from pure white to light green. The optical energy band gap of the Cu doped TiO₂ was determined by plotting the Tauc plot $(\alpha h\nu)^2$ as a function of photon energy ($h\nu$) and fixed from the intercept tangent to the x-axis [1] and presented in Figure 8(b).

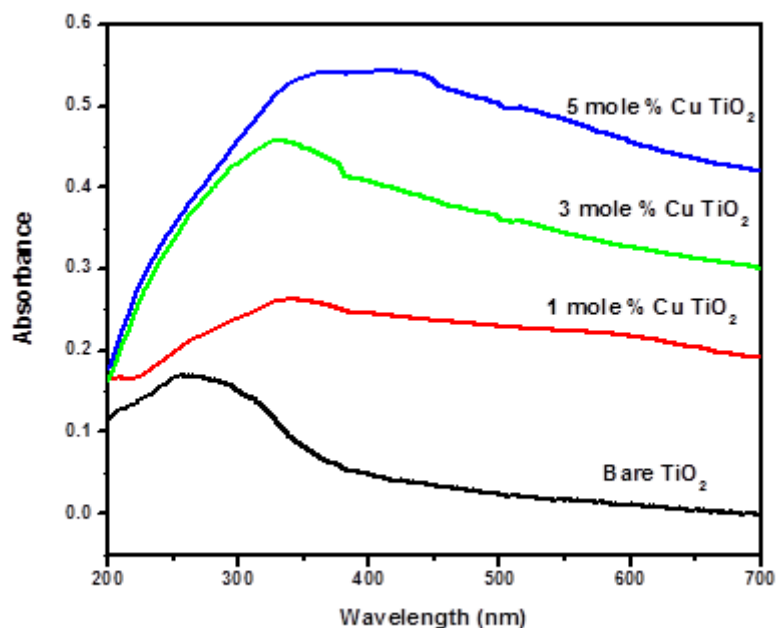


Figure 8(a): UV-Visible DRS (absorption mode) spectra of bare TiO₂ and 1, 3 and 5 mole % Cu doped TiO₂ NPs

The energy band gap decreases from 3.2 to 1.90 eV as the doping of mole % of Cu increases as 1, 3 and 5 mole %. The doping of copper in the TiO₂ lattice, the band gap is lowered to 2.56 eV for 1 mole% Cu, further reduced to 2.31 eV for 3 mole% Cu and 1.90 eV for 5 mole% Cu doping in TiO₂. This absorption enhancement with decrease in band gap in the visible region can be assigned to the formation of dopant level nearer the valance band [4-6]. The decrease in the optical energy band gap of the Cu doped TiO₂ NPs, leads to increase in optical absorption.

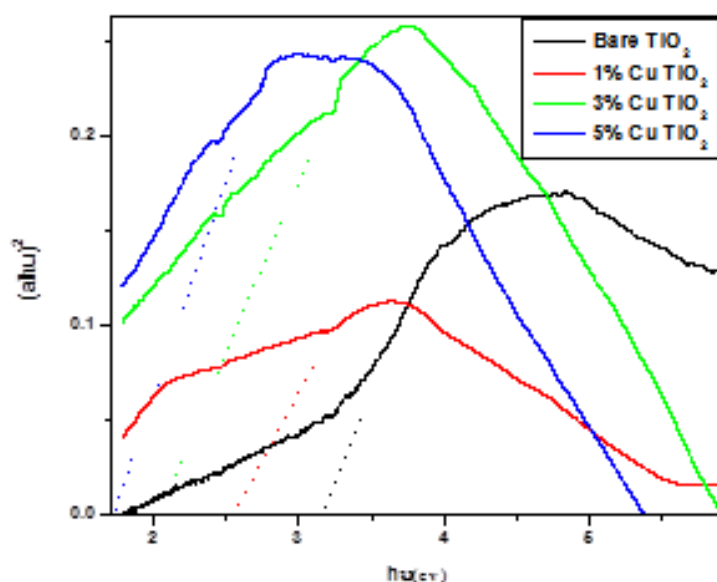


Figure 8(b): Tauc plot $(\alpha h\nu)^2$ as a function of photon energy $(h\nu)$ of TiO₂ and Cu doped TiO₂ NPs with 1, 3, and 5 mole % Cu

IV. CONCLUSION

The Cu doped TiO₂ nanoparticles were successfully synthesized at room temperature by using simple *sol-gel* method. The visible region's optical absorption was improved by the Cu²⁺ ion doping in TiO₂, according to research using UV-visible diffuse reflectance spectroscopy. As the mole% of Cu is doped, the energy band gap shrinks from 3.2 to 1.90 eV. The non-spherical shape of Cu-doped TiO₂ NPs, with an average diameter of 8–9 nm of their particle size, is shown by FESEM and HR-TEM investigation. Using a variety of spectral and microscopic methods, the impact of Cu doping on the optical and structural characteristics of the TiO₂ was investigated. Strong proof of the pure anatase phase and tetragonal structure is provided by XRD analysis of all the desired NMs. The addition of Cu as a dopant on TiO₂ was tuning the band gap into visible region and providing the higher surface area to the TiO₂ NPs to avert agglomeration, which confirmed by UV-DRS, XRD, SEM with EDAX and HR-TEM analysis. After Cu doping, a notable changing for the surface morphology is observed; the surface becomes smooth and lots of grains are homogeneously dispersed onto the catalyst. The tailored surface morphology by Cu doping makes the TiO₂ grains well presenting as the photocatalytic sites, meanwhile the formed micro pores on the surface of Cu doped TiO₂ also result in a large specific surface area which is helpful for the catalytic activities on their surfaces. The synthesized mole % of Cu doped TiO₂ NPs, having higher surface area, lower optical energy band gap, lower charge transfer resistance, lesser charge recombination rate; which enhanced the overall absorption in the visible region.

V. REFERENCES

- [1]. G. Cheng, M. S. Akhtar, O.-B. Yang, F. J. Stadler, ACS Appl. Mater. Interfaces 2013, 5, 6635–6642.
- [2]. V. c. Stengl, D. Popelková, P. Vláčil, J. Phy. Chem.C 2011, 115, 25209–25218.
- [3]. J. T. Robinson, S. M. Tabakman, Y. Liang, H. Wang, H. Sanchez Casalongue, D. Vinh, H. Dai, J. Am. Chem. Soc. 2011, 133, 6825–6831.
- [4]. W. Choi, A. Termin, M.R. Hoffmann, J. Phys. Chem. 98 (1994) 13669.
- [5]. T. Umebayashi, T. Yamaki, H. Itoh, K. Asai, J. Phys. Chem. Solids 63 (2002) 1909.
- [6]. J. Ben Naceur, R. Mechiakh, F. Bousbih, R. Chtourou, Appl. Surf. Sci. 257 (2011) 10699.
- [7]. Y. Yao, L. Guan, Y. Ma, M. Yao, J. Mater. Sci. Mater. Electron. 28, 3013 (2017)
- [8]. H. Gao, Z. Mo, Y. Wang, X. Niu, Z. Li, Mater. Sci. Mater. Electron. 28, 14543(2017)
- [9]. Y. Liu, D. Zhang, Mater. Sci. Mater. Electron. 28, 4965 (2017)
- [10]. D. Guerrero-Araque, D. Ramírez-Ortega, R. Gómez, P. Acevedo- Peña, Mater. Sci. Mater. Electron. 28, 9859 (2017)
- [11]. L. Gurunathan, V. Ponnusamy, Mater. Sci. Mater. Electron. 28, 18666 (2017)
- [12]. P. Govindhan, C. Pragathiswaran, Mater. Sci. Mater. Electron. 28, 5063 (2017)
- [13]. M.R.D. Khaki, M.S. Shafeeyan, A.A.A. Raman, W.M.A.W. Daud, Application of doped photocatalysts for organic pollutant degradation— A review. J. Environ. Manage. 198, 78–94 (2017)
- [14]. O. Aviam, G. Bar-Nes, Y. Zeiri, A. Sivan, Accelerated biodegradation of cement by sulfuroxidizing bacteria as a bioassay for evaluating immobilization of low-level radioactive waste. Appl. Environ. Microbiol. 70, 6031 (2004)
- [15]. M.L. Krumme, S.A. Boyd, Reductive dechlorination of chlorinated phenols in anaerobic upflow bioreactors. Water Res. 22, 171–177 (1988)

- [16]. M.R.D. Khaki, M.S. Shafeeyan, A.A.A. Raman, W.M.A.W. Daud, Evaluating the efficiency of nano-sized Cu doped TiO₂/ ZnO photocatalyst under visible light irradiation. *J. Mol. Liq.* (2017). <https://doi.org/10.1016/j.molliq.2017.11.030>
- [17]. O. Carp, C.L. Huisman, A. Reller, Photoinduced reactivity of titanium dioxide. *Prog. Solid State Chem.* 32, 33–177 (2004)
- [18]. A. Fujishima, T.N. Rao, D.A. Tryk, Titanium dioxide photocatalysis. *J. Photochem. Photobiol. C* 1, 1–21 (2000)
- [19]. U.I. Gaya, A.H. Abdullah, Heterogeneous photocatalytic degradation of organic contaminants over titanium dioxide: a review of fundamentals, progress and problems. *J. Photochem. Photobiol. C* 9, 1–12 (2008)
- [20]. S.R. Pouran, A. Bayrami, A.A.A. Raman, W.M.A.W. Daud, M.S. Shafeeyan, A. Khataee, Comprehensive study on the influence of molybdenum substitution on characteristics and catalytic performance of magnetite nanoparticles. *Res. Chem. Intermed.* 44, 883–900 (2018)
- [21]. S.R. Pouran, M.S. Shafeeyan, A.A.A. Raman, W.M.A.W. Raman, A. Bayrami, Transition metal-substituted magnetite as an innovative adsorbent and heterogeneous catalyst for wastewater treatment, in *Adsorption Processes for Water Treatment and Purification* (Springer, Cham, 2017), pp. 225–247
- [22]. S.R. Pouran, A.A. Aziz, W.M.A.W. Daud, M.S. Shafeeyan, Effects of niobium and molybdenum impregnation on adsorption capacity and Fenton catalytic activity of magnetite. *RSC Adv.* 5, 87535–87549 (2015)
- [23]. S.R. Pouran, A. Bayrami, A.A. Aziz, W.M.A.W. Daud, M.S. Shafeeyan, Ultrasound and UV assisted Fenton treatment of recalcitrant wastewaters using transition metal-substituted-magnetite nanoparticles. *J. Mol. Liq.* 222, 1076–1084 (2016)
- [24]. S.R. Pouran, A. Bayrami, M.S. Shafeeyan, A.A.A. Raman, W.M.A.W. Daud, A comparative study on a cationic dye removal through homogeneous and heterogeneous Fenton oxidation systems. *Acta Chim. Slov.* (2018). <https://doi.org/10.17344/acsi.2017.3732>
- [25]. J.-Y. Park, K.-I. Choi, J.-H. Lee, C.-H. Hwang, D.-Y. Choi, J.-W. Lee, Fabrication and characterization of metal-doped TiO₂ nanofibers for photocatalytic reactions. *Mater. Lett.* 97, 64–66 (2013)
- [26]. Sandip B. Deshmukh, Kalyani H. Deshmukh, Maheshkumar L. Mane, and Dhananjay V. Mane, *Macromol. Symp.* 2021, 400, 2100071. DOI: 10.1002/masy.202100071
- [27]. Mangesh G. Bhosale, Radhakrishna S. Sutar, Sandip B. Deshmukh, Meghshyam K. Patil Photocatalytic efficiency of sol-gel synthesized Mn-doped TiO₂ nanoparticles for degradation of brilliant green dye and mixture of dyes, *J Chin Chem Soc.* 2022;1–14. DOI: 10.1002/jccs.202200248

Study of Structural and Electrical Properties of Zinc Sulphide Films Prepared By Spray Pyrolysis Techniques

Asif Karim, Sayed Mujeeb

Sir Sayyed College of Arts, Commerce and Science, Aurangabad, Maharashtra, India

ARTICLE INFO

Article History:

Published : 27 January 2025

Publication Issue :

Volume 12, Issue 10

January-February 2025

Page Number :

70-73

ABSTRACT

A thin film of zinc sulphide (ZnS) has been deposited by chemical spray techniques using a mixed aqueous solution of zinc sulphate (ZnSO₄) and thiourea (Sc (NH)₂)₂. The spray solution with molar concentrations of 0.1M, 0.2M, and 0.3M ZnS thin films was grown onto a hot glass substrate at a substrate temperature 500 0C. The X-ray diffraction pattern (XRD) of all the films deposited shows a hexagonal Wurtzite crystal-type structure. Microstructure has been analysed using scanning electron microscopy (SEM).

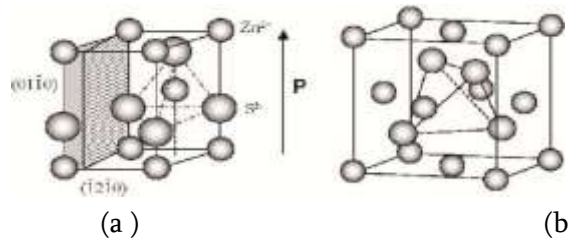
I. INTRODUCTION

Zinc sulphide has grown in interest owing to its possible applications in optoelectronics. It is an important II-IV semiconductor material for the development of various technologies of solid-state devices. Zinc Sulphide has a direct band gap of about 3.50 eV in the UV region. Zinc Sulphide films are used in optoelectronics devices, Light-emitting diodes, displays, and multilayer displays (1,2)Zinc has hexagonal Wurtzite and cubic zinc Blend structure. The relation determines the lattice constant (a) for cubic structure.

$a = d(h^2 + k^2 + l^2)^{1/2}$ where (hkl) are Miller indices

For hexagonal lattice constant (a) determined from the relation

$$\frac{1}{d^2} = \frac{4}{3} \left(\frac{h^2 + hk + k^2}{a^2} \right) + \frac{l^2}{c^2}$$



(a)The Wurtzite ZnS Structure. (b) The Zinc Blend Structure for the II-IV Semiconductors (4)

ZnS thin films have been deposited by various techniques including spray pyrolysis, chemical bath deposition (CBD), photochemical deposition, Metal-organic chemical vapour deposition techniques (MOCVD), electron beam evaporation, Vacuum deposition techniques, photochemical deposition techniques and pulse LASER deposition techniques .(6,14)

Every thin film deposition technique has its advantages and disadvantages. Chemical spray pyrolysis is a well-established technique for depositing thin films of various technologically important materials. Various chalcogenides such as Zn, Co, Cd, Hg, Pb sulphides and selenides have been deposited using this technique. In the present case, the chemical spray pyrolysis technique has been used for the deposition of ZnS thin films, as it is simple, relatively less expensive and convenient for large-area deposition. In recent years, interest in the deposition of thin films of a material using different deposition techniques has considerably increased.

The purpose of the present work is to investigate the effect of the preparative parameters of the spray pyrolysis technique on ZnS thin films. The effect of the molar concentration of the starting solution on the structural characteristics of the films (crystallinity, phases and crystallographically preferred orientations) has been studied using X-ray diffraction. The molar concentration variations also affect the electrical properties. The structural and electrical properties have been investigated by using a scanning electron microscope and two-probe method.

II. EXPERIMENTAL:

Zinc sulphide thin films are deposited on glass substrates using a spray pyrolysis technique in an air atmosphere. The deposition method involves the thermal decomposition of an aqueous solution of zinc sulphate and thiourea. Initially, a solution of 1M was prepared and from this source solution, the solutions of 0.1M, 0.2M, 0.3M and 0.4M concentrations were obtained. The resulting solutions were sprayed onto heated glass substrates held at a constant temperature of 500 °C keeping the other process parameters at optimized condition. Structural study was carried out using X-ray diffraction and SEM. X-ray diffraction spectra were obtained using CuK α ($\lambda=1.5406\text{\AA}$) radiation and scanning angle 2θ was varied in the range between 10° to 90° . The interplanar distance, lattice parameter, preferential growth orientations and grain size were evaluated from these spectra. Scanning electron micrographs (SEM) were obtained using JOEL JSM- 6360A equipped with an energy-dispersive X-ray spectrometer (EDAX) facility. Transmittance and absorbance measurements were carried out using a spectrophotometer in a wavelength range 300 nm to 1100 nm.

Two probe methods have been used to measure the resistivity of the film at room temperature.

III.RESULT AND DISCUSSION:

3.1. Structural properties:

All the deposited ZnS films were white and homogeneous with a good adherence to the substrate. Generally ZnS material has the hexagonal, wurtzite-type structure or cubic, zinc blende-type structure. X-ray diffraction patterns of ZnS thin films prepared with different concentrations are shown in Fig.1. Comparison of interplanar (d) values with JCPDC data shows that the phase present in the deposited films belongs to pure hexagonal wurtzite structure without any impurity phases.

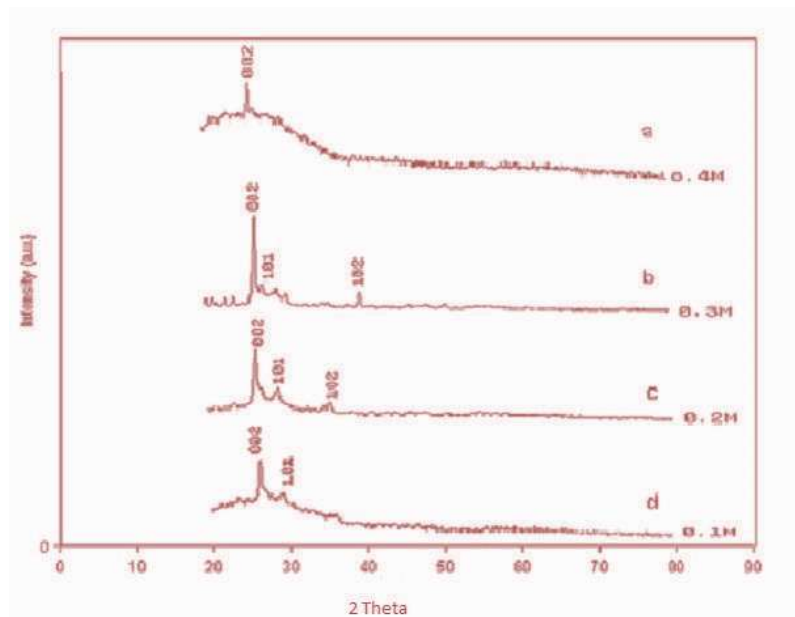


Fig 1 XRD patterns of ZnS films deposited at different concentrations of solution.

It is also noted that as the concentration of the solution increases, the intensity of (002) peak increases and this peak becomes narrower indicating an improvement of the crystallinity. It is also observed that the thickness of the films increases with increasing concentration. The effect of concentration on the grain size (GS) of the obtained phase was also investigated. The grain size has been determined from the (002) diffraction peak using the Scherrer formula. The grain size calculated by Scherrer's formula from XRD data was found to increase with increasing concentration and lies in the range 25 to 35 nm. The raising of molar concentration did not lead to the formation of any other impurity phases. The preferred orientation is seen from the increase in the intensity (002) plane with an increase in mole concentration.

Fig. 2 shows typical micrographs of ZnS thin films. The micrographs show a nearly uniform polycrystalline nature of the films and also show that the grain size decreased with a decrease in concentration. The elemental analysis was done only for Zn and S it was found to be 54.3: 43.5. Other peaks present in the spectra were of O, Na, and Cl. The presence of these elements is due to oxidation during the deposition on the hot substrate or the presence of these elements in the glass substrate.

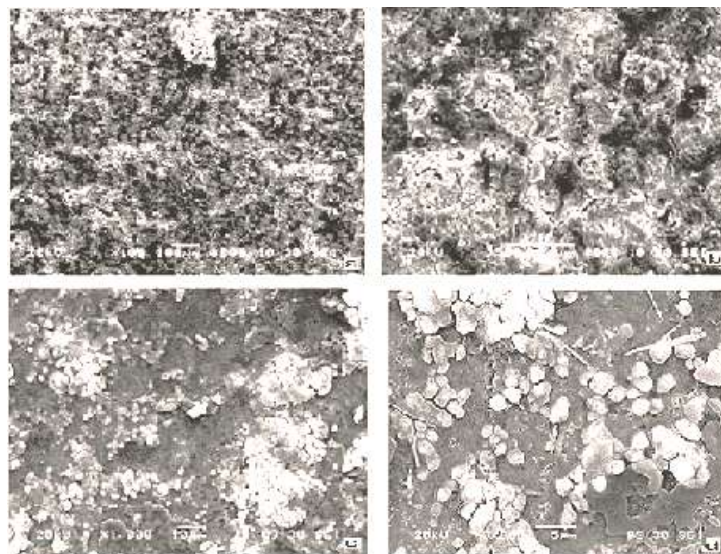


Fig. 2 SEM micrograph of ZnS thin films.

3.2. Electrical properties:

Fig. 3 shows the typical plot of temperature vs. resistance for ZnS thin film at room temperature for 0.1M. From the analysis of curves, it is observed that resistance decreases with an increase in temperature, which confirms the semiconducting nature of the deposited film.

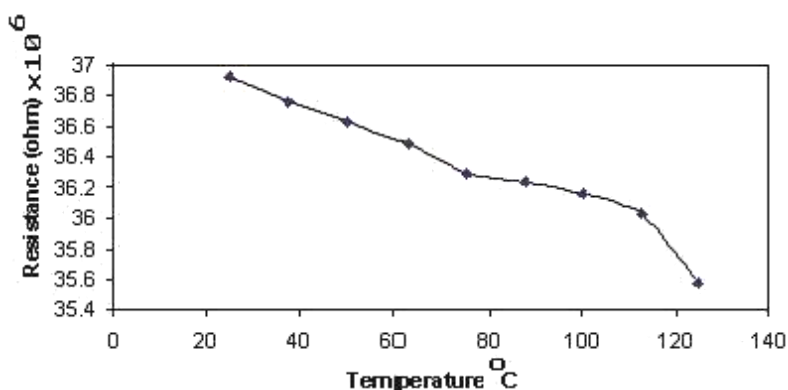


Fig. 3 Temperature vs. resistance for ZnS thin films.

IV. CONCLUSIONS

Good quality ZnS films were deposited using the spray pyrolysis method. The spray deposition of thin films of 0.1M, 0.2M, 0.3M and 0.4M concentration solutions at substrate temperature 5000C is found to be optimum for deposition of good quality films at the specified spray condition. Thin films of ZnS with hexagonal (wurtzite) phases have been prepared by the spray pyrolysis method. The decreases in resistance with an increase in temperature confirms the negative temperature coefficient of the deposited thin films.

V. REFERENCES

- [1]. K. Skwok and X. Sun, "Thin solid films", Vol.335,1998, p.229.
- [2]. A. Antony, K.V. Mirali, R. Manoj, M.K. Jayaraj, Mater Chem. Phy, Vol 90,2005. P. 106
- [3]. Y. Sirotin and M. Shaskolskaya," Fundamental of Crystal physics", Mir Publication, Moscow,1982.
- [4]. J. Mohammed "The study of structural and optical properties for thin film (PbS) and (ZnS)" , M.Sc. Thesis, University of Tikrit.2002.
- [5]. J. Sing "Optical properties of condensed matter and Application" , John Wiley & Sons,2006.
- [6]. A.U. Ubale, V.S. Sangawar and D.K. Kulkarni, Bull. of Mate.Sci. Vol.30 (2007), 147
- [7]. B. Elidrissi, M. Addou, M. Regragui, A. Bougrine, A. Kachouane, C.Bernede Mat. Chem. and Physics 68 (2001) 175
- [8]. A.U. Ubale and D.K. Kulkarni, Bull. of Mate. Sc. Vol.28 (2005),43.
- [9]. M. Gunasekaran, R. Gopalkrishanan, P. Ramasamy. Materials Letters 58 (2003) 67-70.
- [10]. Kook Won Seo, Seok Hwan Yoon, Seung S and Bull. Korean Chem. Soc. 26 (2005) 1582.
- [11]. Lytvyn, Khomchonko, Krystab, Lytvyn, Mazin, Prokopenk4 (2001) 19. A. Necmeddin Yazici, Mustafa Oztas, Metin Bedir: Journal of
- [12]. A.V. Feitosa, M.A.R. Miranda, J.M. Sasaki, M.A. Arajo-Silva, Braz. J. of Phy. 34 (2004) 1.
- [13]. B.R. Sampkal, R.S. Mane and C.D. Lokhande, Mat. Res. Bull. 35 (2000) 177.
- [14]. H. H. Afifi. , S. A. Mahmoud, A. Ashour Thin Solid Films, 263 (1995) 248
- [15]. Li Wenyi, Cai Xum Chen Qiulong, Zhou Zhibin, Mat. Lett. 59 (2004) 1.



Comprehensive Insights into Phenol Sulfonamides: Synthesis, Mechanistic Pathways, and Applications

Sumit R. Nikume*, Atul B. Patil, Ratnamala S. Bendre*

*School of Chemical Sciences, Kavayitri Bahinabai Chaudhari North Maharashtra University, Jalgaon-425001, Maharashtra, India

ARTICLE INFO

Article History:

Published : 27 January 2025

Publication Issue :

Volume 12, Issue 10

January-February 2025

Page Number :

74-84

ABSTRACT

Sulfonamides of phenol represent a crucial class of compounds with diverse applications in medicinal chemistry, environmental science, and synthetic organic chemistry. Their structural versatility enables a broad spectrum of biological activities, particularly as antimicrobial activity. This review discusses the synthesis, mechanistic insights, and key applications of phenolic sulfonamides, incorporating recent advancements in structural modifications and functionalization techniques. Additionally, their interaction with biological targets, environmental impact, and future research has been reviewed.

Keywords: Sulfonamides, Phenols, Synthesis, Medicinal Chemistry, Environmental Transformation, Catalysis

I. INTRODUCTION

Sulfonamides are an essential class of organic compounds described by the presence of a sulfonyl functional group attached to an amine [1,2]. These compounds have been widely explored due to their pharmacological significance, particularly as antimicrobial agents [3,4]. The introduction of a phenolic moiety into the sulfonamide framework enhances their chemical reactivity and biological functionality, leading to the development of more potent bioactive molecules [5-7].

Phenolic sulfonamides exhibit a broad spectrum of biological activities, including antibacterial, antifungal, anticancer, and enzyme inhibitory properties. Their ability to act as carbonic anhydrase inhibitors has been extensively studied, highlighting their potential in treating diseases such as glaucoma, epilepsy, and cancer [8-10]. Additionally, phenolic sulfonamides are gaining attention in synthetic chemistry due to their role in various catalytic and functionalization reactions, which further expands their applicability in drug development [11,12].

Recent advancements in synthetic methodologies have allowed for more efficient and selective modifications of phenolic sulfonamides, improving their pharmacokinetic properties and bioavailability. Furthermore, the environmental impact of sulfonamide-based pharmaceuticals has become a crucial research area, as their

persistence in soil and water bodies raises concerns regarding antibiotic resistance and ecological toxicity [13]. Therefore, a comprehensive understanding of their synthesis, chemical behavior, and biological significance is essential for the continued development of sulfonamide-based therapeutics and industrial applications. This review aims to provide an analysis of phenolic sulfonamides, focusing on their synthesis, structural modifications, mechanism of action, and diverse applications in medicinal and environmental chemistry. By integrating recent findings and emerging trends, this work seeks to contribute to the ongoing advancements in the field of sulfonamide research.

II. CLASSIFICATION OF PHENOLIC BASED SULFONAMIDES

Sulfonamide research into five major categories of domains: synthesis and functionalization, biological activity, environmental effects, structural studies, and drug discovery. The synthesis and functionalization section highlights various chemical modifications that enhance sulfonamide derivatives' structural diversity and functionality in **table 1**.

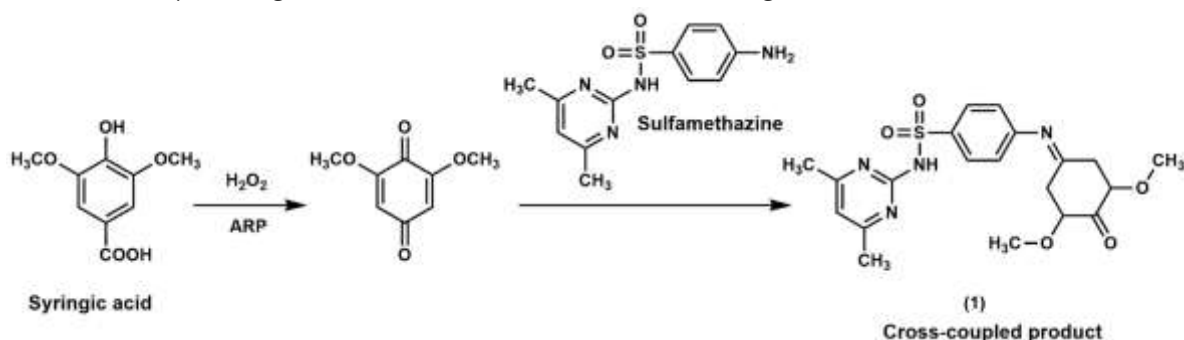
Table 1: Classification of Sulfonamide

Category	Research Focus	References
Synthesis & Functionalization	Cyclization & Ring Formation [14,15]	Crich et al., 2004; Liang & Ciufolini, 2010
	Sulfonylation & Acylation [16,17]	Reddy & Pasha, 2011; Massah et al., 2013
	Nitration & Halogenation [18]	Kilpatrick et al., 2013
	Metal Complexation [19]	Maurya & Patel, 2008
	Novel Synthetic Routes [20]	Smolobochkin et al., 2016
Biological & Pharmacological Activity	Carbonic Anhydrase Inhibitors [21,22]	Garaj et al., 2005; Innocenti et al., 2008
	Antimicrobial & Antibiotic Properties [23,24]	Ricken et al., 2013; Capasso & Supuran, 2015
	Anticancer Activity [25,26]	Gul et al., 2017; Bilginer et al., 2022
	Enzyme Inhibition [27,28]	Sarıkaya et al., 2010; Korkmaz et al., 2015
Environmental Effects & Degradation	Oxidative Transformation [29]	Bialk et al., 2005
	Microbial Biodegradation [23]	Ricken et al., 2013
	Soil & Water Contamination [30,31]	Schwarz et al., 2015; Paumelle et al., 2021
Structural & Computational Studies	Hydrogen Bonding Analysis [32]	Adsmond & Grant, 2001
	Quantum Chemical Calculations [33]	Shainyan et al., 2012
	Molecular Docking & Drug Design [34]	Durdagi et al., 2011
Drug Discovery & Future Applications	FDA Drug Analysis [35]	Scott et al., 2022
	Bio-isosteres & Medicinal Chemistry [36]	Dunker et al., 2024
	Novel Therapeutic Targets [24]	Capasso & Supuran, 2015

The biological activity section presents their roles as enzyme inhibitors, antibiotics, and anticancer agents, emphasizing their pharmaceutical significance. The environmental effects and degradation section discusses their persistence and transformation in ecosystems, underlining concerns regarding contamination and biodegradation. The structural and computational studies section provides insight into molecular interactions and stability, aiding drug development. Finally, the drug discovery and future applications section reflects their role in FDA-approved drugs, bioisosteric modifications, and therapeutic innovations. Together, these classifications demonstrate the versatility of sulfonamides in scientific research and their potential for further advancements.

III. LITERATURE STUDY

To grasp their change in natural organic matter, Bialk et al. (2005) reported the oxidative cross-coupling of sulfonamide (1) antibacterial agents with model humic components represented in Scheme 1. The work shows that covalent connections with humic materials result from major alteration of sulfonamides during incubation with phenoloxidases and manganese oxides. The authors provide proof that this chemical addition can lower the mobility and bioavailability of sulfonamides in the surroundings, therefore raising questions about their persistence and possible contribution to antimicrobial resistance. The results underline the need of knowing the environmental destiny of drugs and their interactions with natural organic matter [29].



Scheme 1: ARP-Mediated cross coupling of sulfamethazine with syringic acid

Three phenolic compounds phenol, 3,5-difluorophenol, and clioquinol were examined by Innocenti et al. (2008) as inhibitors of carbonic anhydrase. While clioquinol proved to be the most strong inhibitor tested overall, the research showed that phenol particularly suppressed CA isozymes I–IV, IX, XII, and XIV. The authors suggested that the phenolic hydroxyl group functions as a new "zinc-water binding group," implying a different inhibitory mechanism than conventional sulfonamide inhibitors (2), thereby stressing the possibility for the development of new CA inhibitors presented in figure 1 [37].

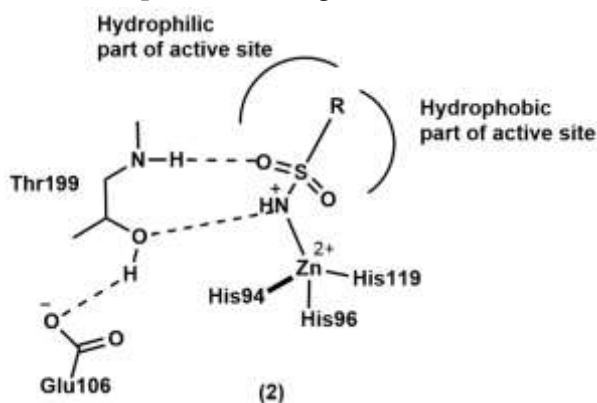


Figure 1: Schematic representation for interaction of CAIs with the CA active site sulfonamide inhibitors

The direction of hydrogen bonds in H-complexes developed from dimethylsulfone (3), N,N-dimethylmethanesulfonamide (4), and N,N-dimethyltrifluoromethanesulfonamide (5) with methanol and phenol was examined by Oznobikhina et al. (2009). The work found two forms of complexes using quantum chemical calculations (DFT method: bidentate complexes including both lone pairs of oxygen atoms and nonlinear structures). Reflecting the basicity of the sulfonyl group in the sequence dimethylsulfone > N,N-dimethylmethanesulfonamide > N,N-dimethyltrifluoromethanesulfonamide, the angle defining the directionality of the hydrogen bond varied greatly is given in figure 2. The results help to better grasp sulfonamides' hydrogen-bonding activity and self-association capacity [38].

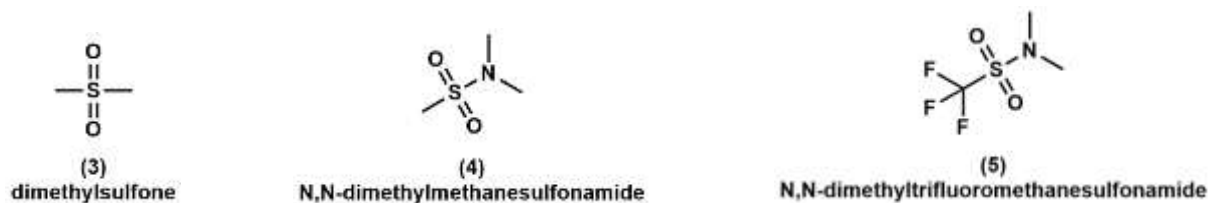


Figure 2: Structures containing sulfonyl group

Sarıkaya et al. reported several phenolic acids, including ellagic acid, gallic acid, ferulic acid, caffeic acid, quercetin, p-coumaric acid, p-hydroxybenzoic acid, and syringic acid, exhibited noteworthy inhibitory action against human carbonic anhydrase (hCA) isozymes I and II. Additionally, while this study primarily focused on phenolic acids, it referenced acetazolamide (AAZ) (6), a well-known sulfonamide-based carbonic anhydrase inhibitor, for comparison. Sulfonamides remain a clinically significant class of CA inhibitors widely used in the treatment of glaucoma, epilepsy, and other disorders [27].

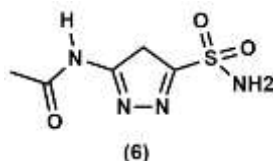
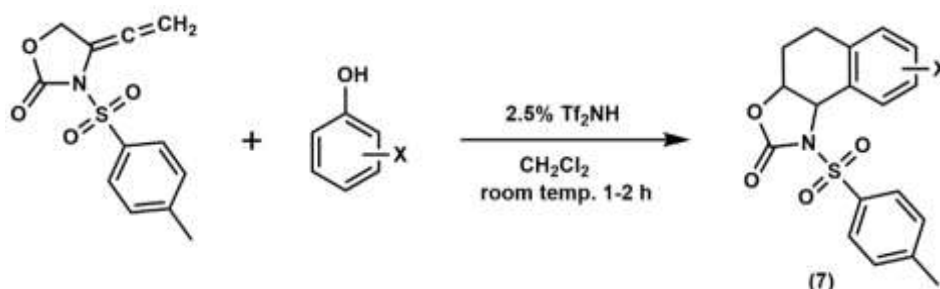


Figure 3: Acetazolamide (sulfonamide-based carbonic anhydrase inhibitor)

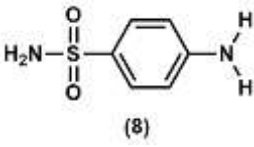
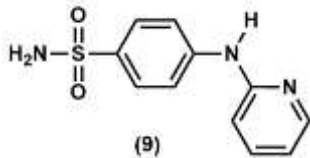
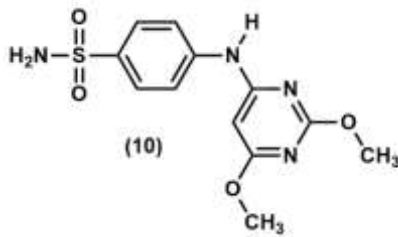
Using Brønsted acid catalysis, hashimoto et al. (2010) synthesized functionalized chromanes (7) via a formal [3 + 3] cycloaddition reaction between allene sulfonamides and phenols are given in scheme 2. The work suggested a mechanism wherein intramolecular cyclization followed a stepwise process of intermolecular hydroarylation. The authors improved reaction conditions to get large yields of chromane derivatives, therefore proving the possibility of this approach for synthesis of physiologically active chemicals. This study provides a simple methodology utilizing widely accessible starting materials and emphasizes the rare nature of Brønsted acid-catalyzed methods in chromane synthesis [39].



Scheme 2: Cycloaddition reaction between allene sulfonamides and phenols

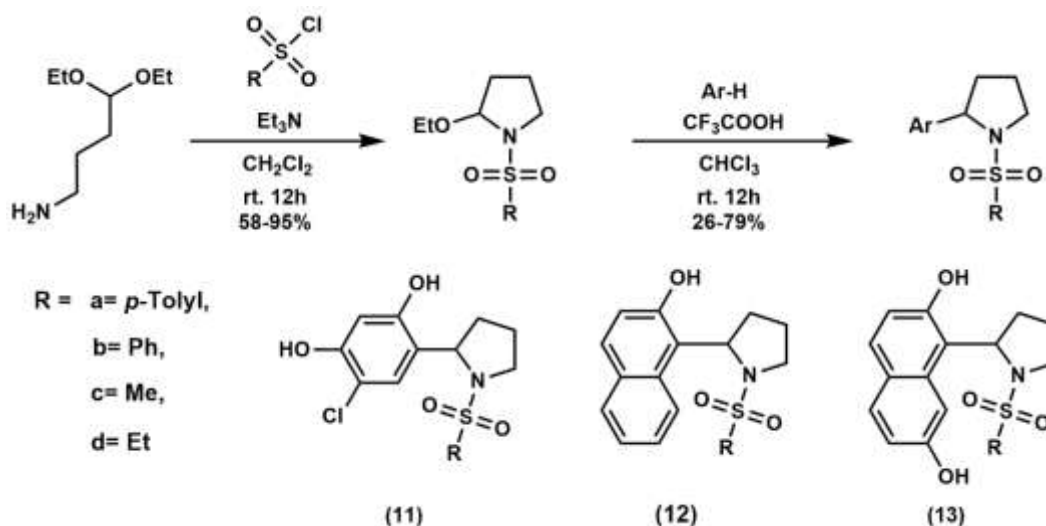
With laccase from *Trametes versicolor*, Schwarz et al. (2015) showed the enzymatic transformation and bonding of sulfonamide (8), (9) and (10) antibiotics to model humic compounds are given in table 2. The research showed that sulfonamides create nonextractable residues resistant to extraction techniques via fast transformation and sequestration in soil. Emphasizing the significance of knowing their destiny and behavior in soil systems, the authors found many bonding mechanisms including covalent binding and discussed the environmental consequences of sulfonamide persistence in agricultural soils [30].

Table 2: Selected compounds of sulfonamide (enzymatic transformation and bonding of sulfonamide antibiotics)

Structures			
C. Name	Sulfanilamide	Sulfapyridine	Sulfadimethoxine
M.F.	C ₆ H ₈ N ₂ O ₂ S	C ₁₁ H ₁₁ N ₃ O ₂ S	C ₁₂ H ₁₄ N ₄ O ₄ S

(*Note: C. Name- Common Name; M.F.- Molecular formula)

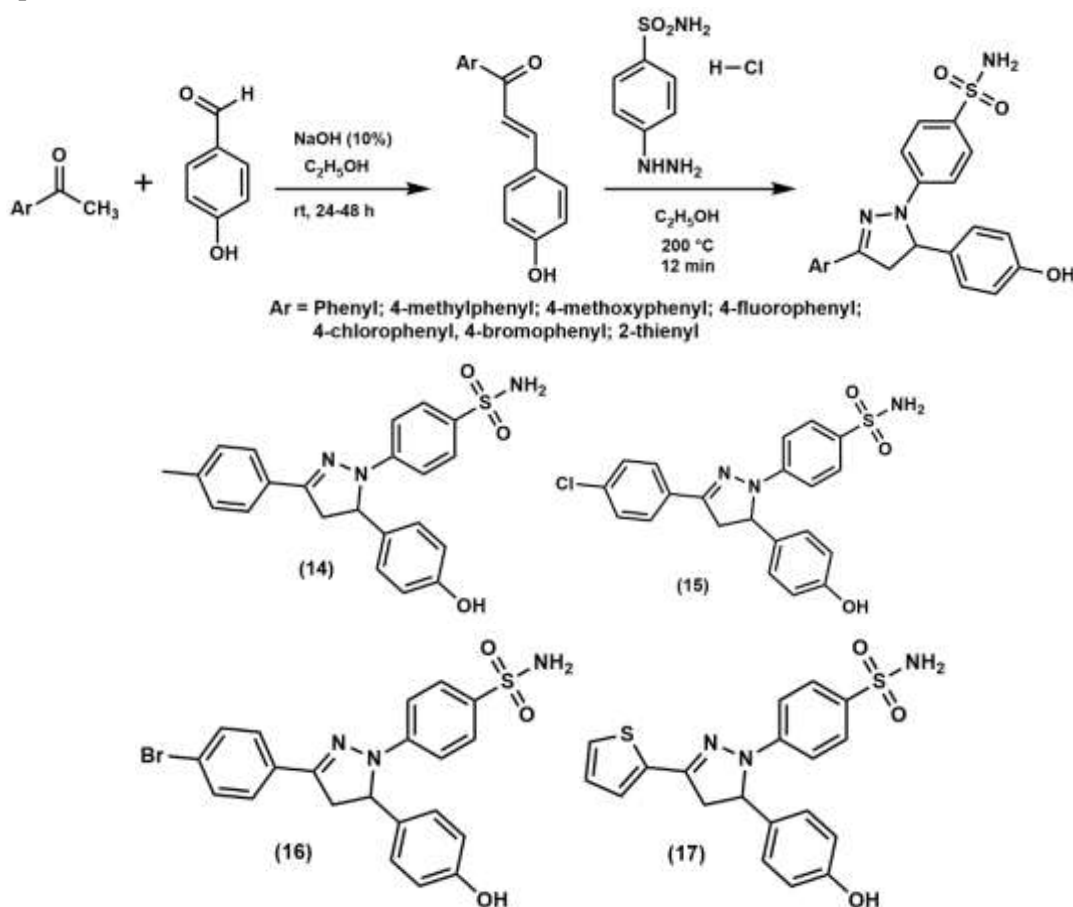
Using the reaction of phenols with N-(4,4-diethoxybutyl)sulfonamides in the presence of trifluoroacetic acid, Smolobochkin et al. (2016) devised a unique technique for synthesis of 2-aryl-1-sulfonylpyrrolidines (11), (12) and (13) in given scheme 3. The research emphasizes the benefits of this approach over current synthetic techniques often including expensive catalysts and severe conditions: high yields and gentle reaction conditions. NMR spectroscopy, IR spectroscopy, and X-ray structural analysis corroborated the structures of the synthesized compounds, therefore proving the possibility of this method for generating physiologically active sulfonamide derivatives [20].



Scheme 3: Synthesis of phenolic based 2-aryl-1-sulfonylpyrrolidines

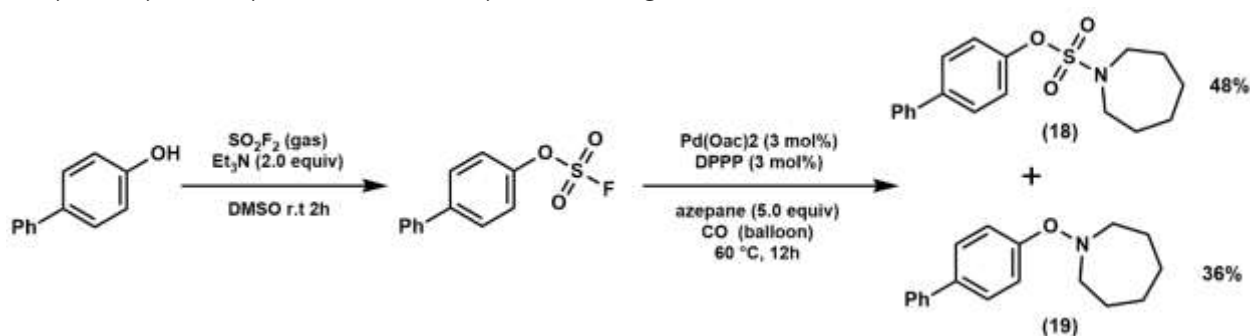
Specifically for 4-[5-(4-hydroxyphenyl)-3-aryl-4,5-dihydro-1H-pyrazol-1-yl]benzenesulfonamide compounds, Gul et al. (2017) described the microwave-assisted synthesis and bioevaluation of novel sulfonamide derivatives are given in scheme 4 verified the chemical structures of the synthesised compounds by using of NMR and

HRMS methods. These compounds cytotoxic activities were assessed in relation to human oral squamous cell carcinoma cell lines, therefore exposing notable anticancer effects. While compounds **16** and **17** showed low inhibition constants (K_i) against carbonic anhydrase I and II, suggesting their potential as lead compounds for further development in cancer therapy, compounds **14**, **15**, and **16** showed strong potency selectivity expression (PSE) values [40].



Scheme 4: Pyrazol based sulfonamide structures contain phenolic moiety

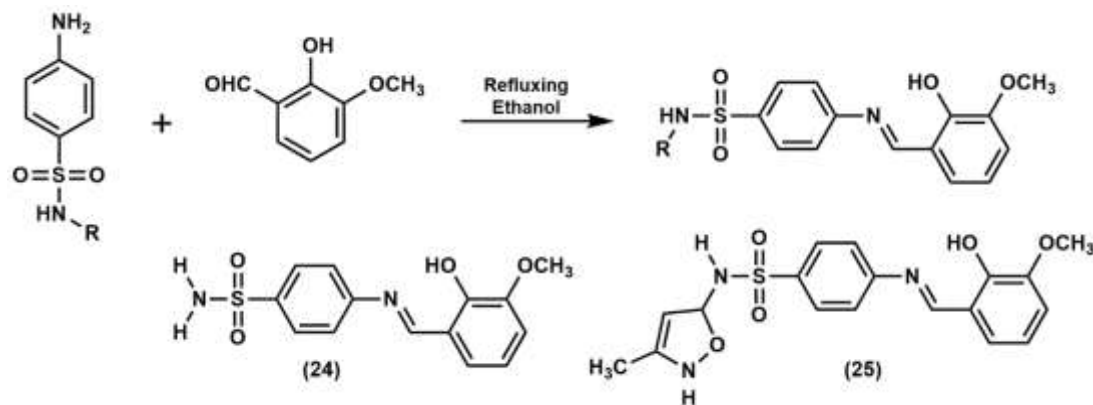
By use of palladium-catalyzed dehydroxylative coupling of phenols and amines in the presence of carbon monoxide, Fang et al. (2018) devised a unique one-pot method for the synthesis of arylcarboxylic amides and sulfonamide is given in scheme 5. Using acyclic amines, this approach shows that the process offers exclusive selectivity for arylcarboxylic amides while cyclic amines generate sulfonamides (**18**) [41].



Scheme 5: Formation of sulfonamide from phenolic compounds

For their possible antioxidative action, Havránková et al. (2020) showed a set of 1,3,5-triazine analogues with different structural motifs including aminobenzene sulfonamide and chalcone. On a mildly acidic resin, the

Sumrra and colleagues focused on the synthesis, characterisation, and biological screening of new sulfonamide-derived Schiff bases and associated transition metal complexes. Two ligands, L¹ (**24**) and L² (**25**), were prepared in this work by condensation of sulfonamide derivatives with certain aldehydes is given in scheme 7. X-ray diffraction, NMR, and IR spectroscopy were among the many methods used to define the produced compounds. Significant antibacterial and antioxidant action of the ligands and their metal complexes against many bacterial and fungal strains was found by biological tests. The results imply that these molecules have possible bioactive effects, so they are candidates for further pharmacological development [43].



Scheme 7: Synthesis of sulfonamide ligand

IV. CONCLUSION

Phenolic sulfonamides constitute a significant class of compounds with diverse applications spanning medicinal chemistry, environmental science, and catalysis. Their structural versatility facilitates potent biological activity, including antimicrobial, anticancer, and enzyme-inhibitory properties. Recent advancements in synthetic methodologies have enabled precise functionalization, enhancing their pharmacological potential and expanding their role in drug discovery. Additionally, environmental concerns surrounding the persistence of sulfonamide derivatives necessitate further studies on their biodegradation and ecological impact. Future research should focus on optimizing synthetic routes, improving bioavailability, and exploring novel therapeutic targets to maximize the utility of phenolic sulfonamides in scientific and pharmaceutical applications.

V. REFERENCES

- [1]. A. Oving, J. Bhattacharyya, Sulfonamide drugs: structure, antibacterial property, toxicity, and biophysical interactions, *Biophys. Rev.* 13 (2021) 259–272. <https://doi.org/10.1007/s12551-021-00795-9>.
- [2]. D.A. Smith, *Metabolism, Pharmacokinetics and Toxicity of Functional Groups: Impact of Chemical Building Blocks on ADMET*, Royal Society of Chemistry, 2010.
- [3]. A) Foye, W. O. *Antibacterial Agents, Sulfonamides*, Kirk-Othmer Encyclopedia of Chemical Technology (2000). B) Macielag, M. J., Bush, K., & Weidner-Wells, M. A., *Antibacterial agents, overview*. Kirk-Othmer Encyclopedia of Chemical Technology (2000). <https://doi.org/10.1002/0471238961.1921120606152505.a01>
<https://doi.org/10.1002/0471238961.1921120606152505.a01.pub2>

- [4]. H. Azevedo-Barbosa, D.F. Dias, L.L. Franco, J.A. Hawkes, D.T. Carvalho, From Antibacterial to Antitumour Agents: A Brief Review on The Chemical and Medicinal Aspects of Sulfonamides, *Mini Rev. Med. Chem.* 20 (2020) 2052–2066. <https://doi.org/10.2174/1389557520666200905125738>.
- [5]. J. Hu, X. Li, F. Liu, W. Fu, L. Lin, B. Li, Comparison of chemical and biological degradation of sulfonamides: Solving the mystery of sulfonamide transformation, *J. Hazard. Mater.* 424 (2022) 127661. <https://doi.org/10.1016/j.jhazmat.2021.127661>.
- [6]. C. Tan, Q. Zhang, X. Zheng, H. Liu, P. Chen, W. Zhang, Y. Liu, W. Lv, G. Liu, Photocatalytic degradation of sulfonamides in 4-phenoxyphenol-modified g-C₃N₄ composites: Performance and mechanism, *Chem. Eng. J.* 421 (2021) 127864. <https://doi.org/10.1016/j.cej.2020.127864>.
- [7]. A.U. Hassan, S.H. Sumrra, Exploring the Bioactive Sites of New Sulfonamide Metal Chelates for Multi-Drug Resistance: An Experimental Versus Theoretical Design, *J. Inorg. Organomet. Polym. Mater.* 32 (2022) 513–535. <https://doi.org/10.1007/s10904-021-02135-6>.
- [8]. D. Guianvarc'h, M. Duca, C. Boukarim, L. Kraus-Berthier, S. Léonce, A. Pierré, B. Pfeiffer, P. Renard, P.B. Arimondo, C. Monneret, D. Dauzonne, Synthesis and Biological Activity of Sulfonamide Derivatives of Epipodophyllotoxin, *J. Med. Chem.* 47 (2004) 2365–2374. <https://doi.org/10.1021/jm031117b>.
- [9]. Z.H. Chohan, Mahmood-ul-Hassan, K.M. Khan, C.T. Supuran, In-vitro antibacterial, antifungal and cytotoxic properties of sulfonamide—derived Schiff's bases and their metal complexes, *J. Enzyme Inhib. Med. Chem.* 20 (2005) 183–188. <https://doi.org/10.1080/14756360500043257>.
- [10]. M. I. H. El-Qaliei, M. El-Gaby, Y. A. Ammar, A. M. Ali, M. F. Hussein, F. A. Faraghally, Sulfonamides: Synthesis and the recent applications in Medicinal Chemistry, *Egypt. J. Chem.* 0 (2020) 0–0. <https://doi.org/10.21608/ejchem.2020.33860.2707>.
- [11]. S. Lu, S.V.H. Ng, K. Lovato, J.-Y. Ong, S.B. Poh, X.Q. Ng, L. Kürti, Y. Zhao, Practical access to axially chiral sulfonamides and biaryl amino phenols via organocatalytic atroposelective N-alkylation, *Nat. Commun.* 10 (2019) 3061. <https://doi.org/10.1038/s41467-019-10940-4>.
- [12]. W. Zafar, S.H. Sumrra, A.U. Hassan, Z.H. Chohan, A review on 'sulfonamides': their chemistry and pharmacological potentials for designing therapeutic drugs in medical science, *J. Coord. Chem.* 76 (2023) 546–580. <https://doi.org/10.1080/00958972.2023.2208260>.
- [13]. C. Dunker, K. Schlegel, A. Junker, Phenol (bio)isosteres in drug design and development, *Arch. Pharm. (Weinheim)* 358 (2025) e2400700. <https://doi.org/10.1002/ardp.202400700>.
- [14]. D. Crich, B. Surve, M. Sannigrahi, CYCLOFUNCTIONALIZATION OF UNSATURATED ALCOHOLS, PHENOLS, ACIDS, AND SULFONAMIDES WITH 1-BENZENE- SULFINYL PIPERIDINE AND TRIFLUOROMETHANESULFONIC ANHYDRIDE, (n.d.).
- [15]. H. Liang, M.A. Ciufolini, Oxidative Spirocyclization of Phenolic Sulfonamides: Scope and Applications, *Chem. – Eur. J.* 16 (2010) 13262–13270. <https://doi.org/10.1002/chem.201001402>.
- [16]. M.B.M. Reddy, M.A. Pasha, Cs₂ CO₃ Catalyzed Rapid and Efficient Conversion of Amines into Sulfonamides; Alcohols and Phenols into Sulfonic Esters, *Phosphorus Sulfur Silicon Relat. Elem.* 186 (2011) 1867–1875. <https://doi.org/10.1080/10426507.2010.544271>.
- [17]. A.R. Massah, R.J. Kalbasi, M. Khalifesoltani, F. Moshtagh Kordesofla, ZSM-5-SO₃ H: An Efficient Catalyst for Acylation of Sulfonamides Amines, Alcohols, and Phenols under Solvent-Free Conditions, *ISRN Org. Chem.* 2013 (2013) 1–12. <https://doi.org/10.1155/2013/951749>.
- [18]. B. Kilpatrick, M. Heller, S. Arns, Chemoselective nitration of aromatic sulfonamides with tert-butyl nitrite, *Chem Commun* 49 (2013) 514–516. <https://doi.org/10.1039/C2CC37481A>.

- [19]. R.C. Maurya, P. Patel, Synthesis, magnetic and special studies of some novel metal complexes of Cu(II), Ni(II), Co(II), Zn(II), Nd(III), Th(IV), and UO₂ (VI) with schiff bases derived from sulfa drugs, viz., Sulfanilamide/Sulfamerazine and o-vanillin, *Spectrosc. Lett.* 32 (1999) 213–236. <https://doi.org/10.1080/00387019909349979>.
- [20]. A.V. Smolobochkin, A.S. Gazizov, E.A. Anikina, A.R. Burirov, M.A. Pudovik, Acid-catalyzed reaction of phenols with N-(4,4-diethoxybutyl)sulfonamides – a new method for the synthesis of 2-aryl-1-sulfonylpyrrolidines, *Chem. Heterocycl. Compd.* 53 (2017) 161–166. <https://doi.org/10.1007/s10593-017-2034-8>.
- [21]. V. Garaj, L. Puccetti, G. Fasolis, J.-Y. Winum, J.-L. Montero, A. Scozzafava, D. Vullo, A. Innocenti, C.T. Supuran, Carbonic anhydrase inhibitors: Novel sulfonamides incorporating 1,3,5-triazine moieties as inhibitors of the cytosolic and tumour-associated carbonic anhydrase isozymes I, II and IX, *Bioorg. Med. Chem. Lett.* 15 (2005) 3102–3108. <https://doi.org/10.1016/j.bmcl.2005.04.056>.
- [22]. A. Innocenti, S. Beyza Öztürk Sarıkaya, İ. Gülçin, C.T. Supuran, Carbonic anhydrase inhibitors. Inhibition of mammalian isoforms I–XIV with a series of natural product polyphenols and phenolic acids, *Bioorg. Med. Chem.* 18 (2010) 2159–2164. <https://doi.org/10.1016/j.bmc.2010.01.076>.
- [23]. B. Ricken, P.F.X. Corvini, D. Cichocka, M. Parisi, M. Lenz, D. Wyss, P.M. Martínez-Lavanchy, J.A. Müller, P. Shahgaldian, L.G. Tulli, H.-P.E. Kohler, B.A. Kolvenbach, ipso -Hydroxylation and Subsequent Fragmentation: a Novel Microbial Strategy To Eliminate Sulfonamide Antibiotics, *Appl. Environ. Microbiol.* 79 (2013) 5550–5558. <https://doi.org/10.1128/AEM.00911-13>.
- [24]. C. Capasso, C.T. Supuran, Bacterial, fungal and protozoan carbonic anhydrases as drug targets, *Expert Opin. Ther. Targets* 19 (2015) 1689–1704. <https://doi.org/10.1517/14728222.2015.1067685>.
- [25]. H.I. Gul, C. Yamali, H. Sakagami, A. Angeli, J. Leitans, A. Kazaks, K. Tars, D.O. Ozgun, C.T. Supuran, New anticancer drug candidates sulfonamides as selective hCA IX or hCA XII inhibitors, *Bioorganic Chem.* 77 (2018) 411–419. <https://doi.org/10.1016/j.bioorg.2018.01.021>.
- [26]. S. Bilginer, S.K. Bardaweel, Y. Demir, I. Gulcin, C. Kazaz, Synthesis, cytotoxicities, and carbonic anhydrase inhibition activities of pyrazoline–benzenesulfonamide derivatives harboring phenol/polyphenol moieties, *Med. Chem. Res.* 31 (2022) 925–935. <https://doi.org/10.1007/s00044-022-02893-z>.
- [27]. S. Beyza Öztürk Sarıkaya, İ. Gülçin, C.T. Supuran, Carbonic Anhydrase Inhibitors: Inhibition of Human Erythrocyte Isozymes I and II with a Series of Phenolic Acids, *Chem. Biol. Drug Des.* 75 (2010) 515–520. <https://doi.org/10.1111/j.1747-0285.2010.00965.x>.
- [28]. N. Korkmaz, O.A. Obaidi, M. Senturk, D. Astley, D. Ekinici, C.T. Supuran, Synthesis and biological activity of novel thiourea derivatives as carbonic anhydrase inhibitors, *J. Enzyme Inhib. Med. Chem.* 30 (2015) 75–80. <https://doi.org/10.3109/14756366.2013.879656>.
- [29]. H.M. Bialk, A.J. Simpson, J.A. Pedersen, Cross-Coupling of Sulfonamide Antimicrobial Agents with Model Humic Constituents, *Environ. Sci. Technol.* 39 (2005) 4463–4473. <https://doi.org/10.1021/es0500916>.
- [30]. J. Schwarz, H. Knicker, G.E. Schaumann, S. Thiele-Bruhn, Enzymatic Transformation and Bonding of Sulfonamide Antibiotics to Model Humic Substances, *J. Chem.* 2015 (2015) 1–11. <https://doi.org/10.1155/2015/829708>.
- [31]. M. Paumelle, F. Donnadieu, M. Joly, P. Besse-Hoggan, J. Artigas, Effects of sulfonamide antibiotics on aquatic microbial community composition and functions, *Environ. Int.* 146 (2021) 106198. <https://doi.org/10.1016/j.envint.2020.106198>.

- [32]. D.A. Adsmond, D.J.W. Grant, Hydrogen bonding in sulfonamides, *J. Pharm. Sci.* 90 (2001) 2058–2077. <https://doi.org/10.1002/jps.1157>.
- [33]. Bagrat.A. Shainyan, Nina.N. Chipanina, Larisa.P. Oznobikhina, The basicity of sulfonamides and carboxamides. Theoretical and experimental analysis and effect of fluorinated substituent, *J. Phys. Org. Chem.* 25 (2012) 738–747. <https://doi.org/10.1002/poc.2910>.
- [34]. S. Durdagi, M. Şentürk, D. Ekinçi, H.T. Balaydın, S. Göksu, Ö.İ. Küfrevioğlu, A. Innocenti, A. Scozzafava, C.T. Supuran, Kinetic and docking studies of phenol-based inhibitors of carbonic anhydrase isoforms I, II, IX and XII evidence a new binding mode within the enzyme active site, *Bioorg. Med. Chem.* 19 (2011) 1381–1389. <https://doi.org/10.1016/j.bmc.2011.01.016>.
- [35]. K.A. Scott, P.B. Cox, J.T. Njardarson, Phenols in Pharmaceuticals: Analysis of a Recurring Motif, *J. Med. Chem.* 65 (2022) 7044–7072. <https://doi.org/10.1021/acs.jmedchem.2c00223>.
- [36]. C. Dunker, K. Schlegel, A. Junker, Phenol (bio)isosteres in drug design and development, *Arch. Pharm. (Weinheim)* 358 (2025) e2400700. <https://doi.org/10.1002/ardp.202400700>.
- [37]. A. Innocenti, D. Vullo, A. Scozzafava, C.T. Supuran, Carbonic anhydrase inhibitors: Interactions of phenols with the 12 catalytically active mammalian isoforms (CA I–XIV), *Bioorg. Med. Chem. Lett.* 18 (2008) 1583–1587. <https://doi.org/10.1016/j.bmcl.2008.01.077>.
- [38]. L.P. Oznobikhina, N.N. Chipanina, T.N. Aksamentova, B.A. Shainyan, Orientation of hydrogen bond in H-complexes of sulfones and sulfonamides, *Russ. J. Gen. Chem.* 79 (2009) 1674–1682. <https://doi.org/10.1134/S1070363209080167>.
- [39]. S. Kuroda, Y. Horino, K. Hashimoto, Synthesis of Functionalized Chromanes via a Formal [3+3]Cycloaddition of Allene Sulfonamides to Phenols, *HETEROCYCLES* 80 (2010) 187. [https://doi.org/10.3987/COM-09-S\(S\)54](https://doi.org/10.3987/COM-09-S(S)54).
- [40]. H.I. Gul, C. Yamali, F. Yesilyurt, H. Sakagami, K. Kucukoglu, I. Gulcin, M. Gul, C.T. Supuran, Microwave-assisted synthesis and bioevaluation of new sulfonamides, *J. Enzyme Inhib. Med. Chem.* 32 (2017) 369–374. <https://doi.org/10.1080/14756366.2016.1254207>.
- [41]. W. Fang, Y. Huang, J. Leng, H. Qin, Pd-Catalyzed One-Pot Dehydroxylative Coupling of Phenols and Amines under a Carbon Monoxide Atmosphere: A Chemical-Specific Discrimination for Arylcarboxylic Amide Synthesis, *Asian J. Org. Chem.* 7 (2018) 751–756. <https://doi.org/10.1002/ajoc.201800037>.
- [42]. E. Havránková, N. Čalkovská, T. Padrtová, J. Csöllei, R. Opatřilová, P. Pazdera, Antioxidative Activity of 1,3,5-Triazine Analogues Incorporating Aminobenzene Sulfonamide, Aminoalcohol/Phenol, Piperazine, Chalcone, or Stilbene Motifs, *Molecules* 25 (2020) 1787. <https://doi.org/10.3390/molecules25081787>.
- [43]. S.H. Sumrra, A.U. Hassan, M. Imran, M. Khalid, E.U. Mughal, M.N. Zafar, M.N. Tahir, M.A. Raza, A.A.C. Braga, Synthesis, characterization, and biological screening of metal complexes of novel sulfonamide derivatives: Experimental and theoretical analysis of sulfonamide crystal, *Appl. Organomet. Chem.* 34 (2020) e5623. <https://doi.org/10.1002/aoc.5623>.



**One Day National Conference On Recent
Advances in Chemical and Biochemical Sciences**



Organized By

Ajintha Education Society's,
Department of Chemistry, Sant Dnyaneshwar Mahavidyalaya,
Soegaon, Maharashtra, India

&

Dr. Babasaheb Ambedkar Marathwada University,
Chhatrapati, Sambhajinagar, Maharashtra, India

Publisher

Technoscience Academy

Website : www.technoscienceacademy.com

Email : editor@ijsrst.com Website : <http://ijsrst.com>